REMOVAL OF ARSENIC AND MERCURY FROM WATER BY CARBON NANOTUBES

BY

SALMAN FALEH AL-KHALDI

A Thesis Presented to the

DEANSHIP OF GRADUATE STUDIES

KING FAHD UNIVERSITY OF PETROLEUM & MINERALS

DHAHRAN, SAUDI ARABIA

In Partial Fulfillment of the
Requirements for the Degree of

MASTER OF SCIENCE

In

ENVIRONMENTAL SCIENCES

July, 2009

DEANSHIP OF GRADUATE STUDIES

This thesis, written by SALMAN F. AL-KHALDI under the direction of his thesis advisor and approved by his thesis committee, has been presented to and accepted by the Dean of Graduate Studies, in partial fulfillment of the requirements for the degree of MASTER OF SCIENCE IN ENVIRONMENTAL SCIENCES.

Thesis Committee

Dr. Bassam S. Tawabini
(Thesis Advisor)

Dr. Muataz Ali Atieh
(Member)

Dr. Abdul-Aziz M. Al-Shaibani
(Department Chairman)

Dr. Mazen M. Khaled
(Member)

Dr. Salam A. Zummo
(Dean of Graduate Studies)

25/7/09
Date

بسم الله الرحمن الرحيم

This Thesis Is Dedicated

To:

My beloved parents for their prayers and my wives for their tender care and efforts

ACKNOWLEDGMENT

First of all, I thank and praise the Almighty Allah, the cherisher and sustainer of the worlds; the most Gracious, the most Merciful and the most High in glory, for giving me an opportunity to pursue knowledge. This work would not have seen the light without the help of Allah almighty then the people around me.

I would like to express my gratitude to King Fahd University of Petroleum and Minerals for awarding me the master degree in the Environmental Sciences Program of the Earth Sciences Department. I really enjoyed being a graduate student in this important discipline of science in this prestigious educational society. I appreciate the support and cooperation from the chairman of Earth Sciences department Dr. Abdulaziz Al-Shaibani in alleviating difficulties we faced throughout the program. Many thanks to Saudi Aramco for the analytical support provided.

My deepest gratitude is also due to the distinguished thesis committee chaired by Dr. Bassam Tawabini for his exceptional efforts, invaluable support and guidance throughout the study. Also, I am grateful to Dr. Muataz Ali for his endless support and guidance. Furthermore, my appreciation is extended to Dr. Mazen Khaled for his encouragement and fruitful comments. Last but not least, I would like to thank Mr. Saad Al-Omar and Mr. Manuel Docdocil for their support on the analytical part of this study. I also want to thank and appreciate Southern Area Laboratories management for their encouragement and support.

Finally, I would like to thank my parents and brothers for her prayers, my wives and children for their sacrifice and understanding throughout this study.

TABLE OF CONTENTS

DEDICATION IV
ACKNOWLEDGEMENT V
TABLE OF CONTENTS VI
LIST OF FIGURES VIII
LIST OF TABLES X
ABSTRACT (ENGLISH) XI
ABSTRACT (ARABIC) XII
NOMENCLATURE XIII
CHAPTER 1: INTRODUCTION 1
CHAPTER 2: SIGNIFICANCE OF THE STUDY 4
CHAPTER 3: LITERATURE REVIEW 7
3.1 ARSENIC 7
3.1.1 The Chemistry of Arsenic 7
3.1.2 Arsenic in Water 9
3.1.3 Toxicity and Health Implications of Arsenic 11
3.1.4 Conventional Removal Techniques of Arsenic 13
3.2 MERCURY 14
3.2.1 The Chemistry of Mercury 14
3.2.2 Mercury in Water 17
3.2.3 Toxicity and Health Implications of Mercury 18
3.2.4 Conventional Removal Techniques of Mercury 20
3.3 CARBON NANOTUBES (CNTS) 23
3.3.1 The Structure of CNTs 27
3.3.2 The Synthesis of CNTs 30
3.3.3 The Properties of CNTs 37
3.3.4 The Applications of CNTs 40
3.4 STUDIES ON METAL REMOVAL USING CNTS 42
3.4.1 Adsorption Efficiency of CNTs 42

3.4.2 Factors affecting the efficiency of CNTs adsorption 43
CHAPTER 4: RESEARCH METHODOLOGY 49
4.1 MULTI-WALLED CARBON NANOTUBES 49
4.2 PREPARATION OF ARSENIC AND MERCURY STOCK SOLUTIONS 49
4.3 BATCH MODE ADSORPTION EXPERIMENT 50
4.4 EXPERIMENTAL DESIGN 52
4.5 ADSORPTION ISOTHERMS MODELS 53
4.6 KINETIC MODELING 56
CHAPTER 5: RESULTS AND DISCUSSION 57
5.1 CHARACTERIZATION OF MWCNTS 57
5.2 REMOVAL OF MERCURY (II) AND ARSENIC (III) FROM WATER BY MWCNTS 60
5.2.1 Removal of Mercury (II) from Water by MWCNTs 60
5.2.2 Removal of Arsenic (III) from Water by MWCNTs 68
5.2.3 Removal of Arsenic (III) from Water by Iron-Impregnated MWCNTs (MWCNT-Fe) 71
5.3 LANGMUIR AND FREUNDLICH ISOTHERM MODELS 81
5.3.1 Langmuir and Freundlich Adsorption Isotherm Models for Mercury (II) 83
5.3.2 Langmuir and Freundlich Adsorption Isotherm Models for Arsenic (III) 86
5.4 ADSORPTION KINETICS 88
5.4.1 Adsorption Kinetics for Mercury (II) 90
5.4.2 Adsorption Kinetics for Arsenic (III) 93
5.5 COMPARATIVE ANALYSIS OF VARIOUS ADSORBENTS FOR MERCURY (II) AND ARSENIC (III) REMOVAL 93
CHAPTER 6: CONCLUSIONS AND RECOMMENDATIONS 99
REFERENCES 102
APPENDIX – A
VITAE

LIST OF FIGURES

	Title	Page
Figure 3.1:	The E_h-pH diagram for Arsenic	8
Figure 3.2:	The transformation, cycling, and movement of Hg in the environment.	17
Figure 3.3:	The structure of C60, buckminsterfullerene	24
Figure 3.4:	Electron micrographs of microtubules of graphitic carbon	25
Figure 3.5:	TEM images of SWCNT	26
Figure 3.6:	A schematic showing a graphene sheet rolled-up into a SWCNT.	27
Figure 3.7:	TEM and schematics images of SWCNT and MWCNT	28
Figure 3.8:	Schematic of the honeycomb structure of a graphene sheet	29
Figure 3.9:	Chirality chart depicting the multitude of (n, m) SWCNT structures	31
Figure 3.10:	Schematic diagram of an arc-discharge apparatus	32
Figure 3.11:	Schematic diagram of Laser ablation apparatus	33
Figure 3.12:	A diagram showing the simplest CVD setup used for CNT growth	35
Figure 3.13:	Effect of pH on the ionization of CNTs	46
Figure 4.1:	Analytical instrumentation used to analyze As and Hg	51
Figure 5.1:	SEM Images of Multi-Walled carbon nanotubes	58
Figure 5.2:	TEM Images of Multi-Walled carbon nanotubes	59
Figure 5.3:	The effect of pH on the removal percentage of Hg (II) by MWCNTs	62
Figure 5.4:	The effect of contact time on the adsorption of Hg (II) by MWCNTs	64
Figure 5.5:	The effect of agitation rate on the adsorption of Hg (II) by MWCNTs	66
Figure 5.6:	The effect of MWCNTs dose on the adsorption of Hg (II)	67

Figure 5.7: The effect of pH on the adsorption of As (III) by MWCNTs 69

Figure 5.8: The effect of contact time on the adsorption of As (III) by MWCNTs.....70

Figure 5.9: The effect of agitation speed on the adsorption of As (III) by MWCNTs.....72

Figure 5.10: The effect of dosage on the adsorption of As(III) by MWCNTs.....73

Figure 5.11: The effect of pH on the adsorption of As (III) by MWCNT-Fe 75

Figure 5.12: The effect of contact time on the adsorption of As (III) by MWCNT-Fe.....78

Figure 5.13: The effect of agitation speed on the adsorption of As (III) by MWCNT-Fe.....79

Figure 5.14: The effect of dosage on the adsorption of As(III) by MWCNT-Fe 80

Figure 5.15: The effect of pH on the adsorption of As (III) by different M-CNTs and R-CNTs 82

Figure 5.16: Adsorption isotherm models for Hg (II) 85

Figure 5.17: Adsorption isotherm models for arsenic (III) 87

Figure 5.18: Test of pseudo-second-order rate equation for adsorption of various initial Hg (II) concentrations onto MWCNTs.....91

Figure 5.19: Test of pseudo-second-order rate equation for adsorption of various initial As(III) concentrations onto MWCNT-Fe 94

LIST OF TABLES

	Title	Page
Table 3.1:	Some common inorganic and organic arsenic compounds	10
Table 3.2:	Comparison of main arsenic removal technologies	15
Table 3.3:	Summary of the qualitative effect of some of the physical and chemical conditions on methylation	19
Table 3.4:	Summary of the major production methods and their efficiency	36
Table 3.5:	Summary of CNTs properties	41
Table 4.1:	Experiment parameters and their variation.	53
Table 5.1:	Parameters of Langmuir and Freundlich adsorption isotherm models for Mercury (II).	84
Table 5.2:	Parameters of Langmuir and Freundlich adsorption isotherm models for As (III).	89
Table 5.3:	Kinetic parameters of Hg (II) adsorbed on MWCNTs.	92
Table 5.4:	Kinetic parameters of As (III) adsorbed on M-CNTs.	95
Table 5.5:	Comparison of various adsorbents and its percentage uptake of Hg (II).	97
Table 5.6:	Comparison of various adsorbents and its percentage uptake of As (III)	98

THESIS ABSTRACT

NAME: SALMAN FALEH AL-KHALDI

TITLE OF STUDY: REMOVAL OF ARSENIC AND MERCURY FROM WATER USING MULTI-WALLED CARBON NANOTUBES

MAJOR FIELD: ENVIRONMENTAL SCIENCES

DATE OF DEGREE: July, 2009

Un-modified and modified multi-walled carbon nanotubes (MWCNTs) produced and optimized by King Fahd University of Petroleum and Minerals (KFUPM) in Dhahran, Saudi Arabia were utilized in this study to remove trivalent Arsenic As (III) and divalent Mercury Hg (II) from water. The effect of solution conditions such as initial solution pH, initial metal ions concentration, dosage of the adsorbent i.e. CNT, contact time and mixing rate were investigated. Generally the percentage uptake increased with an increase in pH from pH 4 to 8. The optimum pH found in this study was 8 which showed 100 % removal of 0.1 ppm Hg (II) ions using 200 ppm of un-modified MWCNTs and 87.8 % of 10 ppm As (III) ions using 400 ppm of Iron-Impregnated MWCNTs from aqueous solution. The adsorption capacity gradually increased with the increase in agitation rate from 50 to 150 rpm, in which higher removal of Hg (II) and As (III) was observed at 150 rpm. The removal of Hg (II) and As (III) was optimal for higher dosage of CNTs, where 10 mg of un-modified MWCNTs contributed to 100 % removal of Hg (II) ions and 40 mg of modified MWCNTs achieved 87.8 % removal of As (III) ions. Both Langmuir and Freundlich isotherms were used to describe As (III) and Hg (III) adsorption process. The short contact time needed to reach equilibrium as well as the high adsorption capacity demonstrates that MWCNTs are good adsorbents for the removal of Hg (II) and As (III) from water.

MASTER OF SCIENCE
KING FAHD UNIVERSITY OF PETROLEUM & MINERALS
DHAHRAN, SAUDI ARABIA

ملخص الدراسة

الاسم سلمان بن فالح بن جاسم الخالدي

عنوان الرسالة إزالة الزرنيخ والزئبق من الماء باستخدام أنابيب الكربون النانوية متعددة الجدران

التخصص علوم البيئة

التاريخ يوليو – 2009

في هذه الدراسة تم استخدام أنابيب الكربون النانوية متعددة الجدران المعدّلة والغير معدّلة، والتي تنتجها وتحسنها جامعة الملك فهد للبترول والمعادن في الظهران بالمملكة العربية السعودية، لإزالة الزرنيخ والزئبق من الماء. لقد تمت دراسة أثر حالات المحلول كالأس الهيدروجيني، وتركيز ايونات المعدن، وجرعة الممتز (في هذه الحالة أنابيب الكربون النانوية متعددة الجدران)، ووقت الاتصال، وسرعة التهيج خلال المزج على فعالية الإمتزاز. عموماً فعالية الإمتزاز زادت بازدياد الأس الهيدروجيني من 4 إلى 8 . وقد وجد في هذه الدراسة أن الأس الهيدروجيني الأمثل لإزالة 100% من أيونات الزئبق (II) باستخدام أنابيب الكربون النانوية متعددة الجدران غير المعدلة هو 8. وعند الأس الهيدروجيني نفسه تمت إزالة 87,8% من الزرنيخ (III) باستخدام أنابيب الكربون النانوية متعددة الجدران المعدلة. كما لوحظ أن فعالية الإمتزاز تزداد تدريجياً بازدياد معدل المزج من 50 إلى 150 دورة في الدقيقة، حيث أن 150 دورة في الدقيقة أعطت الإزالة الأعلى للزئبق والزرنيخ. استخدام جرعات أكبر من أنابيب الكربون النانوية متعددة الجدران أسف عن إزالة أعلى، حيث أن 10 ملغم من أنابيب الكربون النانوية متعددة الجدران غير المعدلة حققت إزالة 100% من أيونات الزئبق (II). و40 ملغم من أنابيب الكربون النانوية متعددة الجدران المعدلة ساهمت في إزالة 87,8% من الزرنيخ (III). لقد تم استخدام ايسوثرمات Langmuir و Freundlich في وصف عملية الإمتزاز لأيونات الزرنيخ (III) والزئبق (II) من الماء. إن الوقت القصير اللازم للوصول إلى التوازن، علاوة على الفعالية العالية للإمتزاز لهو دليل على أن أنابيب الكربون النانوية متعددة الجدران ممتزات فائقة الفعالية لإزالة أيونات الزرنيخ (III) والزئبق (II) من الماء.

NOMENCLATURE

ACNTs	-	Aligned Carbon NanoTubes
As	-	Arsenic
CNT	-	Carbon NanoTubes
CVD	-	Chemical Vapor Deposition
DOC	-	Dissolved Organic Carbon
DOS	-	Density Of States
DWCNT	-	Double Walled Carbon NanoTubes
E_h	-	Redox Potential
EU	-	European Union
FESEM	-	Field Emission Scanning Electron Microscopy
GPa	-	Gigapascal
Hg	-	Mercury
HRTEM	-	High Resolution Transmission Electron Microscopy
IEP	-	Iso-Electrical point
ICP-AES	-	Inductively Coupled Plasma-Atomic Emission Spectrometer
K	-	Kelvin
KFUPM	-	King Fahad University of Petroleum and Minerals
MCL	-	Maximum Contaminant Level
mg/L	-	Milligram per Liter
mg/g	-	Milligram per Gram
MWCNTs	-	Multiwalled Carbon NanoTubes
nm	-	Nanometer
PZC	-	Point of Zero Charge
rpm	-	Round Per Minute
SRB	-	Sulfate-Reducing Bacteria
SWCNT	-	Single Walled Carbon NanoTubes
SEM	-	Scanning Electron Microscopy
TEM	-	Transmission Electron Microscopy
TPa	-	Terapascal
µg/L	-	Microgram per Liter
W/m·K	-	Watts per meter. Kelvin

CHAPTER 1

INTRODUCTION

Water is the new oil of the 21st century and is becoming more valuable due to the increased consumption and demand. Good quality water (i.e. water free of contaminants) is essential to human health and a critical feedstock in a variety of key industries including oil and gas, petrochemicals, pharmaceuticals and food. The available supplies of water are decreasing due to (i) low precipitation, (ii) increased population growth, (iii) more stringent health based regulations, and (iv) competing demands from a variety of users e.g. industrial, agricultural and urban developments. Consequently water scientists and engineers are seeking alternative sources of water. These alternative sources include: seawater, storm water, wastewater (e.g. treated sewage effluent), and industrial wastewater.

Huge volumes of wastewater are generated by many industries. Water recovery, recycle and reuse have proven to be effective and successful in creating a new and reliable water supply, while not compromising public health (USEPA, 1998). Removal of contaminants and reuse of the treated water would provide significant reductions in cost, time, liabilities and labor to industry and result in improved environmental stewardship. Most of the remediation technologies available today, while effective, very often are costly and time-consuming methods. Advances in nanoscale science and engineering suggest that many of the current problems

involving water quality could be resolved or greatly ameliorated using nanosorbents, nanocatalysts, bioactive nanoparticles, nanostructured catalytic membranes and nanoparticle enhanced filtration among other products and processes resulting from the development of nanotechnology (Savage, 2005).

Nanotechnology is one of the latest editions of technological advancements since its boost in the early 1990s. Nanotechnology refers broadly to using materials and structures with nanoscale dimensions, usually ranging from 1 to 100 nanometers (nm). Nanometer-sized particles have been developed to improve the mechanical properties of materials, initiate photographic film development, and serve as vital catalysts in the petrochemical industry. Nanotechnology could substantially enhance environmental quality and sustainability through pollution prevention, treatment, and remediation.

Environmental scientists and engineers are already working with nanoscale structures and many products are increasingly reaching the market. Nanotechnology is not just about the size of very small materials, more importantly it is about the ability to work, observe, manipulate, and build at the molecular level. This results in materials and systems that often exhibit novel and significantly changed physical, chemical, and biological properties due to their size and structure. These new properties include improved catalysis, tunable wavelength sensing ability, and increased mechanical strength (Masciangioli, 2003). In the last decade there has been a significant progress in every application of nanotechnology including nanoparticles,

nanotubes, nanofibers, nanolayers nanodevices and nanostructured biological materials (Meyyappan, 2000).

Among these applications of nanotechnology, it is identified that Carbon Nanotubes (CNTs) emerged with very promising applications (Meyyappan, 2000) since their boost by the report made by Iijima in 1991 (Iijima, 1991). CNTs, a new member of the carbon family, have attracted special attentions to many researchers and engineers because they possess unique morphologies and have showed excellent properties and great potentials such as composite reinforcement, nanodevice component, gas adsorption material and catalyst support phases.

Moreover, CNTs are also good anion and cation adsorption materials for wastewater treatment, as they exhibit exceptionally large specific surface area. In addition to the remarkable mechanical properties, their hollow and layered nanosized structures make them a good candidate as adsorbers (Li *et al.*, 2002).

CHAPTER 2

SIGNIFICANCE OF THE STUDY

Industrial processes such as paper manufacturing, textile processing, food and beverage production, metal processing, and petrochemical refining produce enormous volumes of wastewater which is a valuable resource once properly treated. Removal of contaminants and reuse of the treated water would provide an exceptional alternative of water. Arsenic (As) and Mercury (Hg) are among those contaminants that must be removed from wastewater, due to their high toxicity, health effects and their tendency to accumulate in tissues of living organisms.

Mercury is a highly toxic metal, causing damage to the nervous system even at relatively low levels of exposure. It is particularly harmful to the development of unborn children. It collects in human and animal bodies and can be concentrated through the food chain, especially in certain types of fish. Arsenic is a highly poisonous metal. Arsenic non-cancer effects can include thickening and discoloration of the skin, stomach pain, nausea, vomiting, diarrhea, numbness in hands and feet, partial paralysis and blindness. Arsenic has been linked to cancer of the bladder, lungs, skin, kidney, nasal passages, liver and prostate (USEPA, 2009).

Different methodologies, with varying level of success, have been employed to remove heavy metals from water and wastewater. The efficiency in removing heavy

metals from water depends on the metal itself and its concentration. Biological treatment (aerobic and anaerobic), coagulation, precipitation, membrane filtration, ion exchange, oxidation, in-situ immobilization and adsorption (activated carbon) are common methods of removing As and Hg from wastewater streams. Adsorption is one of these methods which are regarded as the most promising and widely used method among them. Numerous materials were used as adsorbents to remove heavy metal ions from water such as metal oxides, active carbon, sepiolite, chitin, biosorbent, metal sulfides, resin and so on. Nevertheless the search for new and more effective materials to be used as adsorbents is a continuous effort for many researchers (Liang *et al.*, 2006).

One of the emerging technologies is CNTs which is becoming a valuable tool in industrial applications. In this study the efficiency of CNTs in removing As (III) and Hg (II) from water was investigated. The significance of this study is to have a better understanding of the applications of CNTs in preserving the environment and also to hold paramount the safety, health and welfare of the society. Furthermore, this study is also conducted to determine the impact of the different solution conditions on CNTs adsorption efficiency. It is expected that it will lead the way to process and device adjustments that achieve desired arrangements of nanotubes during large-scale production.

RESEARCH OBJECTIVES

The main objective of this study is to evaluate the adsorption efficiency of Arsenic (III) and Mercury (II) by MWCNTs. The specific objectives are:

- To remove Arsenic (As) and Mercury (Hg) from water during the treatment process using MWCNTs.
- To study the effect of solution conditions such as pH, metal ions concentration, dosage of MWCNTs, contact time and mixing rate on the adsorption efficiency.
- To evaluate the adsorption isotherms and kinetics of the experimental data.

CHAPTER 3

LITERATURE REVIEW

3.1 ARSENIC

3.1.1 THE CHEMISTRY OF ARSENIC

Arsenic is a naturally occurring metalloid or semi-metal element belonging to group 15 of the periodic table which comprises nitrogen, phosphorus, arsenic, antimony and bismuth. The ground state electronic configuration of the group's elements is ns^2np^3; which generally results in common oxidation states +3 (III) and +5 (V) (Norman, 1998). Arsenic has an atomic number of 33 and an atomic mass of 74.92. It is odorless, tasteless, and highly toxic which made arsenic the perfect poison in medieval times. It is the twentieth most abundant element in the earth's crust and is present in food, water, and air. It can exist in groundwater or surface water and can enter a water body naturally from geologic formations or by means of contamination from human activities. The primary way that arsenic enters the human body is by eating or drinking, although it can also be inhaled when present in dust. Like other elements, it is possible that the body needs a small amount of arsenic in the diet, but no nutritional role has yet been confirmed (Black, 1999).

The chemistry of arsenic is rather complicated because arsenic can exist, in the natural environment, in four different oxidation states depending on the pH and redox

potential (e.g., E_h) of the water body. A pH and E_h diagram is shown in Figure 3.1. It can exist as As (+V) (arsenate), As (+III) (arsenite), As (0) (arsenic), and

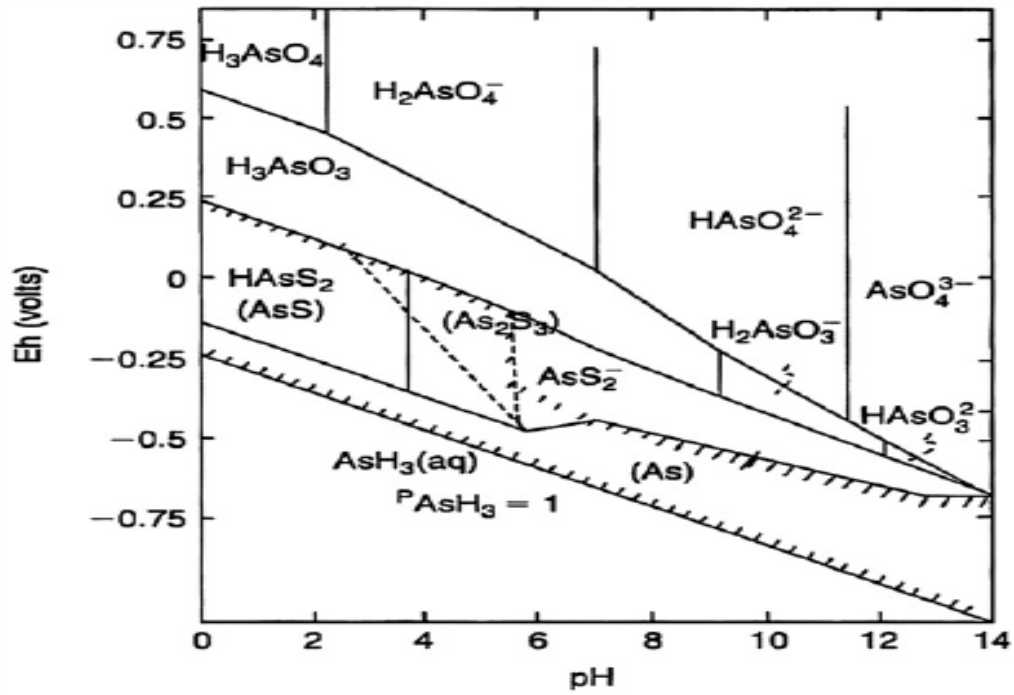

Figure 3.1: The E_h-pH diagram for As at 25°C and one atm. with total arsenic 10-5 mol/L and total sulfur 10-3 mol/L. Solid species are enclosed in parentheses in cross-hatched area, which indicates solubility less than $10^{-5.3}$ mol/L. (Ferguson, 1972).

As (-III) (arsine). In strongly reducing environments, As (0) and As (-III) can exist. Furthermore, in drinking water supplies, arsenic is usually found as As (V) or As (III). Arsenates (H_3AsO_4, $H_2AsO_4^-$, $HAsO_4^{2-}$ or AsO_4^{3-}) are typically present in the mono- and divalent anionic forms in oxygenated waters while arsenite (H_3AsO_3, $H_2AsO_3^-$, and $HAsO_3^{2-}$) is found primarily in moderately reducing conditions such as groundwater (Badruzzaman *et al.*, 2004).

Organic forms of arsenic also exist however they are insignificant in most drinking water sources. The organic chemistry of arsenic is extensive. Carbon-arsenic bonds are quite stable under a variety of environmental conditions of pH and oxidation potential. Some methylarsenic compounds, such as di- and trimethylarsines, occur naturally as a consequence of biological activity. In water solutions, these may undergo oxidation to the corresponding methylarsenic acids. These and other higher organic arsenic compounds such as arsenobetaine and arsenocholine, which are found in marine organisms, are very resistant to chemical degradation (Lauwerys, 1979).

Organic arsenic is found in the environment as methylated forms: dimethylarsinic acid (DMAV); monomethylarsonic acid (MMAV); arsenobetaine (AsBV); arsenocholine (AsCV). Pharmaceutical like 4-hydroxy-3-nitrobenzene arsonic acid (Roxarsone®) is widely used as a growth promoter and antibiotic agent in intensive poultry farming. It must be remarked that MMA and DMA present in the environment are stable methylated mammalian metabolites. However, DMA and sodium salts of MMA can also be present because of their use as herbicides (Villaescusa, 2008). Table 3.1 shows some common inorganic and organic arsenic compounds.

3.1.2 ARSENIC IN WATER

The mobility of arsenic in natural environments is primarily influenced by sorption onto metal-oxides/hydroxides. The sorption of arsenic is dependent on the oxidation state of As, pH conditions, the redox potential, the presence of other

Table 3.1: Some common inorganic and organic arsenic compounds (WHO, 1981).

CAS number	Name	Synonyms	Formula
	Inorganic arsenic, trivalent		
1327-53-3	arsenic (III) oxide	arsenic trioxide arsenous oxide white arsenic	As_2O_3 (or As_4O_6)
13464-58-9	arsenous acid		H_3AsO_3
13768-07-05	arsenenous acid arsenites, salts of arsenous acid	arsenious acid	$HAsO_2$ $H_2AsO_3^-$, $HAsO_3^{2-}$ or AsO_3^{3-}
7784-34-1	arsenic (III) chloride	arsenic trichloride arsenous trichloride	$AsCl_3$
1303-33-9	arsenic (III) sulfide	arsenic trisulfide orpiment, auripigment	As_2S_3
	Inorganic arsenic, pentavalent		
1303-28-2	arsenic (IV) oxide	arsenic pentoxide	As_2O_5
7778-39-4	arsenic acid	orthoarsenic acid	H_3AsO_4
10102-53-1	arsenenic acid arsenates, salts of	metaarsenic acid	$HAsO_3$ $H_2AsO_4^-$, $HAsO_4^{2-}$ or AsO_4^{3-}
	Organic arsenic		
124-58-3	methylarsonic acid	methanearsonic acid	$CH_3AsO(OH)_2$
75-60-5	dimethylarsinic acid	cacodylic acid	$(CH_3)_2AsO(OH)$
4964-14-1	trimethylarsine oxide		$(CH_3)_3AsO$
593-52-2	methylarsine		CH_3AsH_2
593-57-7	dimethylarsine		$(CH_3)_2AsH$
593-88-4	trimethylarsine		$(CH_3)_3As$
98-50-0	arsanilic acid	p - aminobenzene-arsonic acid (4 - aminophenyl) -- arsonic acid	$H_2N-C_6H_4-AsO(OH)_2$
139-93-5	arsphenamine	4,4 - arsenobis (2 - amino-phenol) dihydro-chloride Salvarsan	$HCl \cdot H_2N$, $NH_2 \cdot HCl$ $HO-C_6H_4-As=As-C_6H_4-OH$
121-59-5	carbarsone	[4-[aminocarbonyl-amino] phenyl] - arsonic acid: N - carbamoylarsanilic acid	$(OH)_2OAs-C_6H_4-NHC(=O)NH_2$
554-72-3	tryparsamide	[4 - [2 - amino - 2 - oxoethyly) amino] - phenyl] arsonic acid	$(OH)_2OAs-C_6H_4-NHCH_2C(=O)NH_2$
121-19-7	3 - nitro - 4 - hydroxy-phenylarsonic acid		O_2N, HO, $AsO(OH)_2$
98-72-6	4 - nitrophenylarsonic acid	p - nitrophenylarsonic acid	$O_2N-C_6H_4-AsO(OH)_2$
	arsenobetaine		$(CH_3)_3As + CH_2COOH$
	arsenocholine		$(CH_3)_3As + CH_2CH_2OH$
	dialkylchloroarsine		R_2AsCl
	alkyldichloroarsine		$RAsCl_2$

competing oxyanions, such as phosphate, sulfate, carbonate and silicate and organic matter (Sharma, 2009). Arsenite species are more mobile than arsenate in

groundwater, because uncharged arsenite is less prone to be sorbed to a mineral surface than the arsenate anions. Arsenate has strong affinity for most metal-oxides/hydroxides and clay minerals, and forms surface complexes, whereas arsenite is more selective although it also has an affinity for Fe-oxides/hydroxides (Inskeep, 2002).

In seawater, the concentration of arsenic is usually less than 2 μg/L (Ng, 2005). The levels of arsenic in unpolluted surface water and groundwater vary typically from 1–10 μg/L. In freshwater, the variation is in the range of 0.15–0.45 μg/L. In thermal waters, concentrations of up to 8.5 mg/L and 1.8–6.4 mg/L have been reported in New Zealand and Japan, respectively. Natural geological sources of As to drinking water are one of the most significant causes of arsenic contamination around the world. The World Health Organization (WHO) has set a guideline of 10 μg/L as the drinking water standard (Sharma, 2009). The two inorganic forms most prevalent in aqueous chemistry are the pentavalent arsenate ion, (As (V)), and the trivalent arsenite ion, (As (III)). Organic forms of arsenic also exist that contribute to total arsenic, but they are probably insignificant in most drinking water sources.

3.1.3 TOXICITY AND HEALTH IMPLICATIONS OF ARSENIC

The toxicity of arsenic is dependent on its oxidation state and form i.e. inorganic or organic. Generally inorganic arsenic species are more toxic than organic forms to living organisms, including humans and other animals. The methylated compounds are roughly 1% as toxic as As (III) and arsenite is about four times more toxic than As

(V); insoluble arsenic compounds are less toxic than their soluble counterparts. The higher toxicity of arsenite (AsO_3^{3-}) is attributed to its high affinity for the sulfydryl groups of amino acids e.g. cysteine, and thereby inactivates a wide range of enzymes in intermediate metabolism (Fendorf, 1997).

Arsenic-contaminated waters cannot be distinguished, because arsenic is invisible and does not alter the taste or smell of the water unless concentrations are extremely high. The general public can be exposed to arsenic in several different ways however consuming arsenic-containing water and food (especially marine food) are the most common routes. The extent of chronic exposure can be determined by estimating arsenic concentration in hair and nails since it is laid down in keratin soon after ingestion. Using hair and nails as indicators of exposure to arsenic has a drawback where arsenic concentrations might be influenced by external contamination via air, water, soaps and shampoos. Blood and urine have often been used as an indicator of recent exposure (NRC, 1999).

Although beneficial effects have been reported for some arsenic compounds e.g. reduction of fever, prevention of black-death, healing of boils and treatment of chronic myelocytic leukaemia (Goessler, 2002), its toxicity to human health ranges from skin lesions to cancer of the brain, liver, kidney and stomach (Smith *et al.*, 1992). While acute arsenic poisoning can lead to rapid death, chronic negative health impacts are more common and tend to appear only after several years of exposure. The most commonly observed symptoms identifying people suffering from chronic arsenic poisoning are arsenical skin lesions (e.g. melanosis, keratosis), blackfoot

disease and in more serious cases incidents of gangrene, skin cancer (when ingested), and lung cancers (when inhaled). It is noted, however, that no clear correlation between arsenic concentrations in water and skin cancer has been reported in the USA suggesting that other factors may affect the link between arsenic intake and skin cancer; e.g. dietary factors (Fuhrman, 2004).

The best way to overcome the adverse health effects of arsenic is by providing safe drinking water, because there is no effective treatment to offset arsenic toxicity. Consequently, the World Health Organization (WHO) has recommended 0.01 mg/L as a maximum contaminant level (MCL) for arsenic in drinking water (WHO, 2006). Many countries however, still allow higher arsenic concentrations in drinking water (i.e. 0.05 mg/L) primarily due to the high cost of treatment to lower concentrations. The WHO MCL of arsenic is health-based target guideline below which the presence of arsenic is not considered a significant health risk, even after a lifetime consumption of the water.

3.1.4 CONVENTIONAL REMOVAL TECHNIQUES OF ARSENIC

Providing arsenic-free drinking water has attracted strong interest among scientists and researchers due to the negative health effects of drinking arsenic contaminated water, and to the more stringent regulations that have been imposed for arsenic in many countries e.g. the USA and the EU where the MCL has been reduced from 0.05 mg/L to 0.01 mg/L. Accordingly, tremendous research and projects have

been carried out to develop cost-effective arsenic removal techniques. Several removal methods were proposed and tested for arsenic removal (Fuhrman, 2004).

Treatment processes to remove arsenic can be grouped into conventional treatment (coagulation, lime softening, or iron-manganese removal); sorption processes (ion exchange, activated alumina, and other specialty media); and membrane processes (reverse osmosis, nanofiltration, and augmented micro or ultrafiltration). Mohan and Pittman have extensively reviewed the different arsenic removal technologies with their advantages and disadvantages as shown in table 3.2 (Mohan and Pittman, 2007).

3.2 MERCURY

3.2.1 THE CHEMISTRY OF MERCURY

Mercury is a naturally occurring heavy metal that belongs to group 12 of the periodic table which includes Zinc and Cadmium. The ground state electronic configuration of the group's elements is $(n+1)s^2nd^{10}$. Mercury has three stable oxidation states: the elemental mercury (Hg (0)), mercurous (Hg (I)) and mercuric (Hg (II)). It has an atomic number of 80 and an atomic mass of 200.59 g/mole and its specific gravity is 13.5 times that of water. The melting point and boiling point of mercury are of -38.9^{o}C and 357.3^{o}C respectively. Mercury is the only metal that remains in liquid form at room temperature. Elemental mercury is a silver-white, shiny metal that is traditionally used for industrial, medicinal and cosmetic purposes.

Table 3.2: Comparison of main arsenic removal technologies (Mohan, 2007).

Major oxidation/precipitation technologies	Advantages	Disadvantages
Air oxidation	Relatively simple, low-cost but slow process; *in situ* arsenic removal; also oxidizes other inorganic and organic constituents in water.	Mainly removes As(V) and accelerate the oxidation process.
Chemical oxidation	Oxidizes other impurities and kills microbes; relatively simple and rapid process; minimum residual mass.	Efficient control of the pH and oxidation step is needed.
Major coagulation/coprecipitation technologies	**Advantages**	**Disadvantages**
Alum coagulation	Durable powder chemicals are available; relatively low capital cost and simple in operation; effective over a wider range of pH.	Produces toxic sludges; low removal of arsenic; pre-oxidation may be required.
Iron coagulation	Common chemicals are available; more efficient than alum coagulation on weigh basis.	Medium removal of As (III); sedimentation and filtration needed.
Lime softening	Chemicals are available commercially.	Readjustment of pH is required.
Major sorption and ion-exchange technologies	**Advantages**	**Disadvantages**
Activated alumina	Relatively well known and commercially available.	Needs replacement after 4-5 regeneration.
Iron coated sand	Cheap; no regeneration is required; remove both As (III) and As (V).	Not standardized; produces toxic solid waste.
Ion-exchange resin	Well-defined medium and capacity; pH independent; exclusive ion specific resin to remove arsenic.	High cost medium; high-tech operation and maintenance; regeneration creates a sludge disposal problem; As (III) is difficult to remove; life of resins
Major membrane technologies	**Advantages**	**Disadvantages**
Nanofiltration	Well-defined and high-removal efficiency.	Very high-capital and running cost, pre-conditioning; high water rejection.
Reverse osmosis	No toxic solid waste is produced.	High tech operation and maintenance.
Electrodialysis	Capable of removal of other contaminants.	Toxic wastewater produced.
Other techniques **Foam flotation** **Solvent extraction** **Bioremediation**		

Mercury is primarily found in nature within compounds and inorganic salts. Speciation of mercury is influenced by environmental conditions such as pH, redox potential (E_h), oxygen content, sulfide content, chloride concentration, organic matter content and microbial activity. Similarly, biological and chemical processes control the conversion of inorganic mercury to methylmercury. The properties and chemical behavior of mercury strongly depend on its oxidation state. Many inorganic and organic compounds of mercury can be formed. Inorganic mercuric compounds include mercuric sulphide (HgS), mercuric oxide (HgO) and mercuric chloride ($HgCl_2$). Most inorganic mercury compounds are white powders or crystals, except for mercuric sulphide, which is red and turns black after exposure to light.

Organic mercury or organomercurial compounds also exist naturally when mercury combines with carbon. There is a potentially large number of organic mercury compounds (such as methylmercury, dimethylmercury, phenylmercury, and ethylmercury); however, by far the most common organic mercury compound that microorganisms and natural processes generate from other forms is methylmercury. Figure 3.2 shows a schematic of mercury cycle in the environment. Methylmercury is of particular concern because it can bioaccumulate and biomagnify through the food chain i.e. in many edible freshwater and saltwater fish and marine mammals to levels that are many thousand times greater than levels in the surrounding water (Hontelez, 2005).

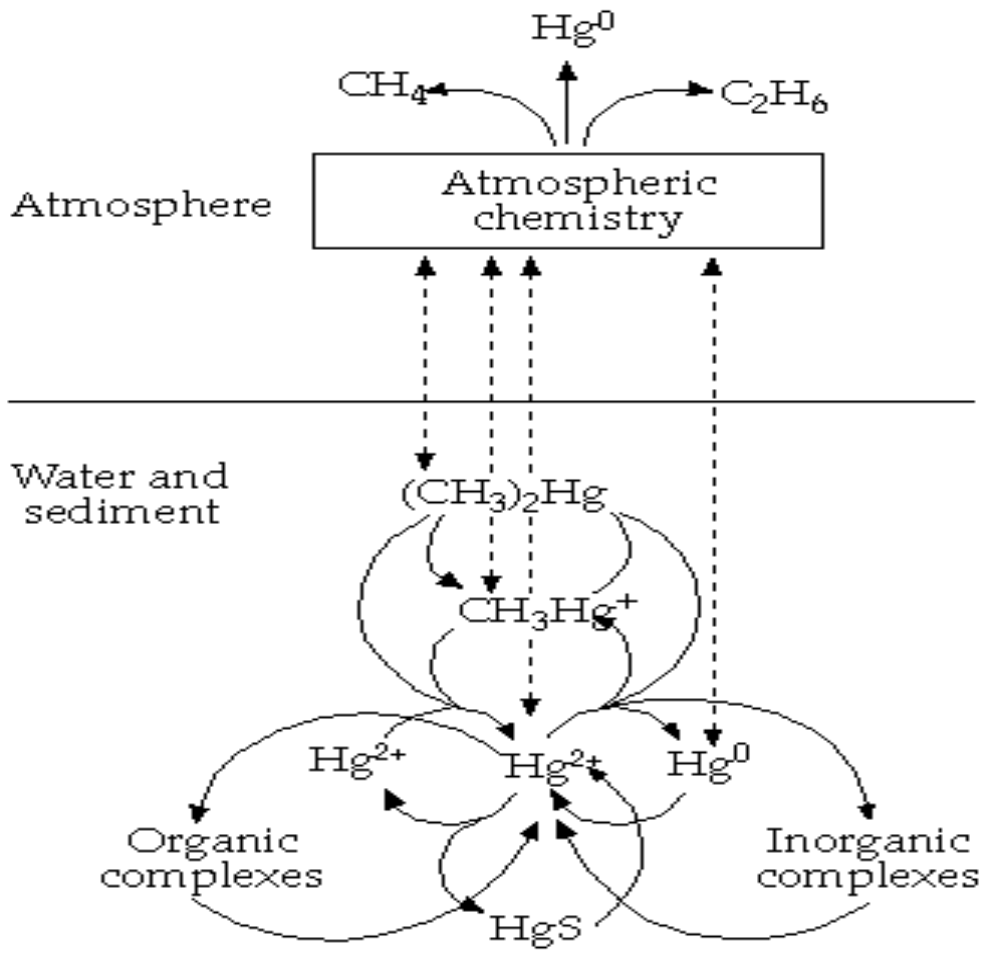

Figure 3.2: The transformation, cycling, and movement of Hg in the environment. Mercury transformations are made primarily by the action of bacteria. Physical conditions, such as temperature and pH, also have major role-determining equilibrium values in mercury transformations, and thus availability to man (Bonaventura, 1997).

3.2.2 MERCURY IN WATER

Natural chemical and biological processes influence mercury speciation hence affecting its solubility in water, toxicity and bioavailability. The solubilities of mercury compounds vary, ranging from negligible (HgCl and HgS) to very soluble ($HgCl_2$) (MADEP, 1996). Inorganic mercury has a high affinity for sediments; a

significant portion of the total mercury in freshwater is in particulate form (Gill, 1990). The total mercury concentration in surface water may decrease as mercury bound to particulate matter settles or is transported downstream (Bonzongo *et al.*, 1996). When organic matter is not present, mercury becomes relatively more mobile in acid soils and can evaporate to the atmosphere or leach to groundwater.

In sediment, freshwater and saltwater environments, mercury is converted from inorganic bivalent mercury Hg (II) to Mono- and dimethylmercury methylmercury primarily by microorganisms such as sulfate-reducing bacteria (SRB). However, In the presence of sulfides, the mercuric ion Hg (II) becomes tightly bound to sulfide as insoluble mercuric sulfide and is not available for methylation. Whereas mercurous ion Hg (I) combines with inorganic compounds *only* and cannot be methylated (Beckvar *et al.*, 1996). Methylation is usually greatest at the sediment water interface, but also occurs in the water column. Table 3.3 summarizes the qualitative effect of some of the physical and chemical conditions on methylation of mercury, as reported in literature.

3.2.3 *TOXICITY AND HEALTH IMPLICATIONS OF MERCURY*

Mercury bioavailability and toxicity is dictated by its species which in turn influenced by the natural chemical and biological processes. Being an element, mercury cannot *be broken down* or degraded into harmless substances. Mercury may change between different states and species in its cycle, but its simplest form is elemental mercury, which itself is harmful to humans and the environment. Once

Table 3.3: Summary of the qualitative effect of some of the physical and chemical conditions on the methylation of mercury (USEPA-OSW-HHRAP, 1998).

Physical or Chemical Condition	**Qualitative Influence on Methylation**
Low dissolved oxygen	Enhanced methylation
Decreased pH	Enhanced methylation in water column
Decreased pH	Decreased methylation in sediment
Increased dissolved organic carbon (DOC)	Enhanced methylation in sediment
Increased dissolved organic carbon (DOC)	Decreased methylation in water column
Increased salinity	Decreased methylation
Increased nutrient concentrations	Enhanced methylation
Increased selenium concentrations	Decreased methylation
Increased temperature	Enhanced methylation
Increased sulfate concentrations	Enhanced Methylation
Increased sulfide concentrations	Enhanced methylation

mercury has been liberated from either ores or fossil fuel and mineral deposits hidden in the earth's crust and released into the biosphere, it can be highly mobile cycling between the earth's surface and the atmosphere. The earth's surface soils, water bodies and bottom sediments are thought to be the primary biospheric sinks for mercury (Hontelez, 2005).

Although most mercury occurs in the inorganic form, methylmercury is the most toxic and readily bioaccumulated form of mercury. The principal target of long-term exposure to low levels of metallic and organic mercury is the nervous system. The principal target of long-term exposure to low levels of inorganic mercury appears to

be the kidneys. Short-term exposure to higher levels of any form of mercury can result in damage to the brain, kidneys and fetuses. Mercury has not been found to be carcinogenic. However, there are significant differences in the toxicity of the major forms of mercury. Mercury has been found to have a deleterious effect upon a wide range of systems including the respiratory, cardiovascular, hematologic, immune and reproductive systems.

The common markers for human mercury exposure are blood, hair and urine mercury concentrations. The mean total mercury levels in whole blood and urine of the general human population are approximately 8 μg/L and 4 μg/L respectively. This background level of mercury can vary considerably, however, with the incidence of dental mercury amalgams and the consumption of fish. Individuals whose diet consists of large amounts of fish can have blood methyl mercury levels as high as 200 μg/L with a daily intake of 200 μg of mercury (Jones, 1996).

3.2.4 *CONVENTIONAL REMOVAL TECHNIQUES OF MERCURY*

Quality of drinking water has become of paramount importance world wide. Presence of mercury in drinking water has been associated to deleterious effects upon a wide range of systems including the respiratory, cardiovascular, hematologic, immune and reproductive systems. Consequently more stringent regulatory controls have been imposed for mercury in many countries. The US EPA has established a maximum contaminant level (MCL) for mercury of 0.002 mg/L in drinking water. Accordingly, extensive research and projects have been performed to develop cost-effective mercury removal techniques. Several removal methods were proposed and

tested for mercury removal. The available technologies for the treatment of mercury include: precipitation/coprecipitation, membrane filtration, ion exchange, adsorption and bioremediation.

Precipitation/Coprecipitation is full-scale, cost-effective and most frequently used technology to treat mercury-contaminated groundwater and wastewater. In this treatment technology, a precipitant is added to the contaminated stream to convert soluble mercury to the relatively insoluble mercury. There are different types of precipitants that can be applied with varying levels of effectiveness for example ferric salts, alum and sulfide. This technology requires pH adjustment for optimal removal of mercury. The most effective precipitation of mercury for the sulfide precipitation occurs within a pH range of 7 to 9 (USEPA, 1997). The most effective precipitation of mercury for the hydroxide precipitation process occurs within a pH range of 7 to 11 (West General Inc., 2005).

The effectiveness of this technology is less likely to be reduced by pH of the treated stream, the presence of other metal contaminants and the excess use of sulfide precipitant can form soluble mercury sulfide species. The reported mercury removal by this technology is greater than 99.0 % with a minimum effluent mercury concentration achieved was 10 to 100 μg/L. However, the cost of this technology is increased by the added cost of treatment of the sludge produced which could be considered a hazardous waste and require additional treatment before disposal as a solid waste or disposal as hazardous waste.

Membrane filtration is effective for the treatment of mercury but is used less frequently because its costs tend to be higher and it produces a larger volume of residuals than other mercury treatment technologies. In addition, it is sensitive to a variety of contaminants and characteristics in the untreated water. Suspended solids, organic compounds, colloids, and other contaminants can cause membrane fouling. There are four types of membrane filtration processes, from largest to smallest filter pore size: microfiltration, ultrafiltration (UF), nanofiltration and reverse osmosis.

In *ion Exchange Treatment***,** various ion exchange resins are used for mercury removal from water. The most efficient are cationic resins with the thiol (-SH) functional group and chelate resins. Their efficiency depends on the initial mercury concentration and the presence of competing ions (copper, lead and iron). Typically, 99.8 % removal was achievable with an effluent mercury concentration of 0.2 – 1 μg/L. Regeneration of the resins with concentrated a sodium chloride solution is necessary.

Adsorption for mercury treatment is more likely to be affected by media characteristics and contaminants other than mercury when compared with precipitation/coprecipitation. Small-capacity systems using these technologies tend to have lower operating and maintenance costs and require less operator expertise. Adsorption tends to be used more often when mercury is the only contaminant to be treated, for relatively smaller systems, and as a polishing technology for the effluent from larger systems.

Adsorption processes have the potential to achieve high efficiencies of mercury removal and low effluent mercury level. The predominant adsorbent is activated carbon and carbon modified with different chemicals (bicarbonate, sulfide, carbon disulfide). Activated carbon is used as a powder (PAC) and disposed or as a granular (GAC) and regenerated usually by heating. Adsorption of mercury on activated carbon is pH dependent with the optimum pH in the 6 to 8 pH range. The level of mercury in the effluent depends on the initial concentration but typically is 0.5 to 10 μg/L with a contact time of at least 20 minutes.

Bioremediation (*in situ* or *ex situ*) has been shown to be effective in several pilot-scale studies. The mechanisms that enable bioremediation to reduce the concentration of mercury are not fully understood. Mechanisms that have been suggested include converting mercury to species that are retained in the biomass or converting it to species that are more easily removed from water by another technology, such as precipitation or adsorption. Bench-scale and additional pilot-scale studies are being conducted to assess the effectiveness of bioremediation technologies for mercury at full scale.

3.3 CARBON NANOTUBES (CNTs)

Carbon is one the most versatile elements in the periodic table for the myriad number of compounds it may form. It has been long known and used throughout history for metal oxides reduction. In 1772, Antoine Lavoisier showed that diamonds are a form of carbon. Graphite, on the other hand, was thought to be a form of lead

until 1779, when Carl Wilhelm Scheele showed that graphite produces the same amount of carbon dioxide gas per gram as amorphous carbon does (Senese, 2000). The most prominent discovery was made by Kroto *et al*. in 1985, when they unintentionally produced fullerenes C60. Figure 3.3 shows the structure of C60, buckminsterfullerene. In 1990, Krätschmer *et al.* developed a technique for synthesizing C60 in macroscopic quantities.

The discovery of fullerenes led to the discovery of Carbon nanotubes (CNTs) by Iijima in 1991. He managed to prepare a new type of finite carbon structure consisting of needle-like tubes grown on the negative end of the carbon electrode used in the arc-discharge evaporation of carbon in an argon-filled vessel (Iijima, 1991). Figure 3.4 shows electron microscope images of CNTs. Although the discovery of CNTs was credited to Iijima, there were earlier studies performed on carbon nanotubes with diameter > 7 nm by Radushkevich and Lukyanovich in 1952 (Bacsa, 2006). Endo and Oberlin have reported the observation of carbon nanotubes by electron microscopy in

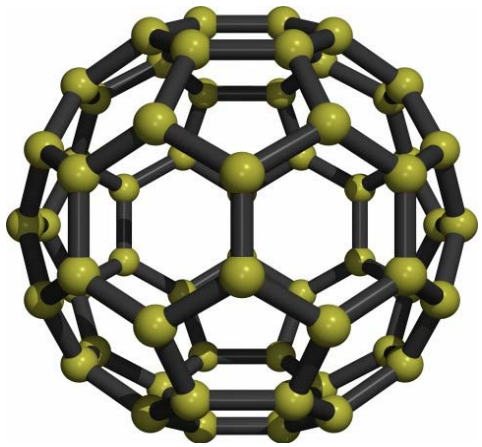

Figure 3.3: The structure of C60, buckminsterfullerene. Source: http://www.physics.uc.edu/~pkent/graphics/c60_big.jpg

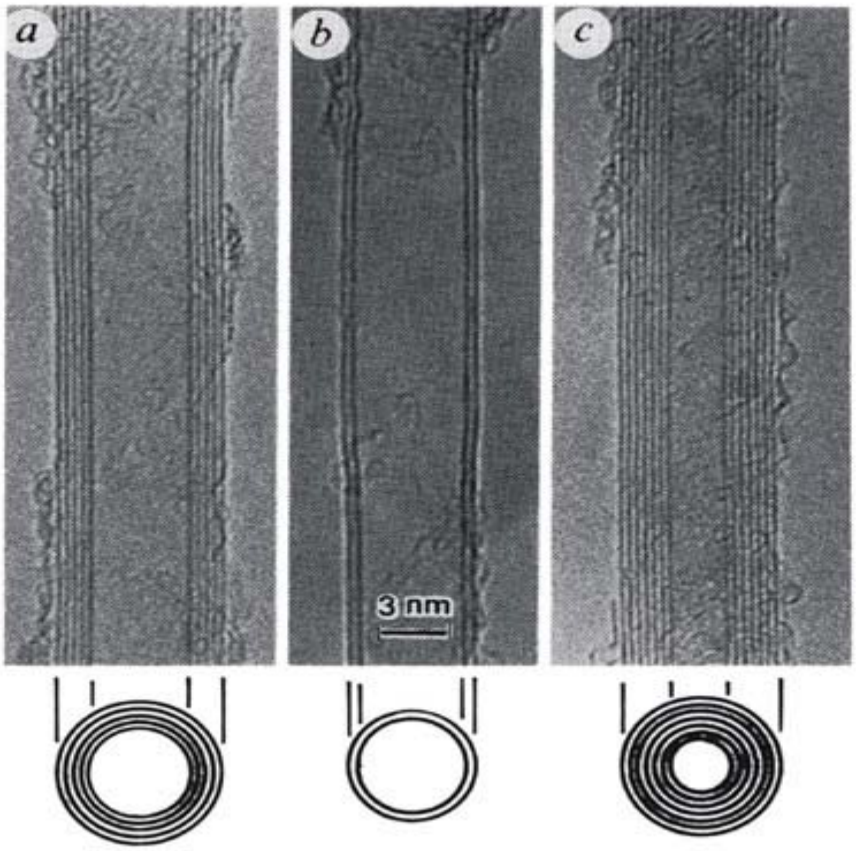

Figure 3.4: Electron micrographs of microtubules of graphitic carbon. Parallel dark lines correspond to the (002) lattice images of graphite. A cross-section of each tubule is illustrated. (a) Tube consisting of five graphitic sheets, diameter 6.7 nm. (b) Two-sheet tube, diameter 5.5 nm. (c) seven-sheet tube, diameter 6.5 nm, which has smallest hollow diameter (2.2 nm) (Iijima, 1991).

1976 (Monthioux, 2006). However, their significance was not widely appreciated until the connection was made between fullerenes and carbon nanotubes both experimentally and theoretically.

CNTs, an emerging material, stirred much speculation among the scientific community about their properties and potential applications. Large-scale synthesis of CNTs was inevitable to experimentally test their properties and potential applications,

which was accomplished in 1992 by Ebbesen and Ajayan. In 1993, Iijima and Ichihashi reported the synthesis of abundant single-shell tubes with diameters of about 1 nm. Figure 3.5 illustrates an image of single-walled nanotubes. Around this same time Bethune and his IBM Almaden colleagues discovered that transition metals such as cobalt can catalyze the formation of single-wall carbon nanotubes (Bethune *et al.*, 1993). In 1996 Thess *et al.* synthesized bundles of single wall carbon nanotubes for the first time. Since then, a new era of intensive research has begun, along with the improvement of the production and characterization techniques, to assess potential CNTs applications.

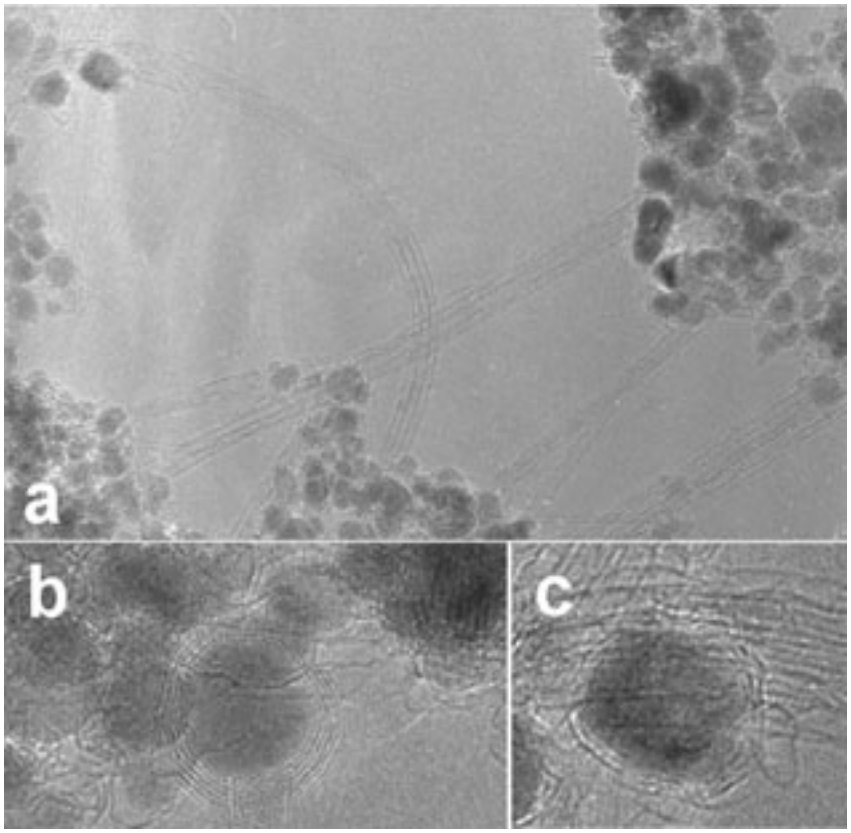

Figure 3.5: TEM images of SWCNT.
http://www.fy.chalmers.se/atom/research/nanotubes/production.xml

3.3.1 STRUCTURE

CNTs are sheets of graphene folded up into seamless cylinders (cf. figure 3.6). They are divided into single-walled carbon nanotubes (SWCNTs) and multi-walled carbon nanotubes (MWCNTs) based on the number of sheets, which can be in the range of 2-50 sheets (Iijima, 1991), in the wall of the nanotubes (cf. figure 3.7). The diameter of MWCNTs ranges from 2 to 30 nm whereas that of SWCNTs is 1–2 nm. The spacing between the sheets of graphene in MWCNTs is 0.34 nm. Zheng *et al.* has synthesized a SWNT of a length of 4.8 cm and indicated the possibility of growing SWNTs continuously without any length limitation (Zheng *et al.*, 2004). Tang *et al.* have reported the fabrication of mono-dispersed SWNTs of diameter as small as 0.4 nm (Tang *et al.*, 1998). A perfect tube is capped at both ends by hemi-fullerenes, leaving no dangling bonds.

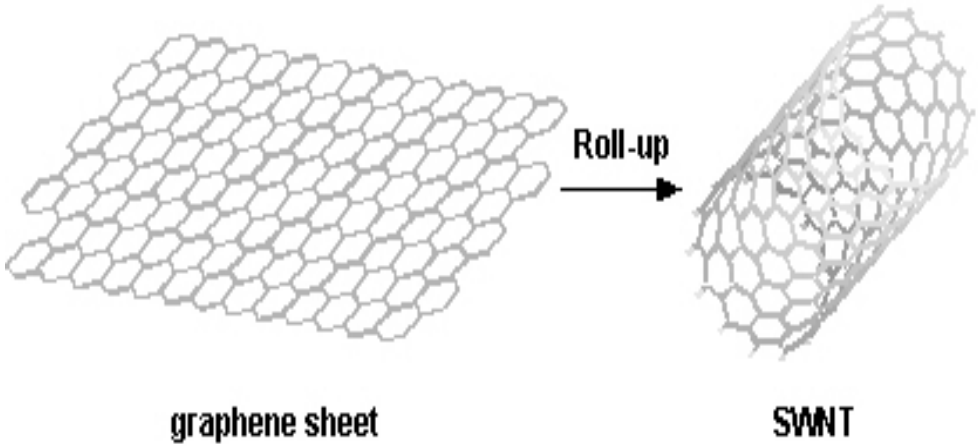

Figure 3.6: A schematic showing a graphene sheet rolled-up into a single walled carbon nanotube. http://www.nanotech-now.com/nanotube-buckyball-sites.htm

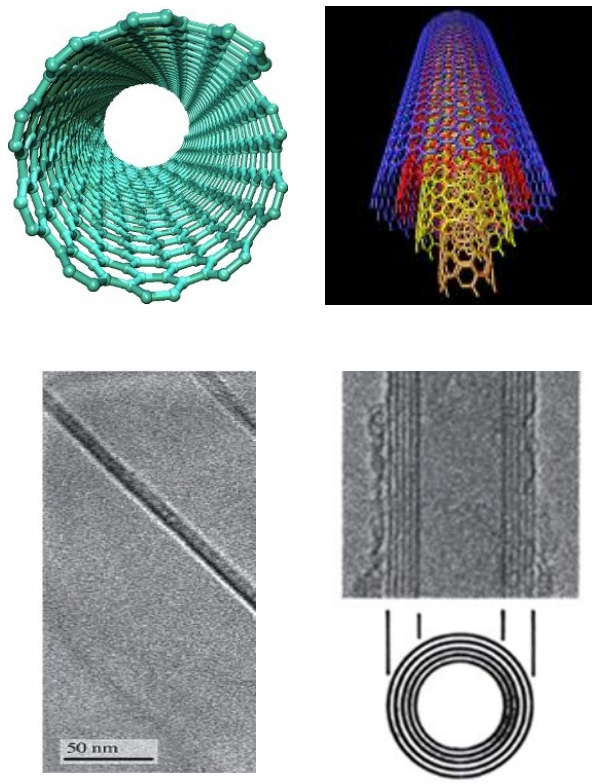

Figure 3.7: TEM and schematics images of SWCNT and MWCNT. (Iijima, 1991)

A carbon nanotube is described by the chiral vector $\overrightarrow{C_h}$, often known as the roll-up vector, where:

$$\overrightarrow{C_h} = n\overrightarrow{a_1} + m\overrightarrow{a_2};$$

The integers (n, m) are the number of steps along the ziz-zag carbon bonds of the hexagonal lattice and $\overrightarrow{a_1}$ and $\overrightarrow{a_2}$ are unit vectors, shown in Figure 3.8. The chiral angle (θ) determines the amount of "twist" in the tube where it can be 0° and 30°;

giving rise to a ziz-zag (0°) and armchair (30°) geometries. The ziz-zag nanotube is (*n,* 0) and the armchair nanotube is (*n, m*). In MWCNTs, each individual tube can have different chirality.

The chirality and diameter of the carbon nanotube influence its electronic properties. CNTs can be either metallic or semiconducting by merely changing the tube's diameter. Furthermore, the energy caps for the semiconducting tubes decrease as the tube's diameter increases. All armchair nanotubes are metallic and zig-zag

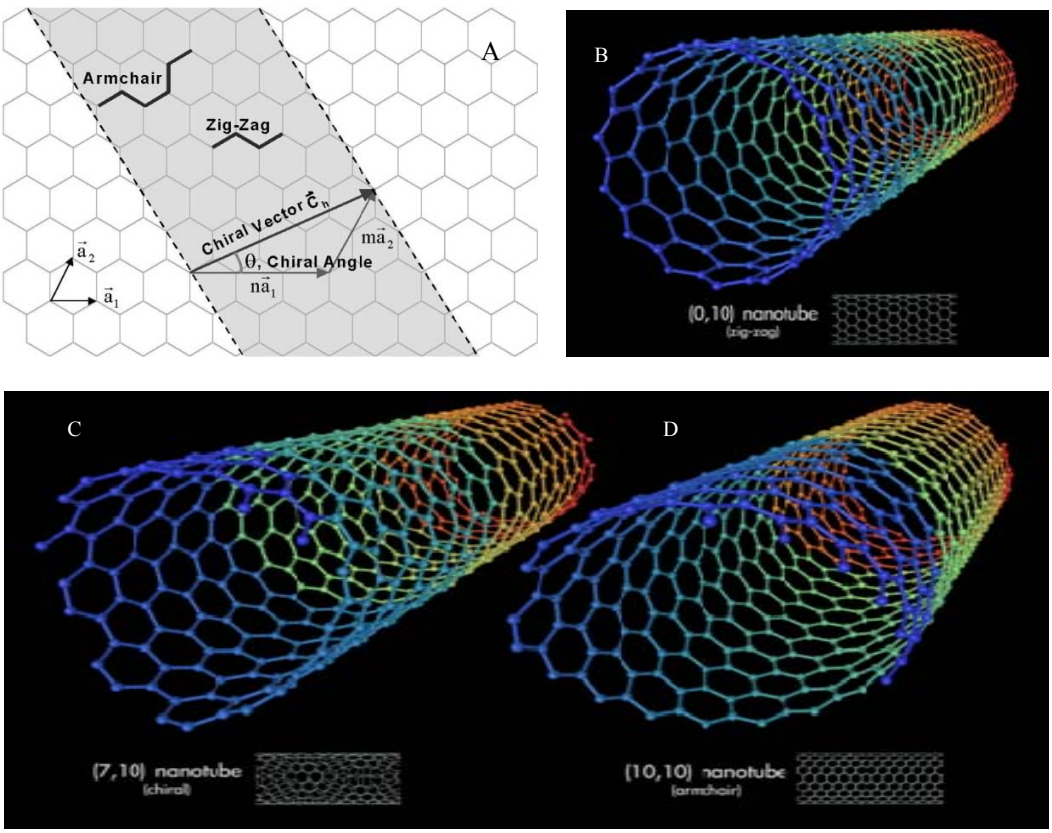

Figure 3.8: Schematic of the honeycomb structure of a graphene sheet (A). SWCNTs can be formed by folding the sheet along the shown lattice vectors leading to armchair (B), zigzag (C), and chiral (D) tubes, respectively. http://en.wikipedia.org/wiki/File:Types_of_Carbon_Nanotubes.png

nanotubes are metallic when *n* is a multiple of three (Satio *et al.*, 1992) (cf. figure 3.9). The C-C bonding in CNTs is composed entirely of sp^2 bonds, similar to those of graphite. This bonding structure, which is stronger than the sp^3 bonds found in diamonds, provides the nanotubes with their unique strength. Concentric sheets of MWCNTs are held together by Van Dar Waals bonds (Thostenson *et al.*, 2001). Under high pressure, nanotubes can merge together, trading some sp^2 bonds for sp^3 bonds, giving the possibility of producing strong, unlimited-length wires.

3.3.2 SYNTHESIS

CNTs exhibit exceptional mechanical, electronic and magnetic properties. In order to exploit these properties, it is necessary to optimize their quality and yield. Real-world applications of nanotubes require the production of large quantities in simple, efficient and cost-effective manner. There have been many remarkable and successful attempts to produce CNTs by various methods; however the three most commonly used techniques are: arc discharge, Laser ablation and chemical vapor deposition (CVD).

CNTs, in the form of MWCNTs, were first produced 1991 by Iijima using the *arc-discharge evaporation* method (cf. figure 3.10). Using this method, Iijima and Ichihashi have synthesized SWCNTs in the gas phase in 1993. Simultaneously, Bethune *et al.* enhanced the production SWCNTs by cobalt catalysis (Bethune *et al.*, 1998). Lambert *at al.* significantly enhanced the synthesis of SWCNTs through the use of binary metal mixtures i.e. Co and Pt (Lambert *at al.*, 1994).

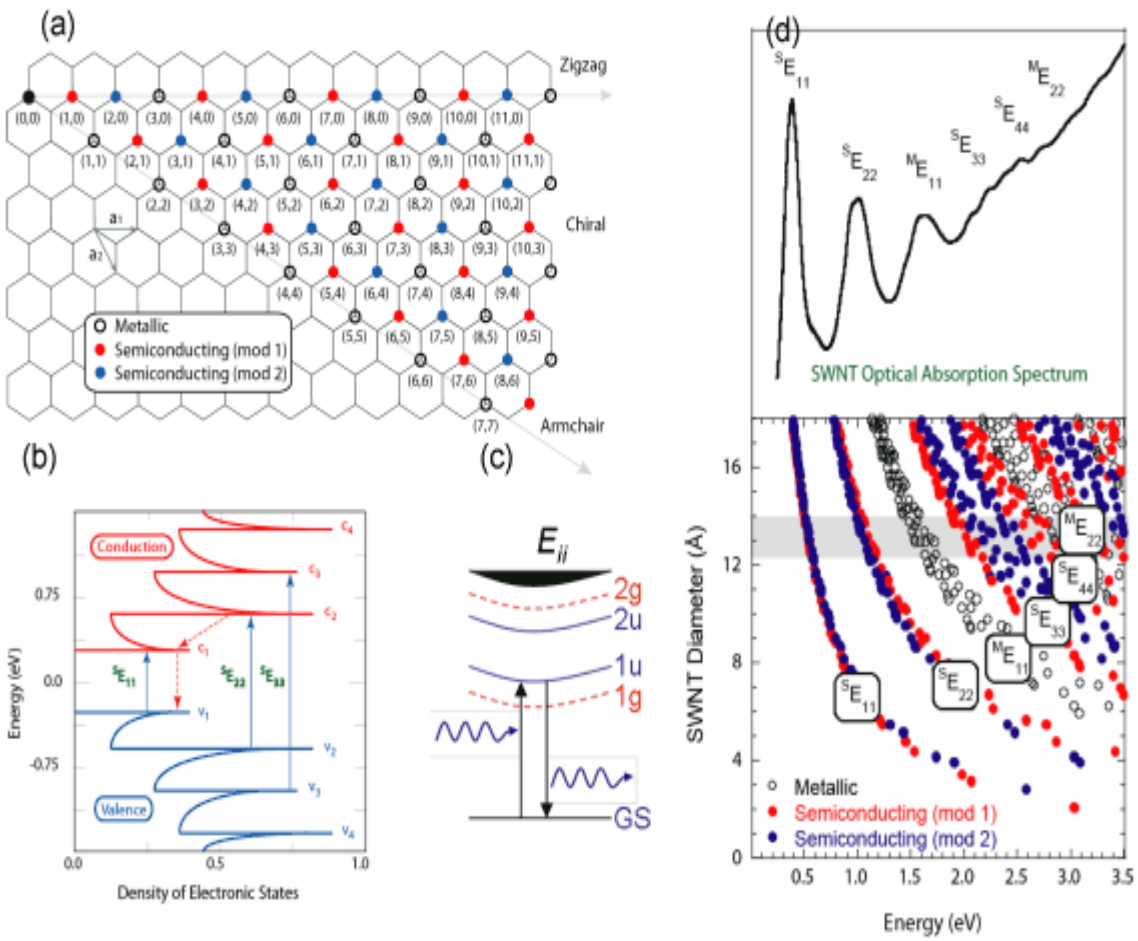

Figure 3.9: (a) Chirality chart depicting the multitude of (n, m) SWCNT structures possible based on the role-up vectors. (b) (top) optical absorption spectrum for SWCNTs and (bottom) "Kataura Plot" of the electronic transitions for SWCNTs. The spectrum is a convolution of the diameter distribution for the sample (shown by the gray box). (c) Depiction of the electronic density of states for a semiconducting nanotube based upon a free-electron model which shows the "spikes" due to 1-dimensional quantum confinement. (d) Schematic of the excitonic model for SWCNT absorption and fluorescence processes whereby odd (u) states are 1-photon active and even (g) states are 1-photon inactive. http://www.sustainability.rit.edu/nanopower/rcn.html

This method creates CNTs through arc-vaporization of two carbon rods placed opposite to each other, separated by approximately 1 mm, in an inert gas-filled

chamber at low pressure. Recent investigations have shown that it is also possible to create CNTs with the arc method in liquid nitrogen (Jung *et al.*, 2003). A direct current of 50 to 100A, driven by a potential difference of approximately 20 V, creates a high temperature discharge between the two electrodes.

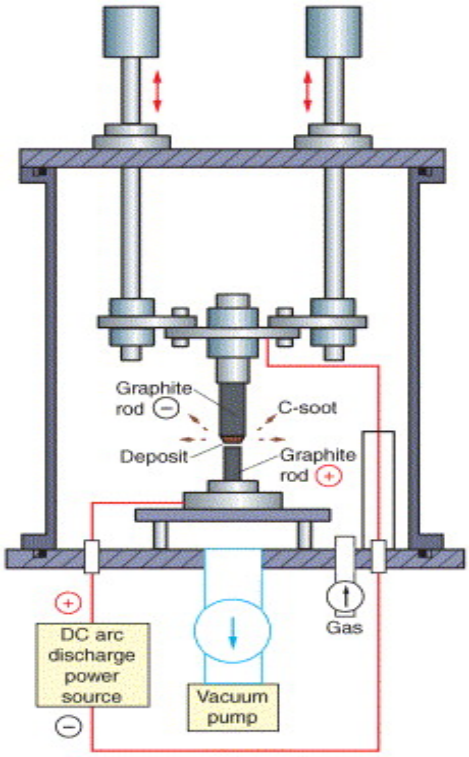

Figure 3.10: Schematic diagram of an arc-discharge apparatus. http://wwwrz.meijo-u.ac.jp/labo/ando/ando-j/1j-image2.gif

The discharge vaporizes small part of the anode graphite rod and deposited on the cathode graphite rod, which includes CNTs (Iijima, 1991). Producing CNTs in high yield depends on the uniformity of the plasma arc, and the temperature of the deposit forming on the graphite rod. Generally, it is hard to grow aligned CNTs (SWNTs, DWNTs, or MWNTs) by arc discharge, although partial alignment of SWNTs can be

achieved by convection or directed arc plasma. On the other hand, the growth temperature of the arc-discharge method is higher than that of other CNT production methods. As a result, the crystallinity and perfection of arc-produced CNTs are generally high, and the yield per unit time is also higher than other methods (Ando, 2004).

In 1995, Guo *et al.* presented a new method for synthesizing SWNTs in which a mixture of carbon and transition metals are vaporized by *laser ablation*. The following year, Thess *et al.* produced SWNTs in yields of more than 70 % by condensation of a laser-vaporized carbon-nickel-cobalt mixture at 1200°C. The formed nanotubes bundled together into crystalline ropes of metallic character (cf. figure 3.11). In this method, samples were prepared by laser vaporization of graphite rods with a 50:50 catalyst mixture of Cobalt and Nickel at 1200°C in flowing argon,

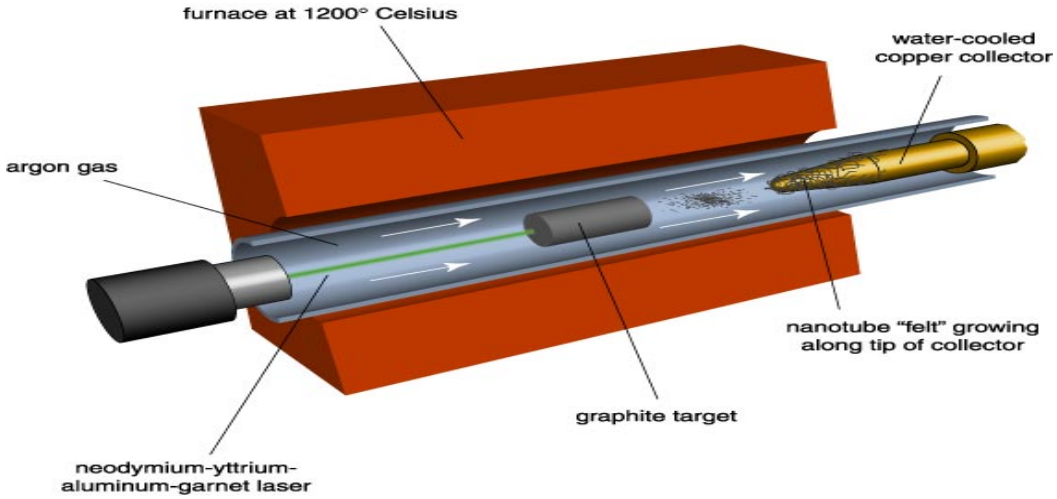

Figure 3.11: Schematic diagram of Laser ablation apparatus reproduced from B. I. Yakobson and R.E. Smalley, American Scientist 85, 324 (1997)

followed by heat treatment in a vacuum at 1000°C to remove the C60 and other fullerenes. The initial laser vaporization pulse was followed by a second pulse, to vaporize the target more uniformly.

The use of two successive laser pulses minimizes the amount of carbon deposited as soot. The second laser pulse breaks up the larger particles ablated by the first one, and feeds them into the growing nanotube structure. By varying the growth temperature, the catalyst composition, and other process parameters, the average nanotube diameter and size distribution can be varied. In contrast to the arc method, direct vaporization allows far greater control over growth conditions, permits continuous operation, and produces nanotubes in higher yield and of better quality (Guo, 1995).

CVD has been used for producing carbon filaments and fibers since 1959 (Ando, 2004). Using CVD, Endo *et al.* grew CNT from pyrolysis of benzene at 1100°C (Endo, M. *et al.*, 1993), while José-Yacamán *et al.* synthesized MWNTs using catalytic decomposition of acetylene over iron particles at 700 °C (José-Yacamán *et al.,* 1993). Later, MWNTs were also grown from ethylene, methane and many other hydrocarbons. Dai *et al.* isolated SWNT grown by disproportionation of carbon monoxide at 1200°C catalyzed by molybdenum particles (Dai *et al.*, 1996). Later, SWNTs were also produced from hydrocarbons using various catalysts (Cheng *et al.*, (1998).

Figure 3.12 shows a diagram of the setup used for CNT growth by CVD in its simplest form. The process involves passing a hydrocarbon vapor (typically for 15-60

minutes) through a tube furnace in which a catalyst material is present at sufficiently high temperature (600-1200°C) to decompose the hydrocarbon. CNTs grow over the catalyst and are collected upon cooling the system to room temperature (Jung *et al.*, 2003). The type of CNTs produced depends on the metal catalyst used during the gas phase delivery and the temperature. In the CVD process SWNTs are found to be produced at higher temperatures with a well-dispersed and supported metal catalyst while MWNTs are formed at lower temperatures and even with the absence of a metal catalyst. Table 3.4 displays a summary of the major production methods, their efficiency and limitations (Daenen *et al.*, 2003).

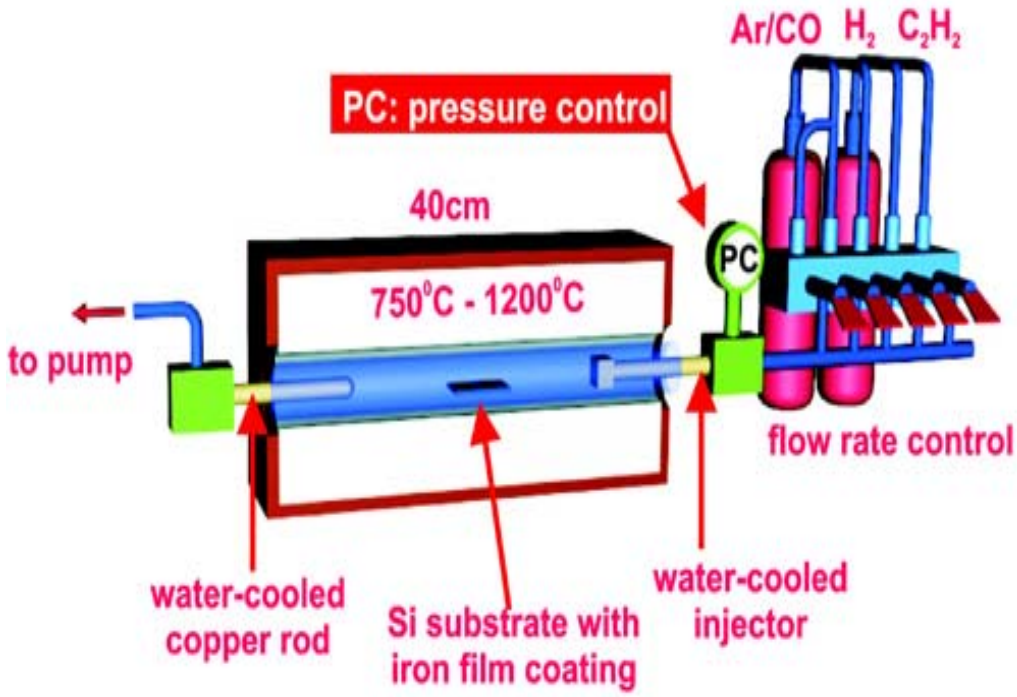

Figure 3.12: A diagram showing the thermal CVD setup used for CNT growth. http://www.fy.chalmers.se/atom/research/nanotubes/images/thermal.jpg

Table 3.4: A summary of the major production methods and their efficiency (Daenen et al., 2003).

Method	Arc discharge method	Chemical vapor deposition	Laser ablation (vaporization)
Who	Ebbesen and Ajayan, NEC, Japan 1992	Endo, Shinshu University, Nagano, Japan	Guo et al. 1995
How	Connect two graphite rods to a power supply, place them a few millimeters apart, and throw the switch. At 100 amps, carbon vaporizes and forms a hot plasma	Place substrate in oven, heat to 600 ^{o}C, and slowly add a carbon-bearing gas such as methane. As gas decomposes it frees up carbon atoms, which recombine in the form of NTs	Blast graphite with intense laser pulses; use the laser pulses rather than electricity to generate carbon gas from which the NTs form; try various conditions until hit on one that produces prodigious amounts of SWNTs
Typical yield	30 to 90%	20 to 100 %	Up to 70%
SWNT	Short tubes with diameters of 0.6 - 1.4 nm	Long tubes with diameters ranging from 0.6-4 nm	Long bundles of tubes (5-20 microns), with individual diameter from 1-2 nm.
MWNT	Short tubes with inner diameter of 1-3 nm and outer diameter of approximately nm	Long tubes with diameter ranging from 10-240 nm	Not very much interest in this technique, as it is too expensive, but MWNT synthesis is possible.
Pro	Can easily produce SWNT, MWNTs. SWNTs have few structural defects; MWNTs without catalyst, not too expensive, open air synthesis possible	Easiest to scale up to industrial production; long length, simple process, SWNT diameter controllable, quite pure	Primarily SWNTs, with good diameter control and few defects. The reaction product is quite pure.
Con	Tubes tend to be short with random sizes and directions; often needs a lot of purification	NTs are usually MWNTs and often riddled with defects	Costly technique, because it requires expensive lasers and high power requirement, but is improving

3.3.3 PROPERTIES

CNTs have attracted the interest of many scientists worldwide. Their nanosize, strength and the remarkable physical properties make them a very exceptional material with a whole range of potential applications. After the successful production of large quantities of CNTs, scientists are experimentally exploring the different properties of CNTs based on previous theoretical, mathematical calculations and new findings. Here, I will touch on some of the proven electrical, mechanical, optical, thermal and chemical merits of CNTs.

Electrical conductivity

As previously mentioned, CNTs can either be metallic, or semiconducting depending on their chirality and diameter (Robertson *et al.*, 1992). The differences in the molecular structure of the tubes dictate conduction properties resulting in different band structures and thus different band gaps. CNTs behave as nanowires, with a density of states (DOS) and an energy gap proportional to the inverse diameter of the tube (Issi**,** *et al.*, 1995) in despite of the tubule chirality (Dresselhaus, 1995). The resistance to conduction is determined by quantum mechanical aspects and was proved to be independent of the nanotube length. A bundle of nanotubes 1 cm^2 in cross section could conduct about one billion Amps. Such high currents would vaporize copper or gold (Collins, 1996).

Optical Activity

Optical spectroscopy studies conducted by Krauss *et al.* suggest that CNTs fluorescence does not show any intensity or spectral fluctuations at 300 K. The lack of intensity blinking or bleaching demonstrates that carbon nanotubes have the potential to provide a stable, single-molecule infrared photon source, allowing for the exciting possibility of applications in quantum optics and biophotonics (Krauss *et al.*, 2005).

Mechanical Strength

The mechanical properties of CNTs can be predicted with some confidence from the known properties of graphene, since the C-C bond in a graphene layer is probably the strongest chemical bond known in nature (Ruoff, 1995). Consequently, CNTs are expected to have high stiffness and axial strength. Treacy *et al.* estimated the Young's modulus of isolated nanotubes to be exceptionally high in the terapascal (TPa) range where the Young's modulus of a material is a measure of its elastic strength. Moreover, Yu *et al.* have experimentally confirmed this value to be 1.4 TPa. Walters *et al.* indicated that CNTs will have a yield strength exceeding 45±7 GPa. Despite their high Young's moduli and yield strengths, Flavo *et al.* showed their extraordinarily flexibility under large strains, and resilience to failure under repeated bending.

Small-diameter SWNTs can be elongated by ≈ 30 % before breaking. Tensile strength experiments performed on MWNTs showed that they break at the outermost layer, with the inner layers being pulled out like a sword from its sheath, and somewhat smaller values for the tensile strength were found for MWNTs (Yu *et al.*, 2000). From these experiments, it was concluded that MWNTs, although difficult to stretch axially, are easy to bend laterally and they could reversibly withstand large lateral distortions (Marinković, 2008). Recently, Suhr *et al.* showed that MWNTs displayed no fatigue failure even at high strain amplitudes up to half a million cycles.

Thermal Conductivity

Until the discovery of CNTs, diamond has been considered to have the highest measured thermal conductivity of any material (Ruoff, 1995). Berber *et al.* have reported the thermal conductivity for an isolated nanotube to be 6600 W/m·K at room temperature; whereas the reported thermal conductivity of a nearly isotopically pure diamond is 3320 W/m·K. The carbon nanotube's thermal conductivity is very high along its axis because vibrations of the carbon atoms propagate easily down the tube. In the direction transverse to its axis, however, the nanotube is much less rigid and the thermal conductivity in that direction is about a factor of 100 smaller.

Chemical Reactivity

The lack of solubility and the difficult manipulation in any solvents have imposed great limitations to the use of CNT. As-produced CNT are insoluble in all organic

solvents and aqueous solutions. However, they have shown great chemical stability. It has also been demonstrated that CNT can interact with different classes of compounds. In addition, CNT can undergo chemical reactions that make them more soluble for their integration into inorganic, organic, and biological systems. Tasis *et al.* have reviewed the chemistry of CNTs the main approaches for the modification of these structures where they can be grouped into three categories: (a) the covalent attachment of chemical groups through reactions onto the π-conjugated skeleton of CNT; (b) the noncovalent adsorption or wrapping of various functional molecules; and (c) the endohedral filling of their inner empty cavity (Stetter, 2004). A summary of the properties of Carbon Nanotubes is presented in Table 3.5 (Tasis, 2006).

3.3.4 APPLICATIONS

The nanosized dimensions, strength and the extraordinary physical properties of these structures make them a very exceptional material with a wide range of potential applications. Since the discovery of CNTs, practical applications have been reported such as chemical sensors, field emission devices (displays, scanning and electron probes/microscopes), catalyst support, electronic devices, high sensitivity nanobalance for nanoscopic particles, nanotweezers, reinforcements in high performance composites, and as nanoprobes in meteorology and biomedical and chemical investigations, medicine/biology (fluorescent markers for cancer treatment, biological labels, drug delivery carriers), anode for lithium ion in batteries, nanoelectronics devices, supercapacitors and hydrogen storage. These are just a few

possibilities that are currently being explored. As research continues, new applications will also develop (Paradise, 2007).

Table 3.5: Summary of CNTs properties (Tasis, 2006).

Mechanical	*Strength, Toughness, Flexibility and Surface/Volume*	
Composites have a CNT Young's Modulus 1 TPa, 5 times that of steel, and tensile strength 45 GPa, 20 times that of steel, a density of 1.4 g/cm^3 (Al: 2.7 g/cm^3); and a strength/weight ratio 500 times greater than Al, steel and Ti and an order of magnitude greater than graphite/epoxy. CNTs have linear elasticity of up to 5-10%. Concentric MWNTs can expand like a telescope. The largest possible surface to volume ratio.		
Electrical	*Conductivity*	High electric conductivity
Suitable for microelectronic, can be semiconducting or metallic CNTs with high current-carrying-capacity stable at J ≈ 10^9 A/cm^2 (1000 times greater than Cu); suitable for field emission tips. Can oscillate tips electrostatically.		
Optical	*Absorption, reflectivity*	High bandwidth
Smallest of fibres and filters or waveguides appear possible; light affects conductivity, field emission tip generates x-ray, IR detection/emission possible.		
Thermal	*Insulators, conductors*	High temperature Stability
Higher Stability than graphite and amorphous carbon. Theory thermal conduction is 6000 W/m K (Cu is 400) to 3 kW/mK, which is greater than that of diamond (2 kW/mK).		
Chemical	*Bonding, reactivity*	High chemical stability
Chemical and biological reactivity can be obtained by functionalization; CNTs possess stability in solvent, acids and bases.		

3.4 STUDIES ON METAL REMOVAL USING CNTS

Since their discovery in 1991, CNTs have been the focus of scientists worldwide owing to their nanosize, large surface area, high mechanical strength and remarkable electrical conductivities which make them superior candidates for a wide range of promising applications. Among the different applications, CNTs have proved to possess great potential applications in environmental protection. Their hollow and layered nanosized structures made them a promising adsorbent material substituted for activated carbon in many ways.

3.4.1 ADSORPTION EFFICIENCY OF CNTS

The adsorption efficiency of CNTs has been investigated by many scientists. The adsorption of heavy metals by nanotubes was studied by many authors for instance Li *et al.* found that CNTs show exceptional adsorption capability and high adsorption efficiency for lead removal from water (Li, *et al.*, 2002). Also it was Li *et al.* who reported that CNTs have much higher fluoride, cadmium (II) and chromium (II) adsorption capabilities than that of AC (Li, *et al.*, 2003). The high adsorption capacity of CNTs to zinc (II) was confirmed by Lu and Chiu (Lu *et al.*, 2006). Kandah and Meunier have evaluated nickel ions removal by CNTs from water (Kandah *et al.*, 2007). The comparison of CNTs with other adsorbents suggests that CNTs have great potential applications in environmental protection particularly in trace metals removal from water.

Furthermore, other researchers have examined CNTs' adsorption capacities to different organic pollutants. Lu and Su concluded that CNTs have a better adsorption performance to natural organic matter compared to granular activated carbon (GAC) (Lu and Su, 2007). Ye *et al.* showed that the adsorption of middle molecular weight toxins by CNTs is 5.5 and 10.8 times of that of macroporous resin and activated carbon, respectively (Ye *et al.*, 2007). More specifically, Long and Yang reported that significantly higher dioxin removal efficiency is found with CNTs than with activated carbon (AC) (Long and Yang, 2001). Peng et al. demonstrated that that it takes only 40 min for CNTs to attain equilibrium for the adsorption of 1,2-dichlorobenzene compared to 20 hours for AC (Peng *et al.*, 2005). Lu *et al.* compared the adsorption of trihalomethanes (THMs) by CNTs and powdered AC and it was evident that it took less time for CNTs to reach equilibrium (Lu *et al.*, 2005). Chin *et al.* have reported that the as-grown SWCNTs have a greater adsorption capacity for o-xylene and p-xylene than the activated carbons when the adsorption capacity is calculated based on surface area (Chin *et al.*, 2007).

3.4.2 FACTORS AFFECTING THE EFFICIENCY OF CNTS ADSORPTION

Although CNTs are efficient adsorbents for the removal of many inorganic and organic pollutants, their adsorption efficiency is influenced by many factors such as the synthesis, purification and modification processes, pH, CNT dosage, contact time and mixing rate. The following subsections are glimpses of the literature documented on the factors influencing the efficiency of CNTs adsorption.

Effect of synthesis, purification and modification processes

The synthesis technique used to produce CNTs dictates the morphologies of the formed CNTs. Consequently, morphologically different CNTs exhibit different adsorption capacities. Li *et al.* have ascertained that the method of producing CNTs influences the adsorption capacity, where they produced four different kinds of CNTs and treated them similarly with nitric acid. The four kinds behaved differently toward the removal of Pb^{+2} from water. Characterization of the four kinds of CNTs showed that each possesses different porosity, specific surface area, particle size and amount of functional groups on the surface. Primarily the kind with more functional groups and secondarily larger surface area was more efficient (Li *et al.*, 2006).

Furthermore, the treatment/purification process of CNTs has been shown to have an impact on the adsorption efficiency of CNTs for metal ions removal. The surface functional groups introduced by the treatment process determine the performance of CNTs. Li *et al.* observed that the adsorption capacity increases remarkably when the CNTs were refluxed with concentrated nitric acid at 140 °C for 1 h (Li *et al.*, 2002). It is known that oxidation of carbon surface can offer not only a more hydrophilic surface structure, but also a larger number of oxygen-containing functional groups, which increase the ion-exchange capability of carbon material (Li *et al.*, 2003). Other researches have reached the same conclusion; explicitly oxidation improves the adsorption capacity of CNTs (Li *et al.*, 2006), (Wang *et al.*, 2007) and (Chen *et al.*, 2007).

It has been shown that supporting CNTs with certain complexes enhances their adsorption capacity. Li *et al.* (2001) confirmed that the adsorption capacity for Al_2O_3 supported on CNTs is about 4 times higher than that of as grown CNTs in the removal of fluoride from water. Peng et al. (2005) attested that CNTs-iron oxide magnetic composites can be used to adsorb contaminants from aqueous effluents and after the adsorption is carried out, the adsorbent can be separated from the medium by a magnetic process. Di *et al.* (2006) noticed that the adsorption capacity for CeO_2 supported on ACNTs (28.3 mg/g) is about 1.5, 2.0 and 1.8 times higher than that of the activated carbon, Al_2O_3 and the ball-milled ACNTs (11.3, 9.3 and 10.2 mg/g), respectively, at equilibrium Cr (VI) concentration of 33.0 mg/l (Di *et al.*, 2006).

Effect of pH

pH is one of the primary factors that influence the site dissociation of CNTs, the hydrolysis, complexation and precipitation of the metal ions. The pH at which the net surface charge is zero is called "*point of zero charge*", pH_{PZC} or IEP. When the pH of the solution is higher than pH_{PZC}, the negative charge on the surface of the CNTs provides electrostatic interactions that are favorable for adsorbing cationic species. The decrease of pH leads to neutralization of surface charge, thus, the adsorption of cations should decrease (cf. Figure 3.13). In other words, as the pH of the solution increases above the pH_{PZC}, the removal efficiency of CNTs towards cationic species increases until equilibrium is reached. At low pH values below the pH_{PZC}, H^+ ions will compete with cationic ions on the surface of the CNTs. Subsequently, pH is an important parameter controlling the metal ion adsorption process.

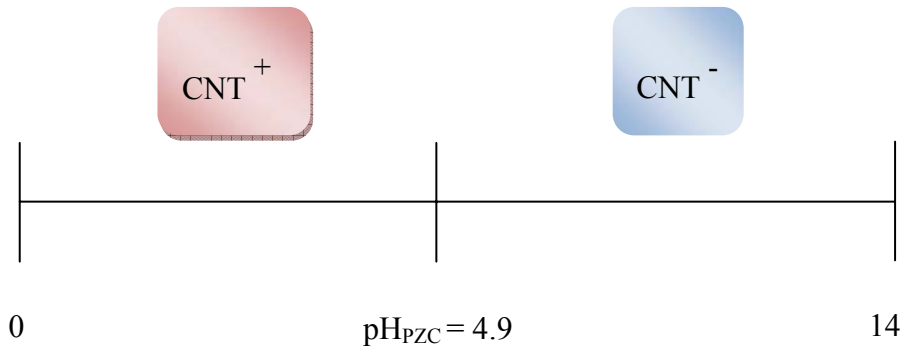

Figure 3.13: Effect of pH on the ionization of CNTs

Li *et al.* found that the removal of Pb^{+2} from water by acid-refluxed CNTs was highly dependent on the pH of the solution, which affects the surface charge of the adsorbent and degree of ionization and speciation of the adsorbates (Li *et al.*, 2002). Stafiej and Pyrzynska observed that the adsorption of cobalt species by CNTs increased with the increase of pH from 3 to 9 (Stafiej and Pyrzynska, 2007). Lu and Chiu have concluded that the adsorption capacity of Zn^{2+} onto CNTs increased with the increase of pH in the pH range of 1–8, fluctuated very little and reached maximum in the pH range of 8–11 and decreased at a pH of 12 (Lu and Chiu, 2006). Among other researchers who have come to the same conclusion.

Effect of Contact Time

Theoretically, as the time increases, the adsorption capacity is expected to increase until equilibrium is reached. The metal binding sites becomes saturated as contact time increases. Wang *et al.* stated that the adsorption of Pb (II) onto acidified MWCNTs increases quickly with contact time at the first 20 min and then reached

equilibrium (Wang *et al.*, 2007). Lu *et al.* demonstrated that the adsorption efficiency for dissolved organic carbon, assimilable organic carbon and trihalomethanes increased steeply with time and then slowly reached equilibrium (Lu *et al.*, 2007).

Effect of CNT Dose

The dosage of CNTs can be associated to the availability of adsorption sites. Based on studies made, the adsorption of metal ions can be enhanced by increasing the adsorbent (CNTs) dosage which provides larger specific surface area and more adsorption sites for binding. Li *et al.* highlighted that the adsorption capacities for Pb^{2+}, Cu^{2+}, and Cd^{2+} increase with increasing of the CNT dosages (Li *et al.*, 2003). The removal ratio for Pb^{2+}, Cu^{2+}, and Cd^{2+} and adsorbents is in general increased with an increase in the amount of adsorbent was confirmed by Hsieh and Horng (Hsieh and Horng, 2007).

Effect of mixing rate

The adsorption capacity increases with the increase of mixing rate. This is because the increase of mixing rate causes the adsorbent to be well dispersed in solution hence increasing the probabilities of adsorbate-adsorbent interaction. Hsieh and Horng have indicated that there is and effect of dispersion on adsorption efficiency (Hsieh and Horng, 2007).

In summary, although the adsorption of some of the heavy metals with CNTs was researched extensively, yet the removal of arsenic (III) and mercury (II) using

MWCNTs and the effect of solution conditions such as pH, dosage of the adsorbent, mixing rate and contact time on the adsorption efficiency is yet to be explored as far as I know.

CHAPTER 4

RESEARCH METHODOLOGY

4.1 MULTI-WALLED CARBON NANOTUBES

Multi-walled carbon nanotubes (MWCNTs) produced and optimized by King Fahd University of Petroleum and Minerals (KFUPM) in Dhahran, Saudi Arabia were used in this study. The MWCNTs were kept dry in a glass bottle at room temperature of 25ºC.

4.2 PREPARATION OF As (III) AND Hg (II) STOCK SOLUTIONS

Certified arsenic (III) and mercury (II) stock solutions (1000 mg/l) were used to prepare the required concentrations to be used in the batch mode adsorption experiments. The solutions were diluted to the required concentrations (i.e. 1 mg/l). The glassware utilized for the experiment was rinsed with 2% nitric acid in order to remove all the impurities that might be present and to prevent further adsorption of the heavy metals to the walls of the glasswares.

The standard solutions were prepared by pipetting 1 ml of As (III) and 0.1 ml of Hg (II) from the stock solutions into a 1-L volumetric flask and mixed thoroughly. The calculations for determining the volume of As (III) and Hg (II) to be taken from the stock solutions are as follows:

$$V_1M_1 = V_2M_2 \quad (1)$$

Where:

V_1 = *Volume of standard solution (L)*

V_2 = *Final desired volume (1L)*

M_1 = *Concentration of the standard solution (1000 mg/L)*

M_2 = *Concentration of the stock solution that we need (1 mg/L)*

After preparing the standard solutions, the pH of the solutions was adjusted using 0.1M HCl and 0.1M NaOH to the required pH i.e. 4, 5, 7, 8 and 9.

4.3 BATCH MODE ADSORPTION EXPERIMENT

Batch mode sorption experiments were performed in glass flasks at room temperature. Weighed amounts of the adsorbent, in this case, the MWCNTs (5 and 10 mg) were added to 125-mL Erlenmeyer flasks containing 50 ml of 1.0 mg/L of As and 0.1 mg/L of Hg. The Erlenmeyer flasks were then mounted on the shaker and shaken at different speeds (50,100,150 and 200 rpm) for 10, 30, 60 and 120 minutes.

After the elapsed time (10, 20, 40, 60 and 120 min) has passed, the suspension was filtered through 0.45µm Millipore filter papers. Afterwards, the filtered solutions were analyzed for As (III) using Hydride Generated Inductively Coupled Plasma-Atomic Emission Spectrometer (HG-ICP-AES) manufactured by Varian, whereas the filtered Hg (II) solutions were analyzed by mercury analyzer system manufactured by P.S. Analytical Ltd., (cf. Figure 4.1). The effects of the dosage of MWCNTs, pH, contact time and the agitation speed were studied.

(a)

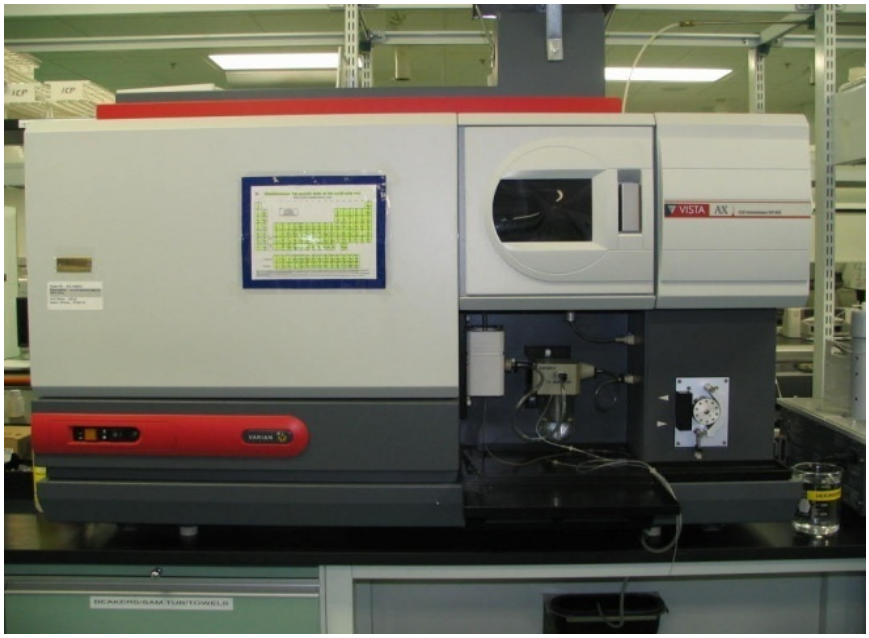

(b)

Figure 4.1: (a) Mercury analyzer system by P.S. Analytical Ltd., England. (b) Inductively Coupled Plasma-Atomic Emission Spectrometer (ICP-AES) by Varian

The amount of As (III) and Hg (II) adsorbed on the MWCNTs was determined by the difference of the initial concentration (C_i) and the equilibrium concentration (C_e). The percentage removed of As (III) and Hg (II) ions from the solution was calculated using the following relationship:

$$\%removal = \frac{C_i - C_e}{C_i} \times 100 \quad (2)$$

The metal adsorption capacity (q_e) was calculated by the following equation:

$$\text{AdsorptionCapacity} q_e \text{ (mg/g)} = \frac{C_i - C_e}{M_s} \times V \quad (3)$$

Where:

V = volume of the solution (L)

M_s = weight of adsorbent (g)

4.4 EXPERIMENTAL DESIGN

Table 4.1 illustrates the experimental parameters and their variations which were used in the batch mode adsorption experiments. The initial concentrations of As (III) and Hg (II) in this study were fixed at 1.0 mg/L and 0.1 mg/L respectively.

Table 4.1: Experiment parameters and their variation

CNTs Dosage (mg)	Agitation Speed (rpm)	pH	Contact Time (min)
5	50	4	10
10	100	5	20
20	150	7	40
40		8	60
		9	120

4.5 ADSORPTION ISOTHERMS MODELS

Adsorption isotherms are mathematical models that describe the distribution of the adsorbate species among liquid and adsorbent, based on a set of assumptions that are mainly related to the heterogeneity/homogeneity of adsorbents, the type of coverage, and possibility of interaction between the adsorbate species. The Langmuir model assumes that there is no interaction between the adsorbate molecules and the adsorption is localized in a monolayer.

The Freundlich isotherm model is an empirical relationship describing the adsorption of solutes from a liquid to a solid surface, and assumes that different sites with several adsorption energies are involved. In order to model the adsorption behavior and calculate the adsorption capacity for the adsorbent, the adsorption isotherms will be studied. The Langmuir adsorption isotherm is perhaps the best known of all isotherms describing adsorption and it is often expressed as:

$$Q_e = \frac{X_m K C_e}{(1 + K C_e)} \quad (4)$$

Where;

> ***Q_e*** *= the adsorption density at the equilibrium solute concentration C_e (mg of adsorbate per g of adsorbent)*
> ***C_e*** *= the equilibrium adsorbate concentration in solution (mg/l)*
> ***X_m*** *= the maximum adsorption capacity corresponding to complete monolayer coverage (mg of solute adsorbed per g of adsorbent)*
> ***K*** *= the Langmuir constant related to energy of adsorption (l of adsorbent per mg of adsorbate)*

The Freundlich isotherm model is an empirical relationship describing the adsorption of solutes from a liquid to a solid surface, and assumes that different sites with several adsorption energies are involved. In order to model the adsorption behavior and calculate the adsorption capacity for the adsorbent, the adsorption isotherms will be studied.

The Langmuir adsorption isotherm is perhaps the best known of all isotherms describing adsorption and it is often expressed as:

$$Q_e = \frac{X_m K C_e}{(1 + K C_e)} \quad (4)$$

Where;

> ***Q_e*** *= the adsorption density at the equilibrium solute concentration C_e (mg of adsorbate per g of adsorbent)*
> ***C_e*** *= the equilibrium adsorbate concentration in solution (mg/l)*
> ***X_m*** *= the maximum adsorption capacity corresponding to complete monolayer coverage (mg of solute adsorbed per g of adsorbent)*
> ***K*** *= the Langmuir constant related to energy of adsorption (l of adsorbent per mg of adsorbate)*

The above equation can be rearranged to the following linear form:

$$\frac{C_e}{Q_e} = \frac{1}{X_m K} + \frac{C_e}{X_m} \tag{5}$$

The linear form can be used for linearization of experimental data by plotting C_e/Q_e against C_e. The Langmuir constants $\mathbf{X_m}$ and **K** can be evaluated from the slope and intercept of linear equation.

In addition, we can describe adsorption with Langmuir if there is a good linear fit. If not then maybe some other model will work. Therefore, we can use Freundlich Isotherm.

$$Q_e = K_F C_e^{1/n} \tag{6}$$

Where;

> ***Q_e*** *is the adsorption density (mg of adsorbate per g of adsorbent)*
> ***C_e*** *is the concentration of adsorbate in solution (mg/l)*
> ***K_f*** *and* ***n*** *are the empirical constants dependent on several environmental factors and* ***n*** *is greater than one.*

This equation is conveniently used in the linear form by taking the logarithm of both sides as:

$$\ln Q_e = \ln K_f + 1/n \ln C_e \tag{7}$$

A plot of ln C_e against ln Q_e yielding a straight line indicates the confirmation of the Freundlich isotherm for adsorption. The constants can be determined from the slope and the intercept.

4.6 KINETIC MODELING

The study of sorption kinetics is applied to describe the adsorbate uptake rate and this rate evidently controls the residence time of adsorbate at solid liquid interface. In order to evaluate the mechanism of sorption of As (III) and Hg (II) by the CNTs, the first-order equation, the pseudo-second-order rate equation and the second-order rate equation are calculated by the below shown equations respectively:

$$\log \frac{q_e - q_t}{q_e} = -\frac{K_L t}{2.303} \tag{8}$$

$$\frac{t}{q_t} = \frac{1}{2K_2 q_e^2} + \frac{t}{q_e} \tag{9}$$

$$\frac{1}{q_e - q_t} = \frac{1}{q_e} + kt \tag{10}$$

Where:

q_e = sorption capacity at equilibrium
q_t = sorption capacity at time (mg/g)
K_L = the Lagergren rate constant of adsorption (1/min)
k = rate constant of the pseudo second-order sorption ($g.mg^{-1}.min^{-1}$)
t = time (min)

The linear plots of log ($q_e - q_t$) versus t; t/q_t versus t and $1/(q_e - q_t)$ versus t of the above equations, q_e, , K_L and k can be determined from the slopes and intercepts.

CHAPTER 5

RESULTS AND DISCUSSION

5.1 CHARACTERIZATION OF CARBON NANOTUBES

High purity multi-walled carbon nanotubes (MWCNTs) were produced by chemical vapor deposition (CVD) technique. The produced MWCNTs were examined under field emission scanning electron microscope (FE-SEM) and transmission electron microscope (TEM). The diameter of the produced MWCNTs varies from 20-40 nm with an average diameter of 24 nm and the length of the CNTs reaches few microns. Figure 5.1 (a) and (b) show low and high magnification SEM images of the produced MWCNTs. From the SEM images, the product is pure and only MWCNTs were observed.

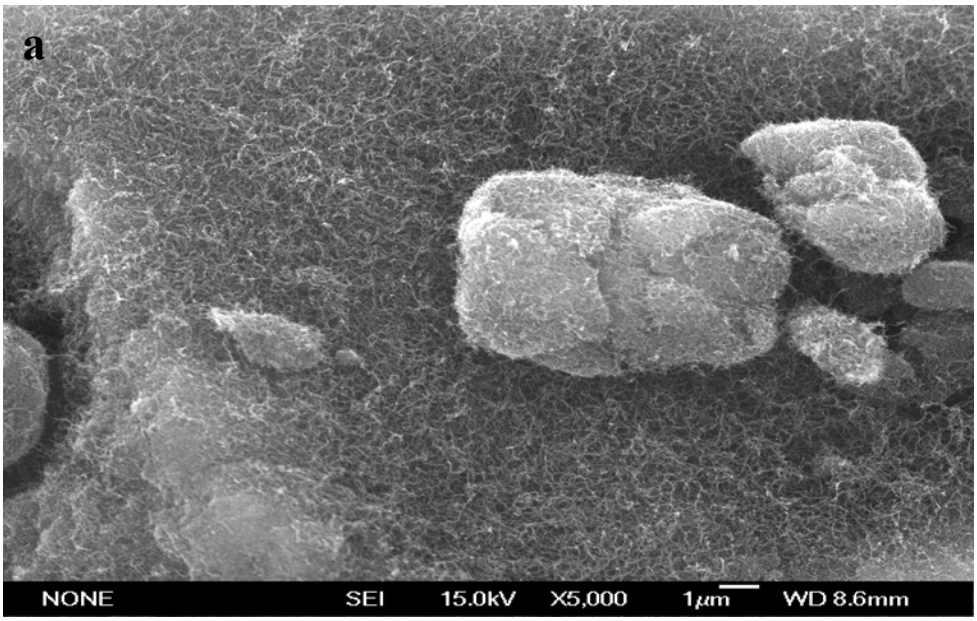

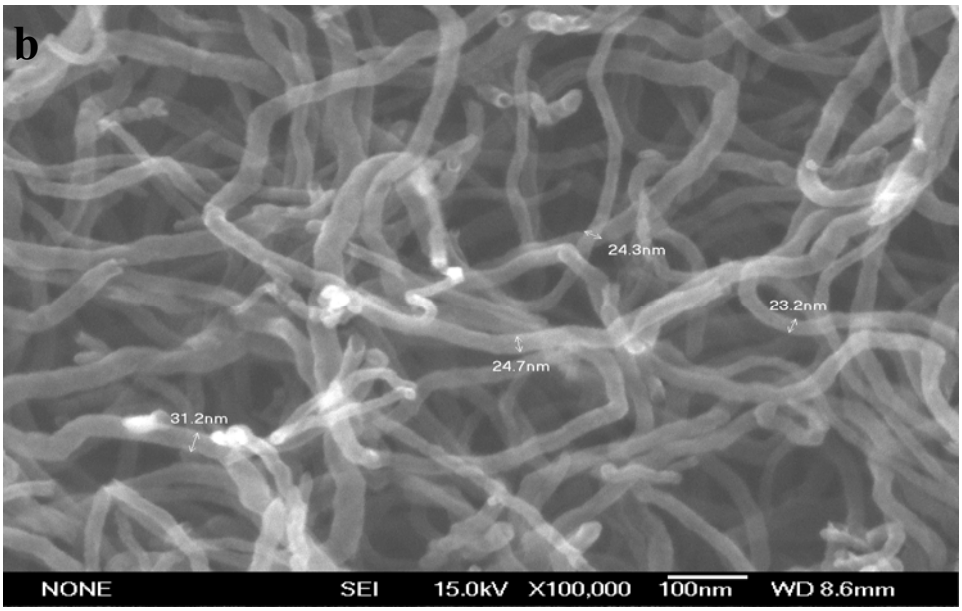

Figure 5.1: SEM Images of MWCNTs at (**a**) at low resolution (**b**) at high resolution.

The structure of the produced nanotubes was characterized by TEM (cf. Figure 5.2 (a)). The TEM samples were prepared by pouring alcohol onto the nanotubes film, then, these films were transferred with a pair of tweezers to a carbon-coated copper grid. It is obvious from the images that all the nanotubes are hollow and tubular in shape. In some of the images, catalyst particles can be seen inside the nanotubes. TEM images indicate that the nanotubes are of high purity, with uniform diameter distribution and contain no structural deformity. Figure 5.2 (b) shows the High Resolution Transmission Electron Microscope (HRTEM) image of the MWCNTs. It shows that a highly ordered crystalline structure of MWCNT is present.

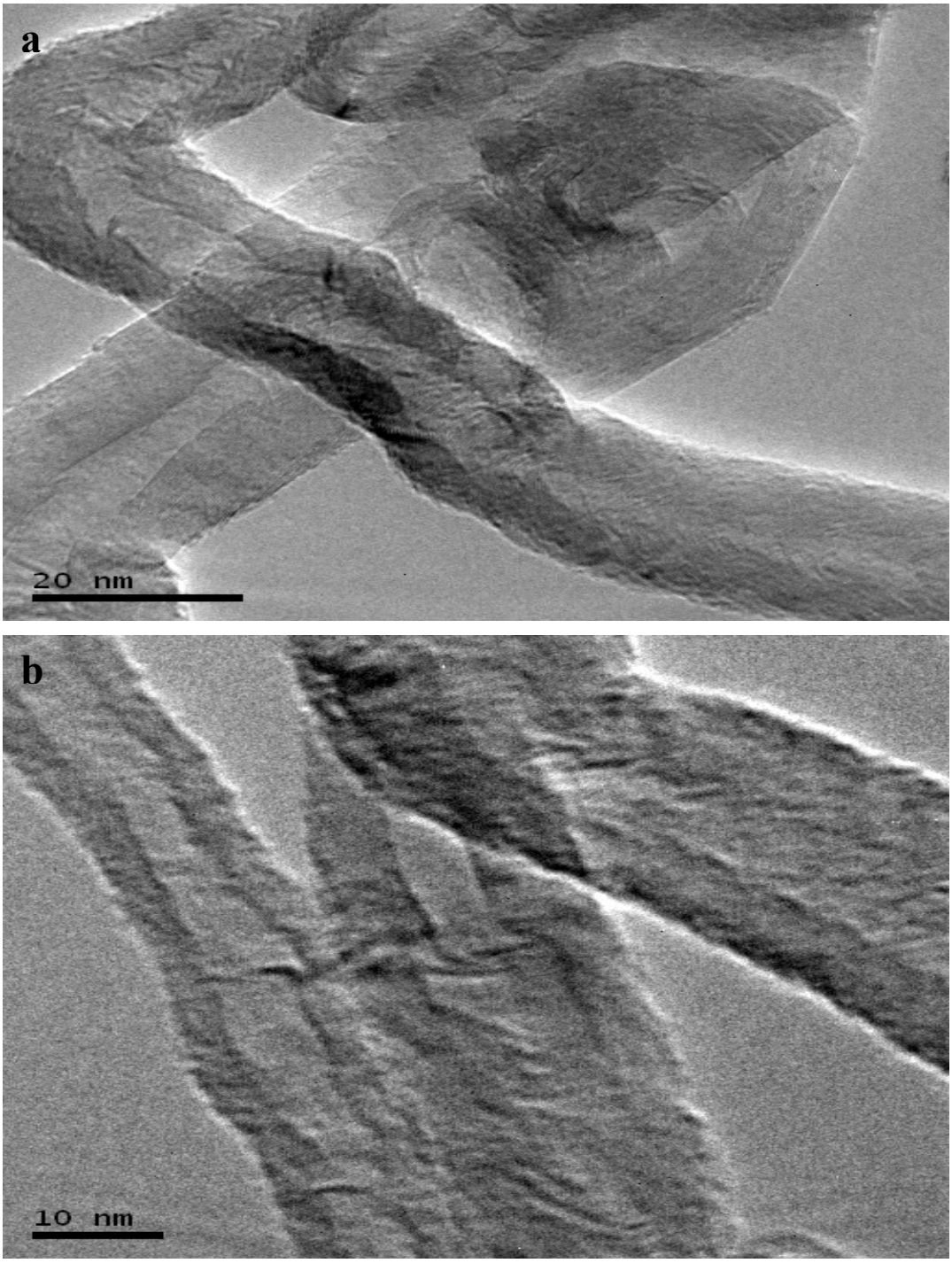

Figure 5.2: TEM Images of MWCNTs (**a**) at low resolution (**b**) at high resolution.

5.2 REMOVAL OF MERCURY (II) AND ARSENIC (III) FROM WATER BY MWCNTs

In this study, the effect of pH, contact time, dosage of the MWCNTs and agitation speed on the uptake of mercury (II) and arsenic (III) were investigated to determine the optimum conditions for the removal of mercury (II) and arsenic (III) from water. The percentage removal of mercury (II) and arsenic (III) was determined to measure the adsorption capacity of CNTs. All experimental data can be seen in Appendix A.

5.2.1 REMOVAL OF MERCURY (II) FROM WATER BY MWCNTS

Effect of pH

The pH of the solution is one of the key parameters controlling adsorption; in which it influences the surface charge of the adsorbent, the degree of ionization and the speciation of the adsorbates (Li *et al.*, 2002) in this case Hg (II). The pH at which the net surface charge of the CNTs is zero is called "point of zero charge", pH_{PZC}. When the pH of the solution is higher than the pH_{PZC}, the negative charge on the surface of the CNTs provides electrostatic interactions that are favorable for adsorbing cationic species. The decrease of pH leads to neutralization of surface charge, thus, the adsorption of cations should decrease. The pH value plays a vital role with respect to the adsorption of Hg (II) ions on The MWCNTs. The removal of Hg (II) by MWCNTs as a function of the pH was studied. The pH of these experiments was varied from 4-9. Precipitation of $Hg(OH)_2$ is expected to occur as

the pH exceeds 8.0. However precipitation was not observed within the pH range evaluated.

Figure 5.3 shows the effect of pH on the adsorption of Hg (II) ion by MWCNTs. The obtained results indicate that the removal of Hg (II) by MWCNTs increases with the pH value from 4.0 to 8.0. The lower adsorption in the acidic region can be attributed in part to the competition between H^+ and Hg^{2+} ions on the same binding sites. Furthermore, as the charge of CNTs surface becomes more negative with the increase of pH, the electrostatic interactions becomes stronger and thus results in higher adsorption of metal species. The functional groups such as hydroxyl (-OH), carboxyl (-COOH) and carbonyl (-C=O) on the CNTs surfaces play an effective role in the gradual increase of the adsorption capacity in the pH range of 5-8.

As the pH increases, the hydroxide ion concentration increases favoring the formation of Hg negative species $Hg(OH)_3^{-1}$ and $Hg(OH)_4^{-2}$ Consequently, the decrease in Hg removal that took place at pH 9.0 can be partially attributed to unavailability of Hg (II) for adsorption. In other words, the free Hg (II) concentration available for adsorption decreases as Hg hydroxides form (Lu and Chiu, 2006). On the Contrary, the obtained data show that at MWCNTs dose of 200 mg/L the adsorption capacity in not affected by pH changes where the MWCNTs dose effect dominate the pH effect. A %100 removal of 0.1 mg/L of Hg (II) was achieved over the whole range of pH values studied i.e. 4-9. It can be observed that, the removal of mercury (II) from water by MWCNTs is pH dependent.

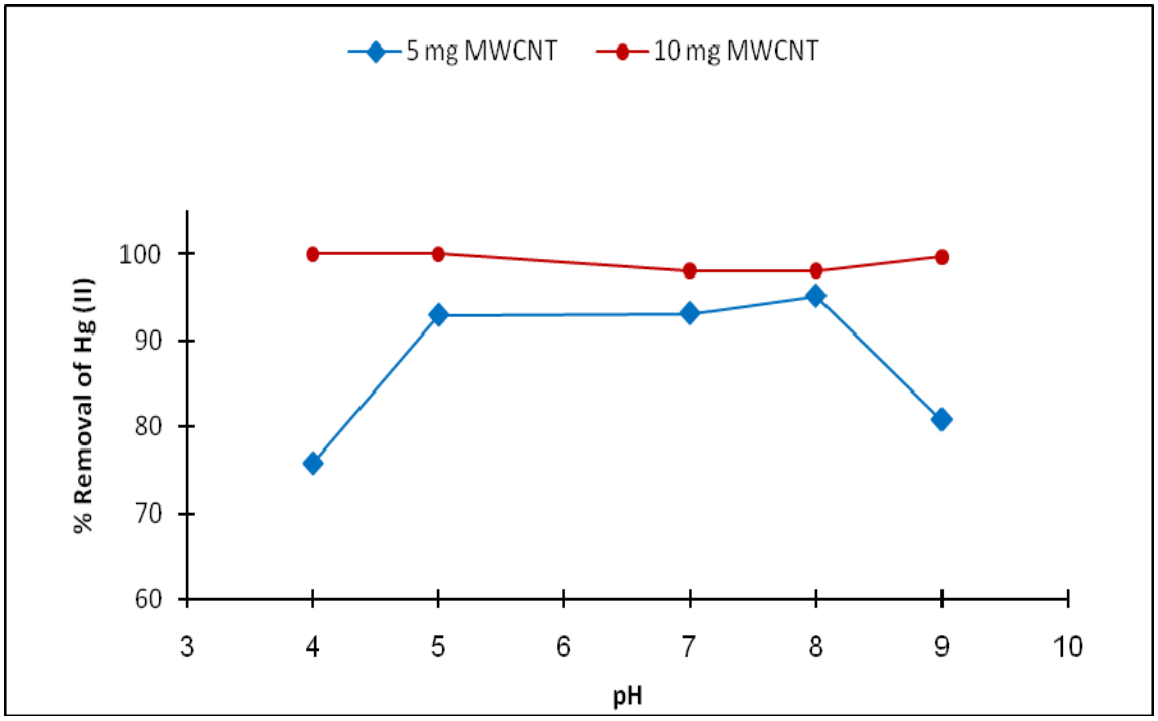

Figure 5.3: The effect of pH on the removal percentage of Hg (II); (C_i = 0.1 mg/L at 150 rpm for 120 min).

The same effect of pH on the adsorption of different heavy metals by CNTs was concluded by Li *et al.*, Stafiej *et al.* and among others on the see for example (Li *et al.*, 2002), (Stafiej and Pyrzynska, 2007) and (Lu and Chiu, 2006).

Effect of contact time

By keeping the dosage of MWCNTs, the mixing rate and the pH of the solution constants, it was observed that Hg (II) adsorption have positive result in terms of time. The amount of Hg (II) adsorbed onto the MWCNTs increased gradually with time until it reached equilibrium. Figure 5.4 shows the effect of contact time on the adsorption of Hg (II) onto MWCNTs. The contact time to reach equilibrium was 120 min. The final capacities for the adsorption of (C_i = 0.1 mg/L) Hg (II) onto MWCNTs reached 0.486 mg/g. The metal binding sites on the surface of the MWCNTs became saturated as contact time increased.

Wang *et al.* stated that the adsorption of Pb (II) onto acidified MWCNTs increases quickly with contact time at the first 20 min and then reached equilibrium (Wang *et al.*, 2007). Lu *et al.* demonstrated that the adsorption efficiency for dissolved organic carbon, assimilable organic carbon and trihalomethanes increased steeply with time and then slowly reached equilibrium (Lu and Su, 2007) and (Lu *et al.*, 2005).

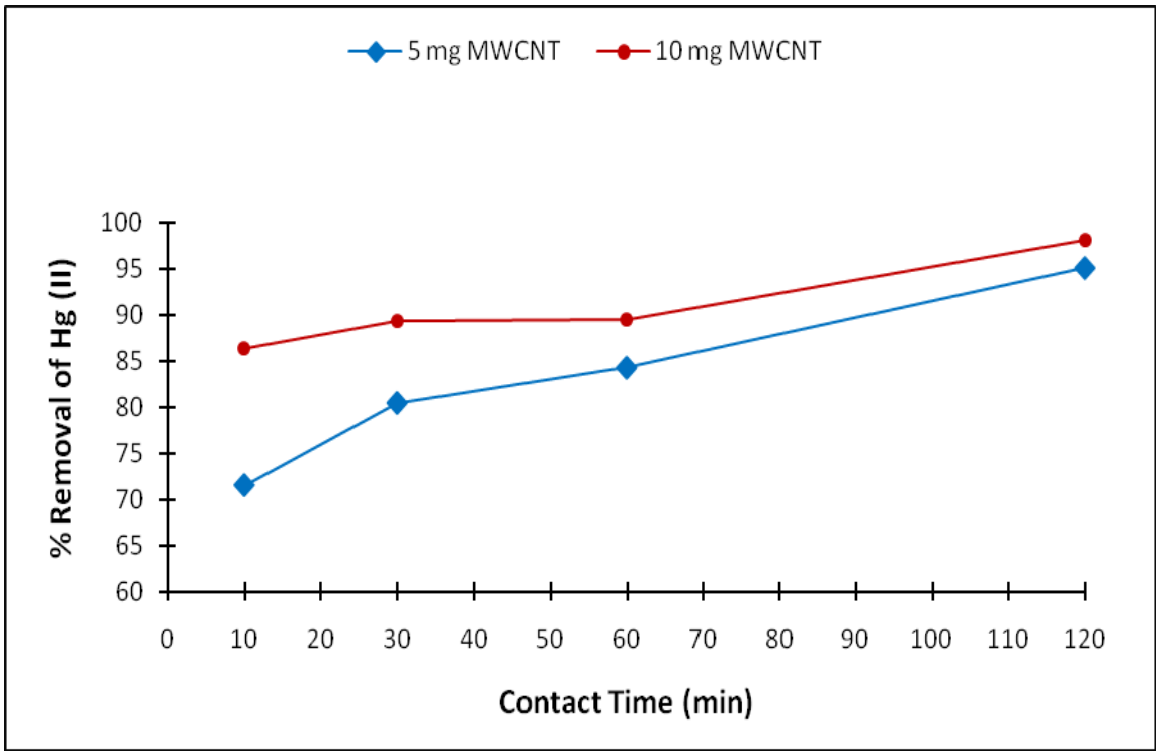

Figure 5.4: The effect of contact time on the adsorption of Hg (II) by MWCNTs (MWCNT dosage = 0.01 g and 0.005 g/50 ml; C_i = 0.1 mg/L; pH = 8; agitation speed = 150 rpm).

Effect of mixing rate

The effect of mixing rate on adsorption capacity of mercury (II) was studied by varying the rate of mixing from 50 to 150 rpm. It was observed that the percentage of mercury removed increased progressively by increasing the rate of mixing as can be seen in Figure 5.5. This can be associated with the fact that the increase of mixing rate improves the dispersion of mercury (II) ions hence increasing adsorbent adsorbate interaction probabilities. Furthermore, mixing will decrease the mass transfer resistance which in turn offers a faster external mass transfer rate of Hg (II) and thus gives more adsorption capacity. Hsieh and Horng have indicated that there is an effect of dispersion on the adsorption efficiency (Hsieh and Horng, 2007).

Effect of MWCNTs Dosage

The batch adsorption experiments were conducted by changing the dosage of MWCNTs 10, 20 and 40 mg. In all experiments, it was obvious that the adsorption of Hg (II) is generally enhanced when the amount of MWCNTs is increased in spite of the pH, agitation speed and contact time as depicted in Figure 5.6. The dosage of MWCNTs can be associated to the availability of adsorption sites consequently adsorption of metal ions can be enhanced by increasing the adsorbent dosage which provides larger surface area and more adsorption sites for binding. Li *et al.* highlighted that the adsorption capacities for Pb^{2+}, Cu^{2+}, and Cd^{2+} increase with increasing of the CNT dosages (Li *et al.*, 2003). The same effect was confirmed by Hsieh and Horng (Hsieh and Horng, 2007).

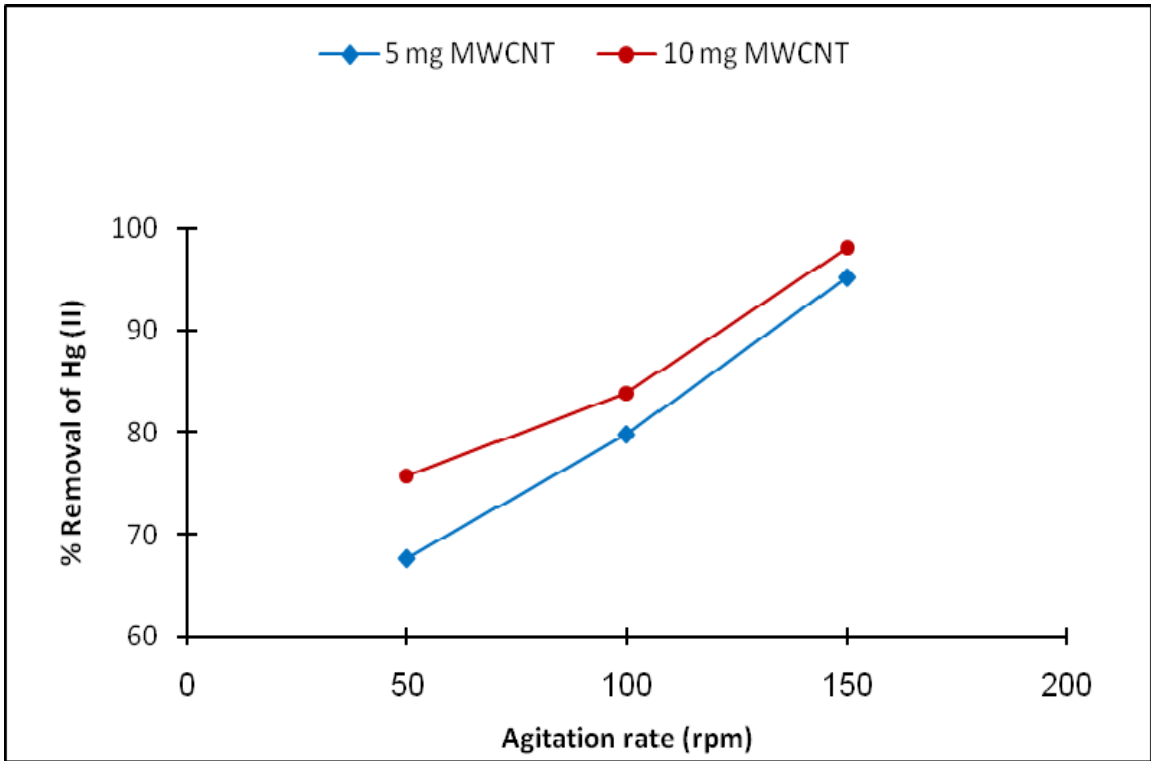

Figure 5.5: The effect of mixing rate on the adsorption of Hg (II) by MWCNTs (MWCNTs dosage = 0.01 g/50 ml; Hg^{2+} conc. = 0.1 mg/L; pH = 8; agitation speed = 150 rpm).

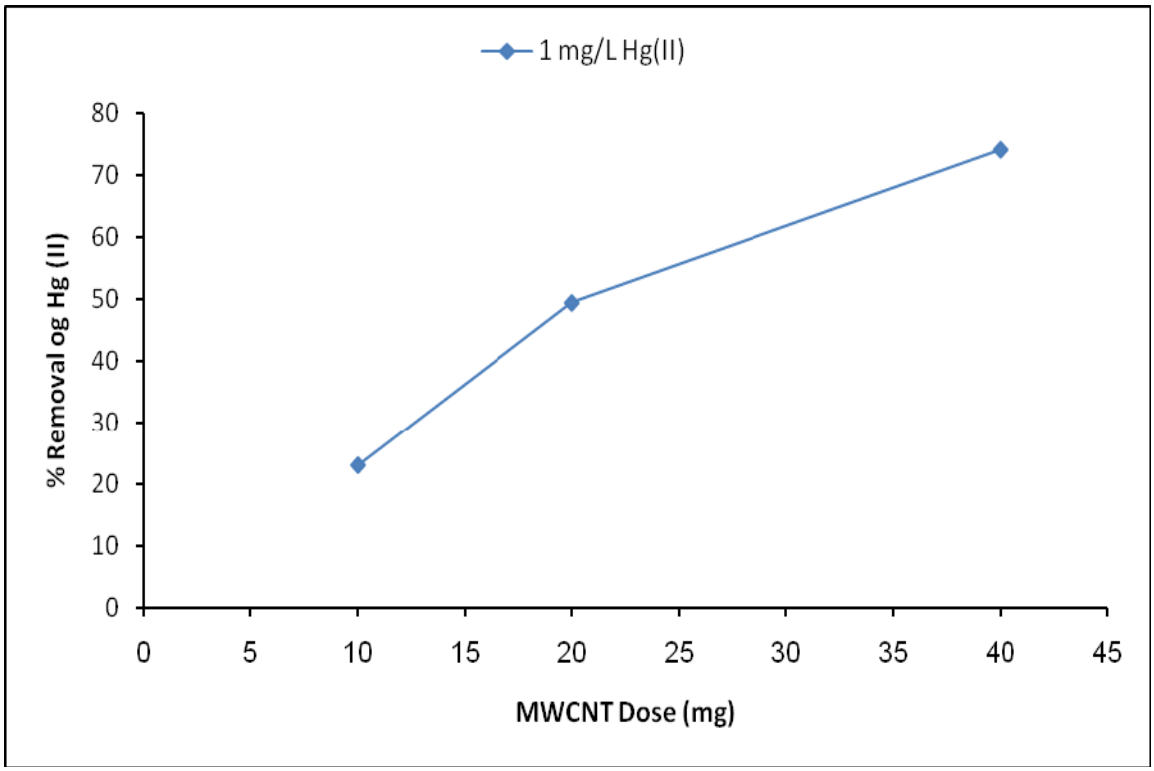

Figure 5.6: The effect of MWCNTs dose on the adsorption of Hg (II) (MWCNTs dosage = 0.01-0.04g/50 ml; Hg^{2+} conc. = 1 mg/L; agitation speed = 150 rpm for 120 min).

5.2.1 REMOVAL OF ARSENIC (III) FROM WATER BY MWCNTS

Effect of pH

The uptake of As (III) by MWCNTs at various pH values (4-9) for an arsenic concentration of 1.0 mg/L was studied to determine the optimum pH. The pH had no effect on the adsorption of As (III) by MWCNTs as shown in Figure 5.7. It is evident from the results acquired that there was no adsorption of As (III) onto the MWCNTs. This behavior of arsenite in the pH range evaluated is not totally clear but may be attributed to the fact that As (III) exists predominantly as the neutral H_3AsO_3 within this pH range (Sharma and Sohn, 2009). The lack of electrostatic interactions between As (III) ions and the as grown MWCNTs might have resulted in no adsorption.

Effect of Contact Time

The adsorption efficiency of As (III) by MWCNTs as a function of the contact time was evaluated by varying the contact time from 10 min to 2 h at an As (III) concentration of 1 mg/L, a dose of MWCNTs of 200 mg/L and at a pH of 8. The data obtained as shown in Figure 5.8 that the adsorption capacity of As (III) by MWCNTs is not affected by the variation of contact time.

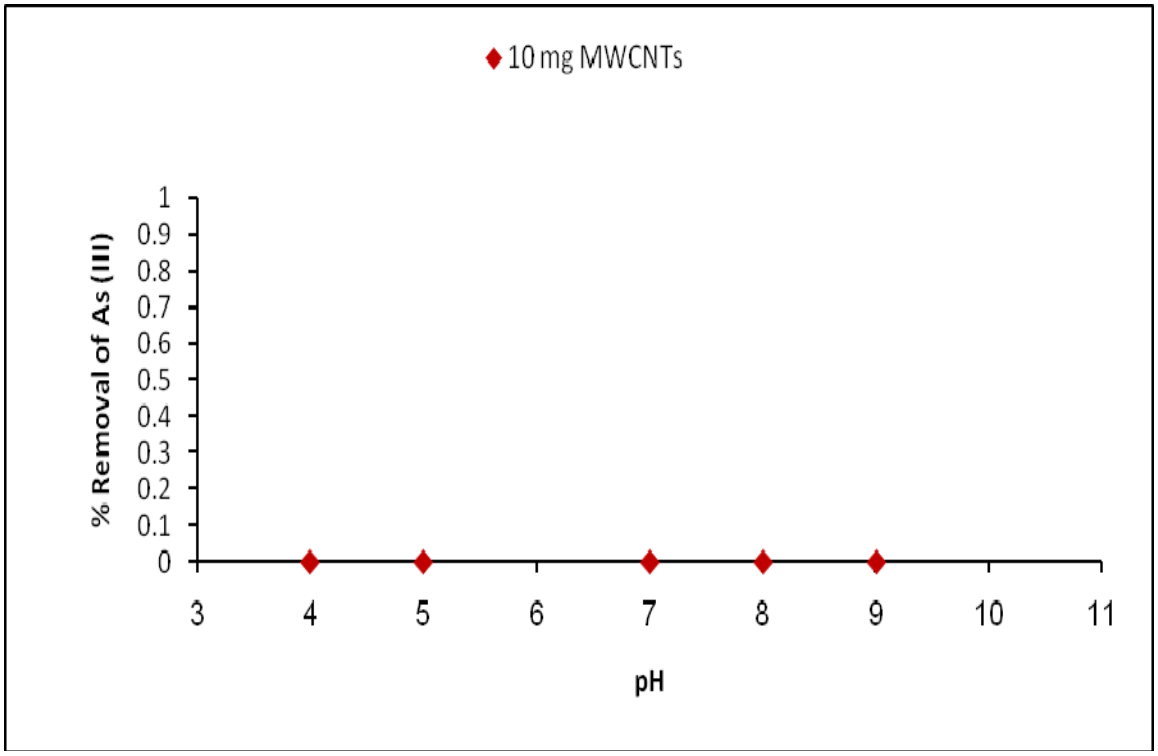

Figure 5.7: The effect of pH on the adsorption of As (III) by MWCNTs (MWCNTs dosage = 0.01 g/50 ml; As^{3+} conc. = 1.0 mg/L; agitation speed = 150 rpm for 120 min).

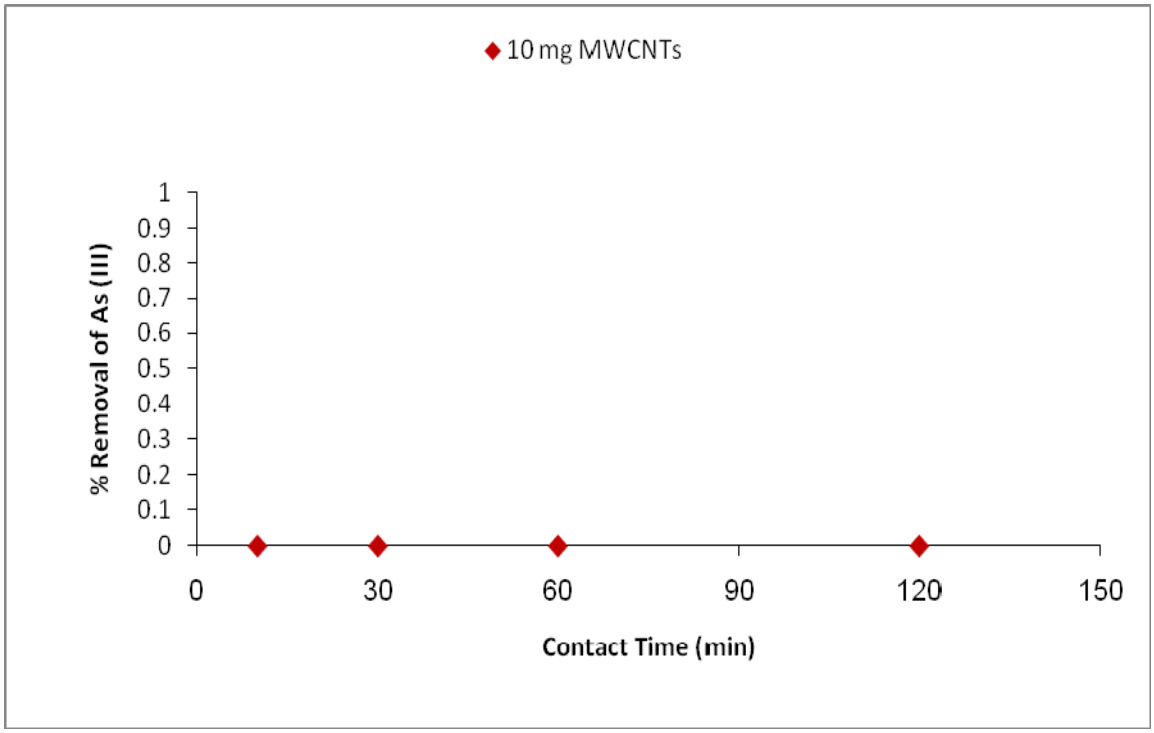

Figure 5.8: The effect of contact time on the adsorption of As (III) by MWCNTs (MWCNTs dosage = 0.01 g/50 ml; As^{3+} conc. = 1.0 mg/L; pH = 8, agitation speed = 150 rpm for 120 min).

Effect of mixing rate

The effect of mixing rate on the adsorption capacity of arsenic (III) by MWCNTs was studied by varying the rate of mixing from 50 to 200 rpm. It was observed that the percentage of arsenic (III) removed by MWCNTs was zero and did not change as the mixing rate changed. The data obtained was graphed in Figure 5.9.

Effect of CNTs Dosage

The amount of MWCNTs in the water is one of the factors which affect the adsorption capacity. The batch adsorption experiments were carried out by using 5 and 10 mg of MWCNTs while the pH, agitation speed and contact time were fixed at 8, 150 rpm and 120 min respectively. The results showed that the adsorption capacity of As (III) is not influenced by the MWCNTs dosage as represented on Figure 5.10.

5.2.3 REMOVAL OF ARSENIC (III) FROM WATER BY IRON-IMPREGNATED CNTS (MWCNT-Fe)

Unfortunately the removal of As (III) by MWCNTs was unsuccessful even after varying the pH, contact time, the dosage of the MWCNTs and mixing rate. Consequently, the adsorption of As (III) by multi-walled Carbon Nanotubes impregnated with Iron Oxides (MWCNT-Fe) was evaluated. It has been demonstrated by a number of researchers that supporting CNTs with certain complexes enhances their adsorption capacity. Li *et al.* confirmed that the adsorption capacity for Al_2O_3 supported on CNTs is about 4 times higher than that of as grown CNTs in the removal

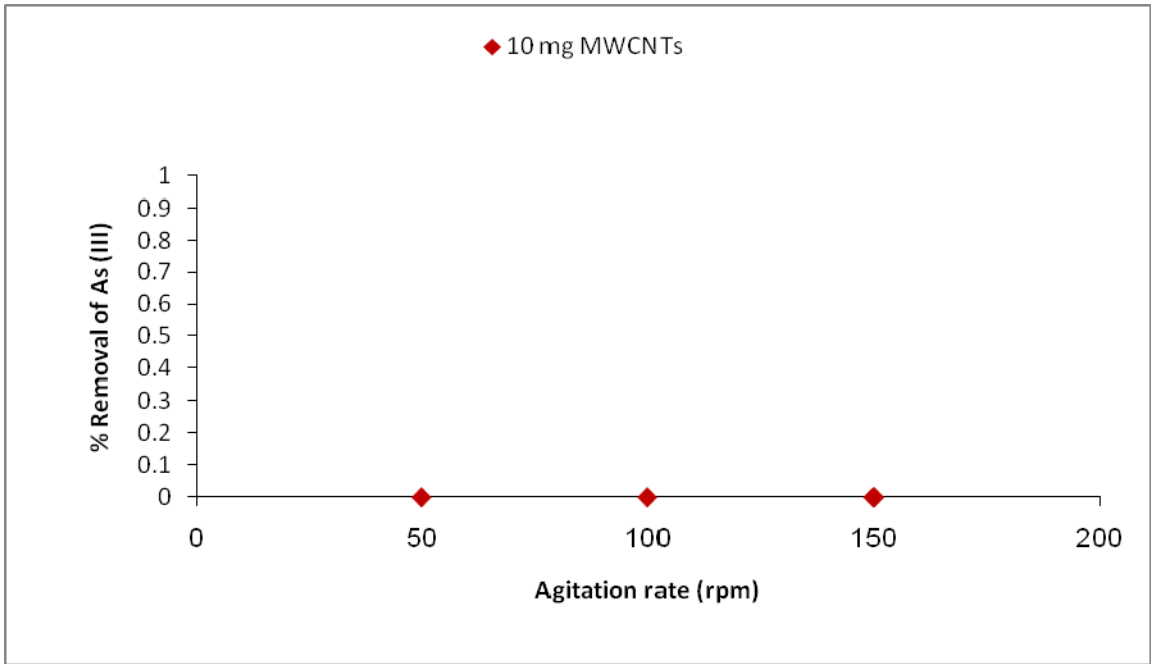

Figure 5.9: The effect of mixing rate on the adsorption of As (III) by MWCNTs (MWCNTs dosage = 0.01 g/50 ml; As^{3+} conc. = 1.0 mg/L; pH = 8 for 120 min).

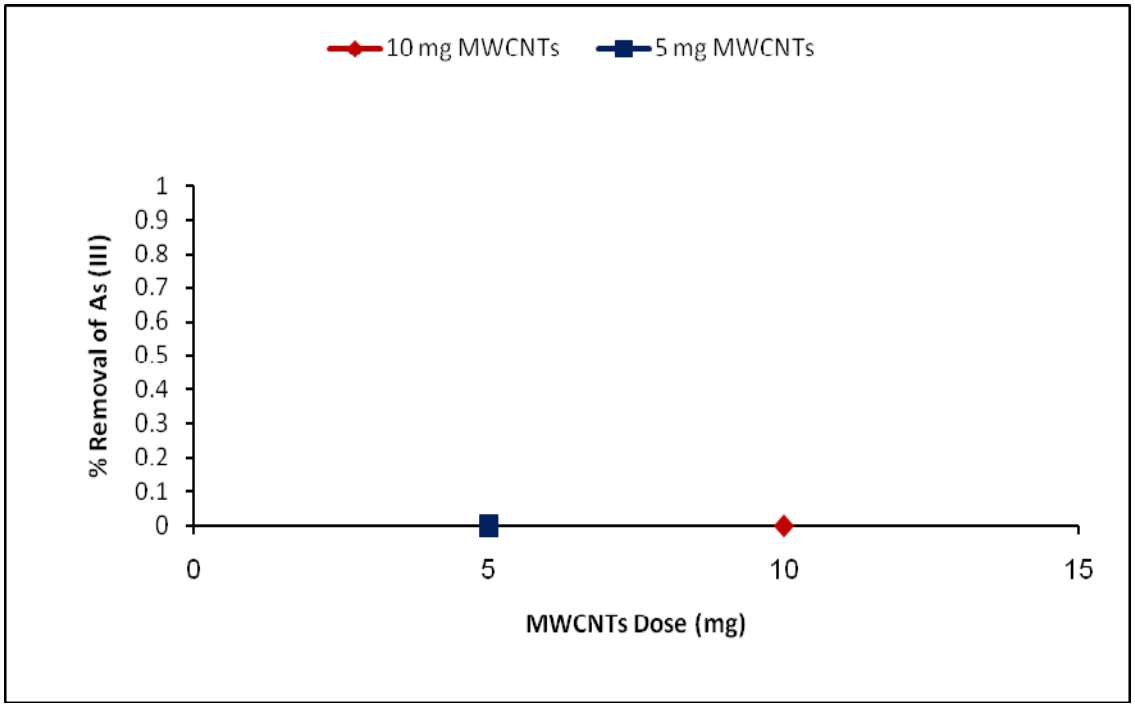

Figure 5.10: The effect of dosage on the adsorption of As (III) by MWCNTs (MWCNTs dosage = 0.01 g and 0.005g /50 ml; As^{3+} conc. = 1.0 mg/L; pH = 8 at rpm = 150 for 120 min).

of fluoride from water (Li *et al.*, 2001). Peng *et al.* demonstrated that CNTs-iron oxide magnetic composites can be used to adsorb contaminants from aqueous effluents and after the adsorption is carried out, the adsorbent can be separated from the medium by a magnetic process (Peng *et al.*, 2005). Di *et al.* noticed that the adsorption capacity for CeO_2 supported on ACNTs (28.3 mg/g) is about 1.5, 2.0 and 1.8 times higher than that of the activated carbon, Al_2O_3 and the ball-milled ACNTs (11.3, 9.3 and 10.2 mg/g), respectively, at equilibrium Cr(VI) concentration of 33.0 mg/l (Di *et al.*, 2006).

Additionally in light of the fact that arsenic has high affinity to iron (Thirunavukkarasu *et al.*, 2003), the adsorption of arsenic (III) by MWCNTs impregnated with iron oxides has been studied. The effect of pH, contact time, dosage of the MWCNT-Fe and mixing rate on the uptake of arsenic (III) were investigated to determine the optimum conditions for the removal of As (III) from water by MWCNT-Fe. The percent removal of arsenic (III) was determined to measure the adsorption capacity of MWCNT-Fe.

Effect of pH

The removal of As (III) by MWCNT-Fe at pH values 4-9 was investigated. The effect of pH on arsenite removal by MWCNTs impregnated with iron oxides is shown in Figure. 5.11. The adsorption of metals and anions can be treated as competitive complex formation and competitive ligand exchange, respectively, with great dependence on pH. As (III) exists predominantly as the neutral H_3AsO_3 in the pH range evaluated which is a poor ligand when compared to As (V).

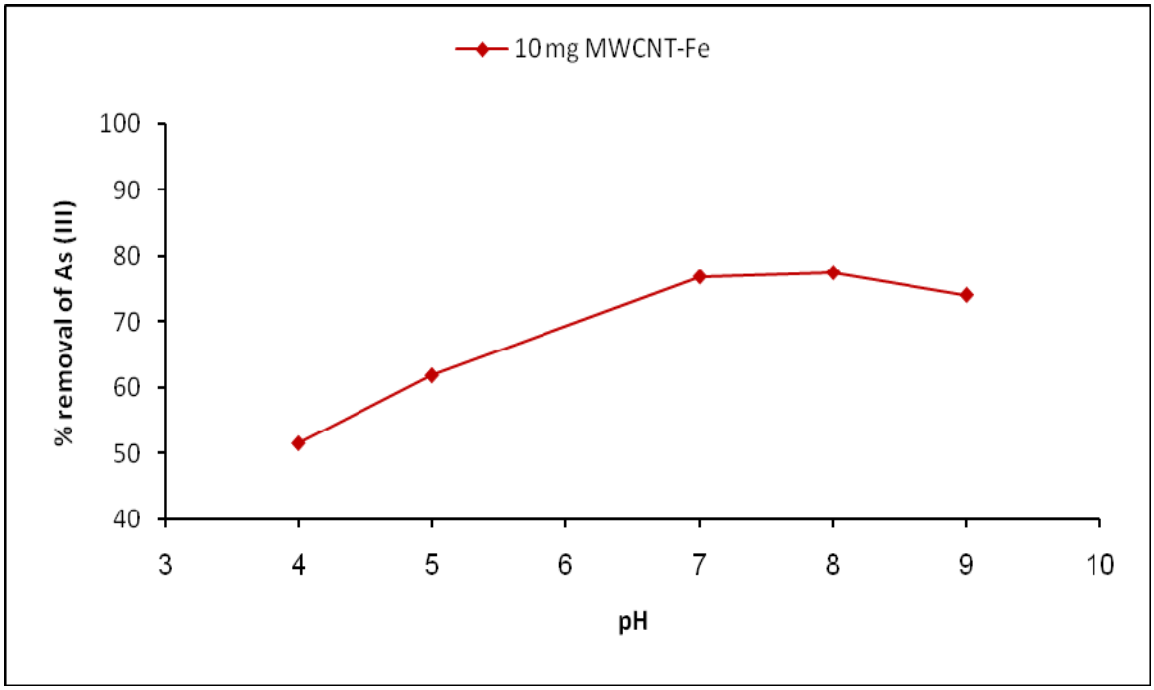

Figure 5.11: The effect of pH on the adsorption of As (III) by MWCNT-Fe (MWCNT-Fe dosage = 0.01 g /50 ml; As^{3+} conc. = 1.0 mg/L; agitation speed = 150 rpm for 120 min).

However, as the pH increases, the greater concentration of hydroxide, which is an excellent ligand, outcompetes the $H_2AsO_3^-$ anion for complexation sites. The same phenomenon of the effect of pH was observed. At acidic pH medium, free metal ions exist in solution while surface functional groups present in the protonated form. On the other hand, at basic pH medium, metals are precipitated as their hydroxides while functional groups on adsorbent surface (carboxyl, phenolic, lactonic) exist in the deprotonated form. Therefore, with the increasing of the pH from 4 to 9 the removal of arsenic in solution will increase and the degree of protonation of the surface will decrease which in turn will increase the adsorption capacity of the trivalent arsenic ion.

There was a gradual increase in the removal of arsenic (As^{3+}) at pH 4 until it reached pH 8. The low adsorption at pH 4 was due to the strong competition of H^+ with As^{3+} on the adsorption sites. When the pH increased the adsorption of arsenic increased gradually. At pH 7-8, the maximum percentage removal of arsenic was about 84.8 %. Above pH 9, the negatively charged $H_2AsO_3^-$ becomes predominant so is the adsorbent surface also negatively charged; thus, electrostatic repulsion results in decreased adsorption.

Effect of Contact Time

The adsorption behavior of As (III) by MWCNT-Fe as a function of contact time was performed by varying the contact time from 10-120 minutes at an As (III) concentration of 1 mg/L, a dose of adsorbent of 200 mg/L and at an optimum pH of 8.

The results shown in Figure 5.12 showed that the adsorption efficiency slightly increases as the contact time increases. The metal binding sites on the surface of the MWCNT-Fe become saturated as the contact time increases.

Effect of mixing rate

The effect of mixing rate on adsorption capacity of arsenic (III) was studied by varying the rate of mixing from 50 to 150 rpm. It has been observed that the percentage of arsenic (III) removed increased with increasing the mixing rate as shown in Figure 5.13. Mixing facilitates proper contact between the metal ions in solution and the MWCNT binding sites and thereby promotes effective transfer of arsenic (III) ions to the carbon nanotubes sites. At 50 rpm and 100 rpm, the adsorption rates monitored were found to be lower than that at 150 rpm. These results indicate that the contact between solids and liquid is more effective at 150 rpm. This is due to the fact that, the increase of agitation speed, improves the dispersion of arsenic ions in solution for better adsorption.

Effect of dosage

The amount of multi-walled carbon nanotubes in water is one of the factors which affect the adsorption capacity. The batch adsorption experiments were carried out using different amounts of MWCNT-Fe 10, 20 and 40 mg. The results in Figure 5.14 showed that the adsorption capacity increased with increasing adsorbent dosage. This is expected because the higher the dose of adsorbent in the solution, the larger the

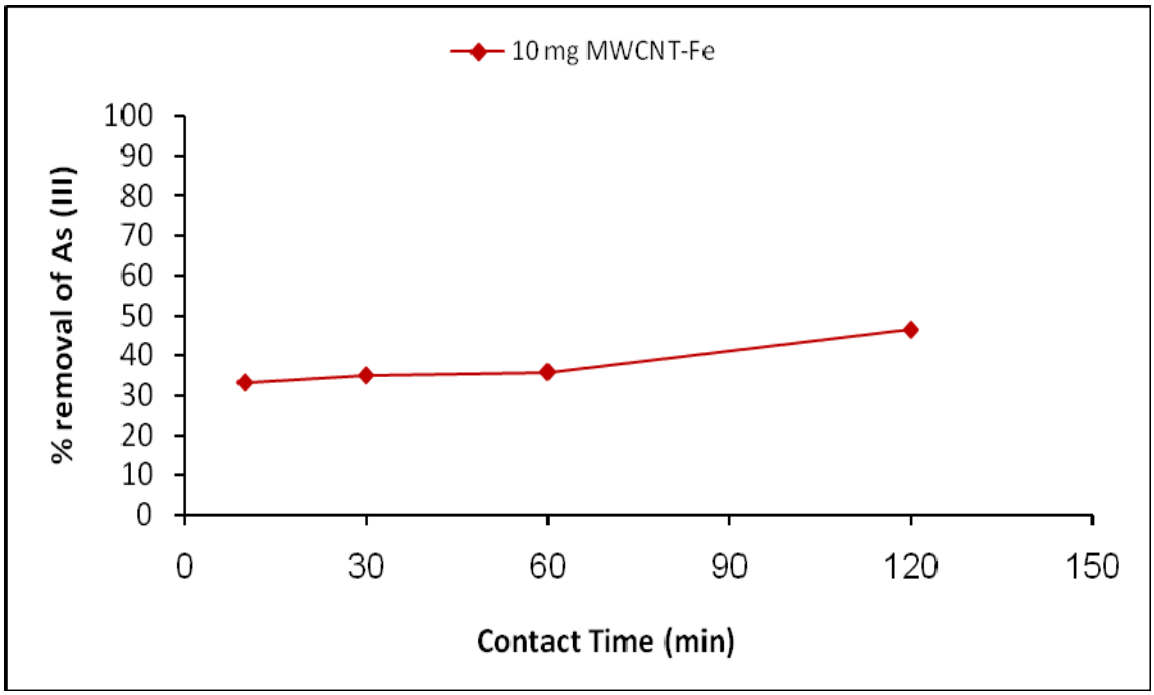

Figure 5.12: The effect of contact time on the adsorption of As (III) by MWCNT-Fe (M-CNTs dosage = 0.01 g/50 ml; As^{3+} conc. = 1.0 mg/L; agitation speed = 100 rpm).

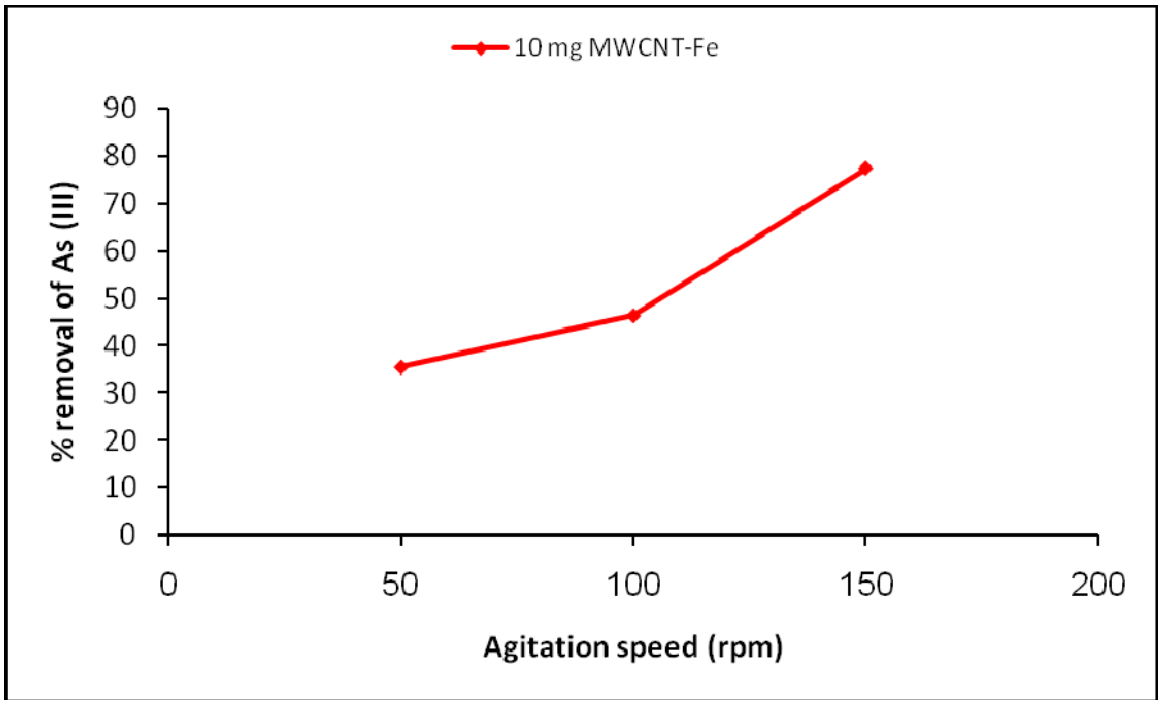

Figure 5.13: The effect of mixing rate on the adsorption of As (III) by MWCNT-Fe (MWCNT-Fe dosage = 0.01 g/50 ml; As^{3+} conc. = 1.0 mg/L; contact time = 120 min).

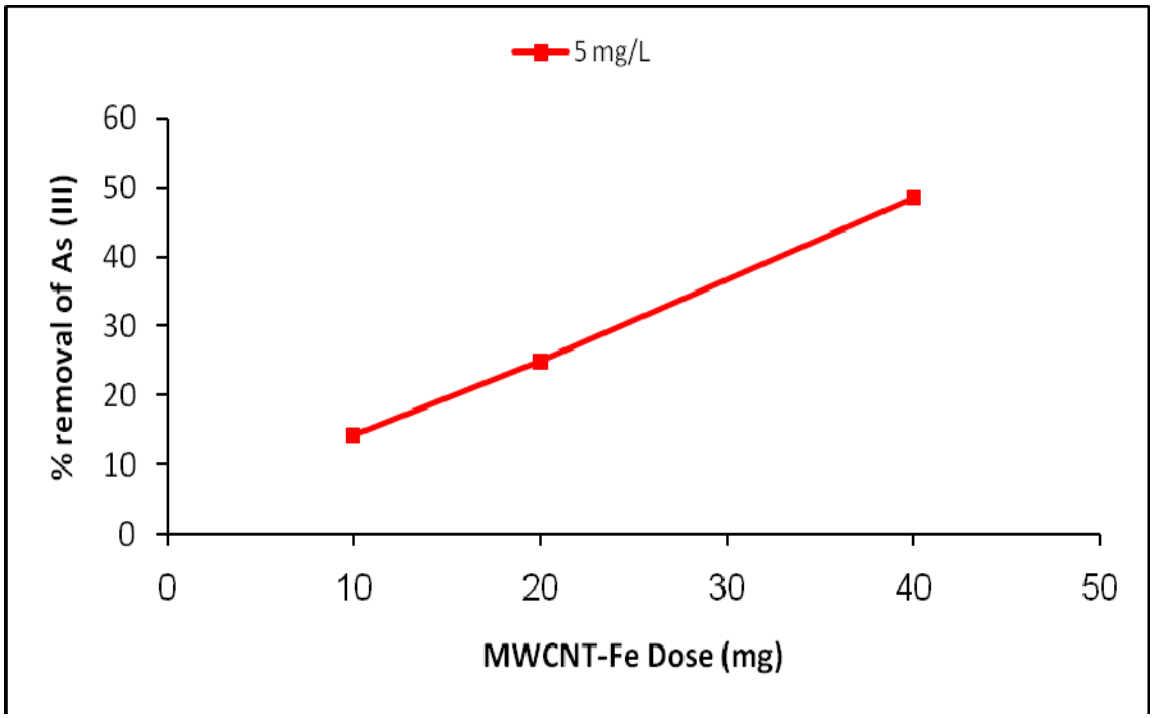

Figure 5.14: The effect of CNTs dosage on the adsorption of As (III) by MWCNT-Fe (MWCNT-Fe dosage = 0.01 g-0.04/50 ml; As^{3+} conc. = 5.0 mg/L; Contact time = 120 min at 150 rpm).

surface area and the greater the availability of binding sites for metal ions. This suggests that after a certain dose of adsorbent, the adsorption sites become occupied and the amount of free ions remains constant even with further addition of the adsorbent. Therefore, the adsorption capacity for arsenic (III) removal is dependent on the adsorbent dosage. It was found, that the maximum removal of arsenic (III) was 77.45 % when 10 mg of MWCNT-Fe were added to 1 mg/L As (III).

Comparative study for As (III) removal from water

A comparison study of the adsorption of arsenic (III) by different M-CNTs and R-CNTs was conducted. MWCNTs impregnated with iron oxides, carboxyl groups and raw MWCNTs were used to remove arsenic (III) from water. The arsenic (III) concentration, contact time, mixing rate and MWCNTs dosage were all kept constant. Figure 5.15 shows that MWCNTs supported by iron oxides was superior to MWCNTs supported by carboxyl groups and MWCNTs. The maximum arsenic (III) removal of 77.45 % was achieved by CNTs supported by iron oxides while CNTs impregnated by carboxyl groups removed only 11% at pH 5.

5.3 LANGMUIR AND FREUNDLICH ISOTHERM MODELS

Langmuir and Freundlich isotherms relate the coverage or adsorption of molecules on a solid surface to concentration of a medium above the solid surface at a fixed temperature. The experimental data for Hg (III) and As (III) adsorption on MWCNTs at different pH values could be approximated by the isotherm models of

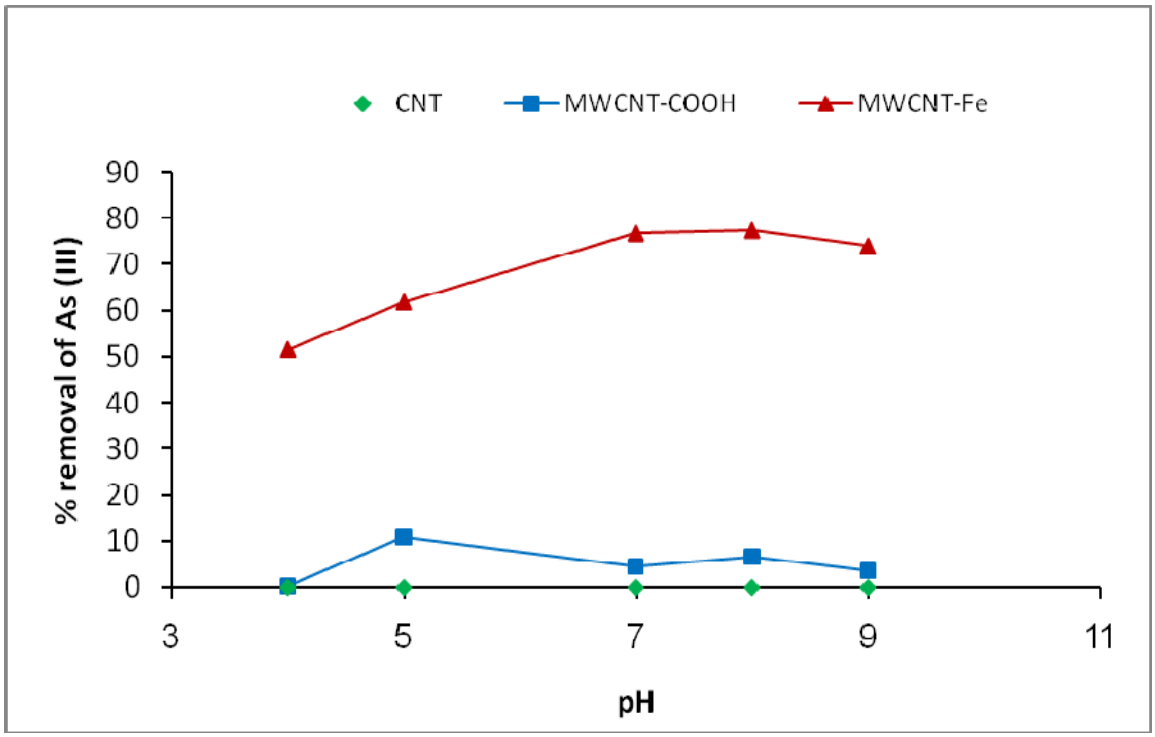

Figure 5.15: The effect of pH on the adsorption of As (III) by different M-CNTs and R-CNTs (CNTs dosage = 0.01 g /50 ml; As^{3+} conc. = 1.0 mg/L; mixing rate= 150 rpm for 120 min).

Langmuir (1) and Freundlich (2):

$$q_e = \frac{q_m K_L C_e}{(1 + K_L C_e)} \quad (1)$$

$$q_e = K_F C_e^{1/n} \quad (2)$$

Where C_e is the equilibrium concentration of mercury (II) or arsenic (III) in (mg/L), q_e is the amount adsorbed in (mg/g) and q_m and K_L are Langmuir constants which are related to adsorption capacity and energy of adsorption, respectively. K_F and n are Freundlich constants related to adsorption capacity and adsorption intensity, respectively. The equations (1) and (2) can be written as:

$$\frac{1}{Q_e} = \frac{1}{q_m K_L C_e} + \frac{1}{q_m} \quad (3)$$

$$\log q_e = \log K_F + 1/n \log C_e \quad (4)$$

5.4.1 LANGMUIR AND FREUNDLICH ADSORPTION ISOTHERM MODELS FOR MERCURY (II)

It can be seen from Table 5.1 that both Langmuir and Freundlich models show good agreement with the experimental data where the data fit the Freundlich model better, with correlation coefficient values of 0.989 and 0.9994 respectively. Figure 5.16 (a) and (b) represent the linear, Langmuir and Freundlich isotherm plots of Hg (II) adsorption on the MWCNTs. The equilibrium data were fitted very well to all sorption isotherms. Therefore, this indicates the applicability of monolayer coverage of Hg (II) ions on the surface of the adsorbent.

Table 5.1: Parameters of Langmuir and Freundlich adsorption isotherm models for Mercury (II)

pH	***Langmuir***				***Freundlich***			
	q_{max}	K_L	r^2	R_L	$1/n$	n	K_F	r^2
8	14.50	0.09	0.989	0.91	0.85	1.17	1.06	0.999

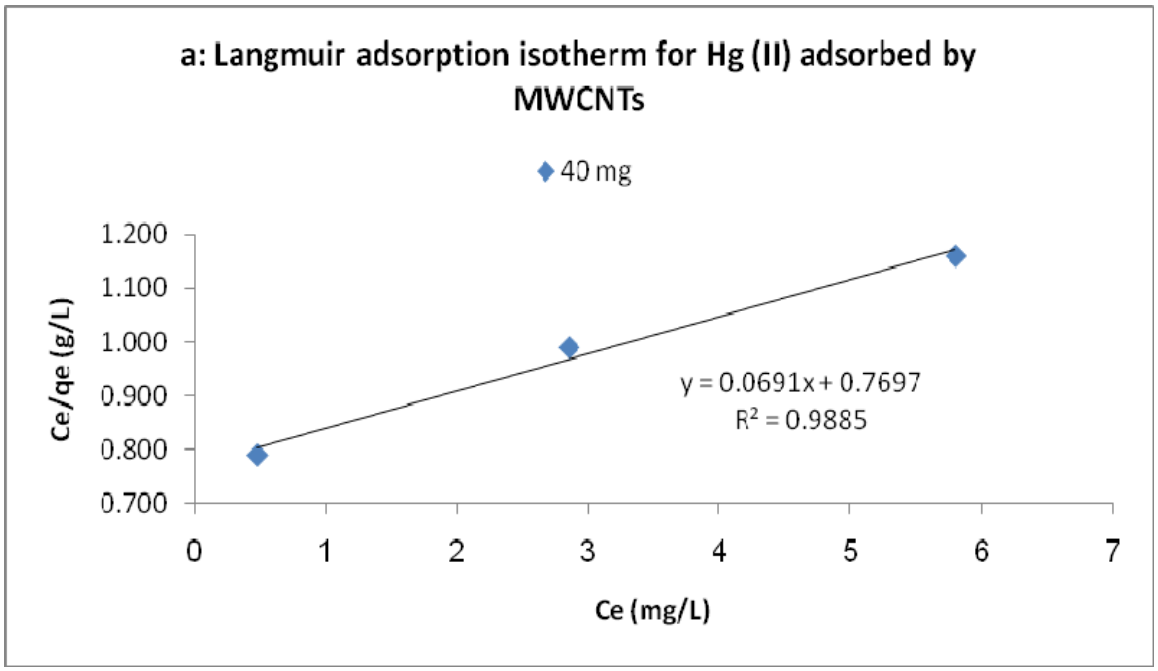

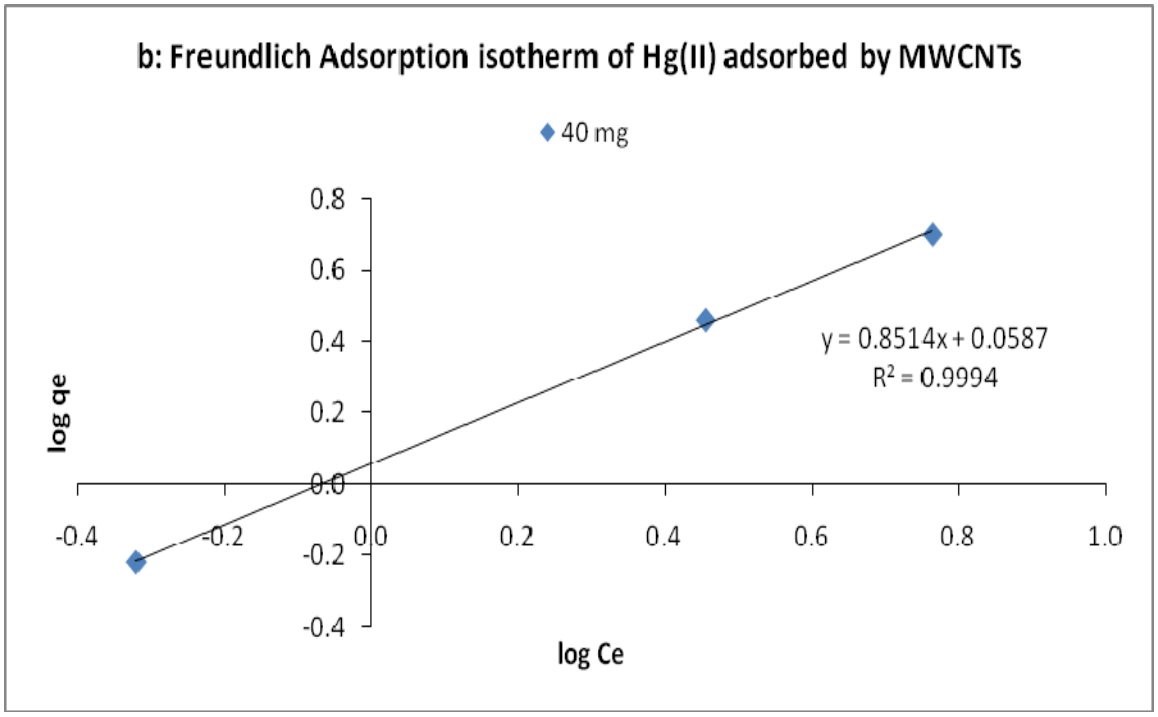

Figure 5.16: Adsorption isotherm models for mercury (II) (a) Langmuir and (b) Freundlich

This is due to the fact that, MWCNTs have greater surface area for metal adsorption. The good correlation coefficients of Langmuir and Freundlich isotherms also indicate that Hg (II) ions strongly adsorbed to the surface of MWCNTs. Therefore, it is verified that MWCNTs have great potential to be a good adsorbent for the removal of Hg (II) ions in water treatment.

The magnitude of $1/n$ quantifies the favorability of adsorption and the degree of heterogeneity of the CNTs' surface. If $1/n$ is less than 1, suggesting favorable adsorption, then the adsorption capacity increases and new adsorption sites form. The favorability of adsorption is also confirmed by calculating separation factor or equilibrium parameter, R_L, which is defined as $1/(1 + K_L C_0)$, where K_L is Langmuir constant and C_0 is initial metal concentration (mg/l). The value of R_L indicates the shape of isotherm to be either unfavorable ($R_L > 1$) or linear ($R_L = 1$) or favorable ($0 < R_L < 1$) or irreversible ($R_L = 0$). The R_L values obtained indicate favorable isotherm shape ($0 < R_L < 1$) for the adsorption of Hg (II) by MWCNTs.

5.3.2 LANGMUIR AND FREUNDLICH ADSORPTION ISOTHERM MODELS FOR ARSENIC (III)

The equilibrium adsorption is important in the design of adsorption systems. Equilibrium studies in adsorption indicate the capacity of the adsorbent during the treatment process. Taking into account that the percentage removal of As (III) by MWCNT-Fe was highest at pH 8, the condition was used to further optimize the adsorption process parameters. The equilibrium curve was modeled in Figure 5.17.

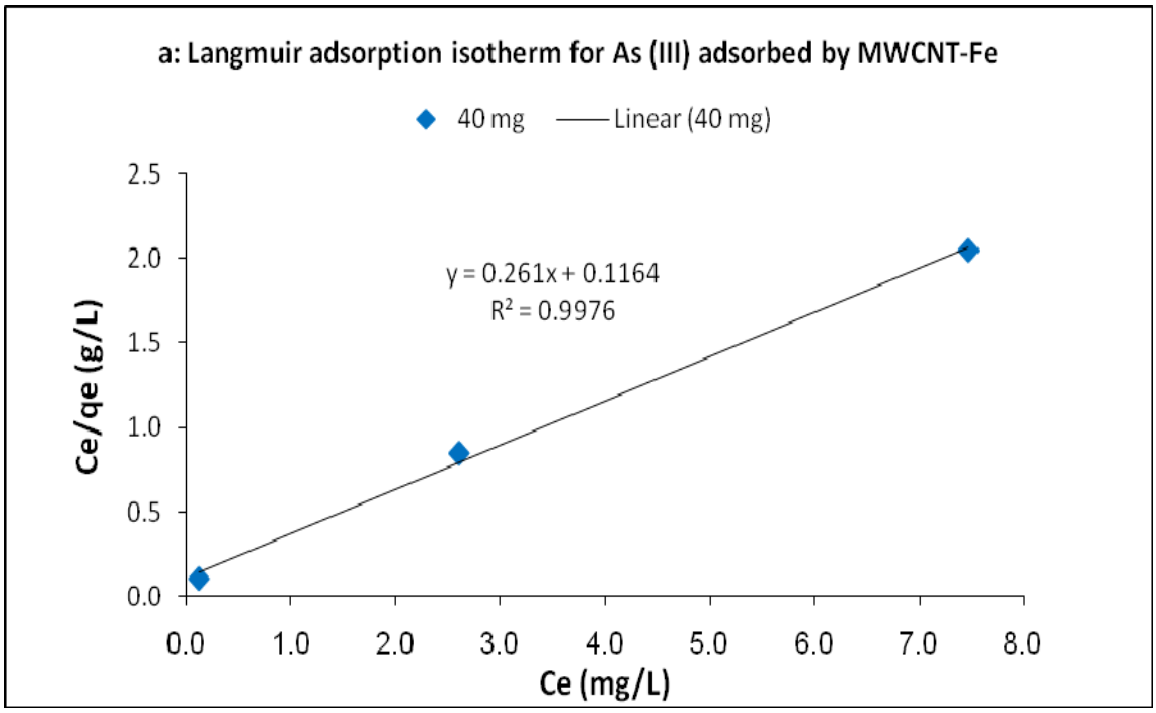

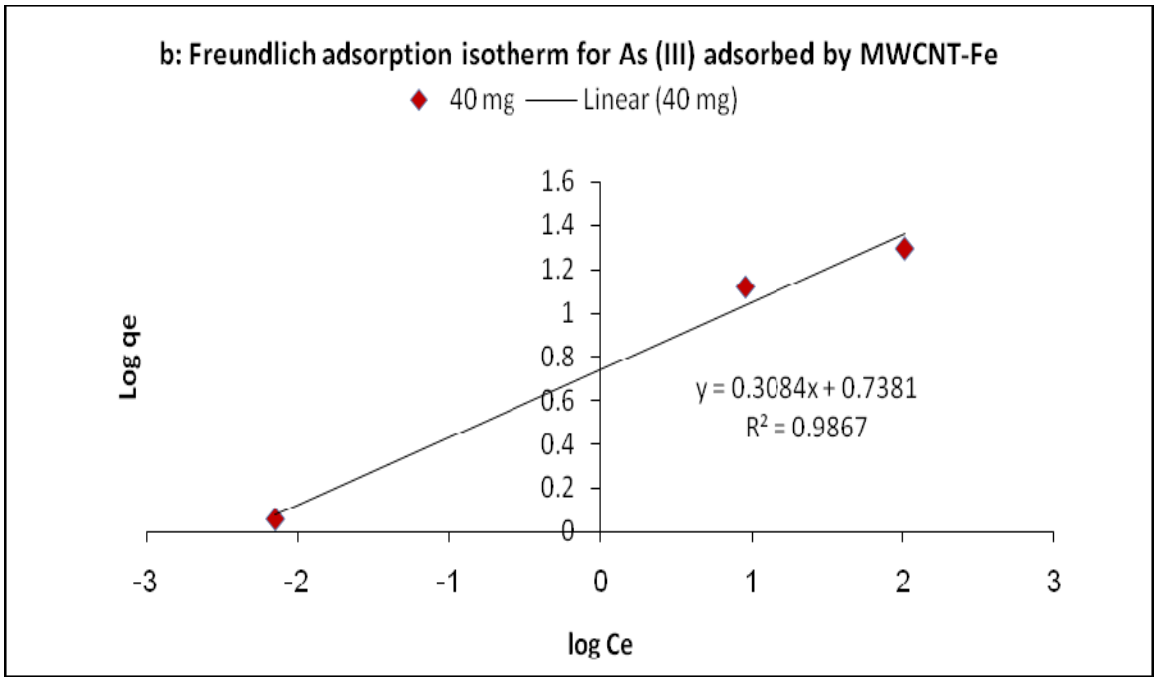

Figure 5.17: Adsorption isotherm models for arsenic (III) :(a) Langmuir (b) Freundlich.

The Langmuir and Freundlich equations were used to describe the data derived from the adsorption of As (III) by MWCNT-Fe over the entire parameters range studied. Based on Figure 5.17, the adsorption capacity (q_{max}) and adsorption intensity were determined from the slope and intercept of the graph respectively. Table 5.2 summarizes the results of both adsorption isothermal models.

Both Langmuir and Freundlich isotherm models fit the experimental data; however Langmuir Isotherm shows better fit model with higher correlation coefficient (R^2=0.998) compared to Freundlich Isotherm (R^2=0.987). This is indicative of the applicability of monolayer coverage of As (III) ions on the surface of the adsorbent. This is due to the fact that, M-CNTs have greater surface area for metal adsorption. The good correlation coefficient of Langmuir isotherm also indicates that As (III) ions strongly adsorbed to the surface of MWCNT-Fe. Therefore, it is verified that MWCNTs have great potential to be a good adsorbent for the removal of As (III) ions in water treatment. The favorability of adsorption of As (III) and the degree of heterogeneity of the MWCNT-Fe surface have been confirmed by the magnitudes of $1/n$ and R_L.

5.4 ADSORPTION KINETICS

The study of sorption kinetics is applied to describe the adsorbate uptake rate and this rate evidently controls the residence time of adsorbate at solid liquid interface. In order to evaluate the mechanism of sorption of Hg (II) and As (III) by MWCNTs and MWCNT-Fe respectively, the first-order equation, the pseudo- second-order rate

Table 5.2: Parameters of Langmuir and Freundlich adsorption isotherm models for arsenic

pH	***Langmuir***				***Freundlich***			
	q_{max}	K_L	r^2	R_L	$1/n$	n	K_F	r^2
8	3.83	2.24	0.998	0.32	0.31	3.24	2.09	0.987

equation and the second-order rate equations were calculated by the below shown equations respectively:

$$\log \frac{q_e - q_t}{q_e} = -\frac{K_L t}{2.303} \quad (1)$$

$$\frac{t}{q_t} = \frac{1}{2K_2 q_e^2} + \frac{t}{q_e} \quad (2)$$

$$\frac{1}{q_e - q_t} = \frac{1}{q_e} + kt \quad (3)$$

Where:

q_e = sorption capacity at equilibrium

q_t = sorption capacity at time (mg/g)

K_L = the Lagergren rate constant of adsorption (1/min)

k = rate constant of the pseudo second-order sorption ($g.mg^{-1}.min^{-1}$)

t = time (min)

The linear plots of log ($q_e - q_t$) versus t; t/q_t versus t and $1/(q_e - q_t)$ versus t of the above equations. q_e, K_L and k can be determined from the slopes and intercepts.

5.4.1 ADSORPTION KINETICS FOR MERCURY (II)

In order to evaluate the adsorption rate of Hg (II) onto MWCNTs, a pseudo-second-order rate equation was implemented to simulate the kinetic of adsorption. From the linear plot of t/q_t versus t (Figure 5.18) the value *of k* was calculated from the slope and intercept and summarized in Table 5.3. The correlation coefficient of the pseudo-second order rate equation for the linear plot is 0.9975, which suggests

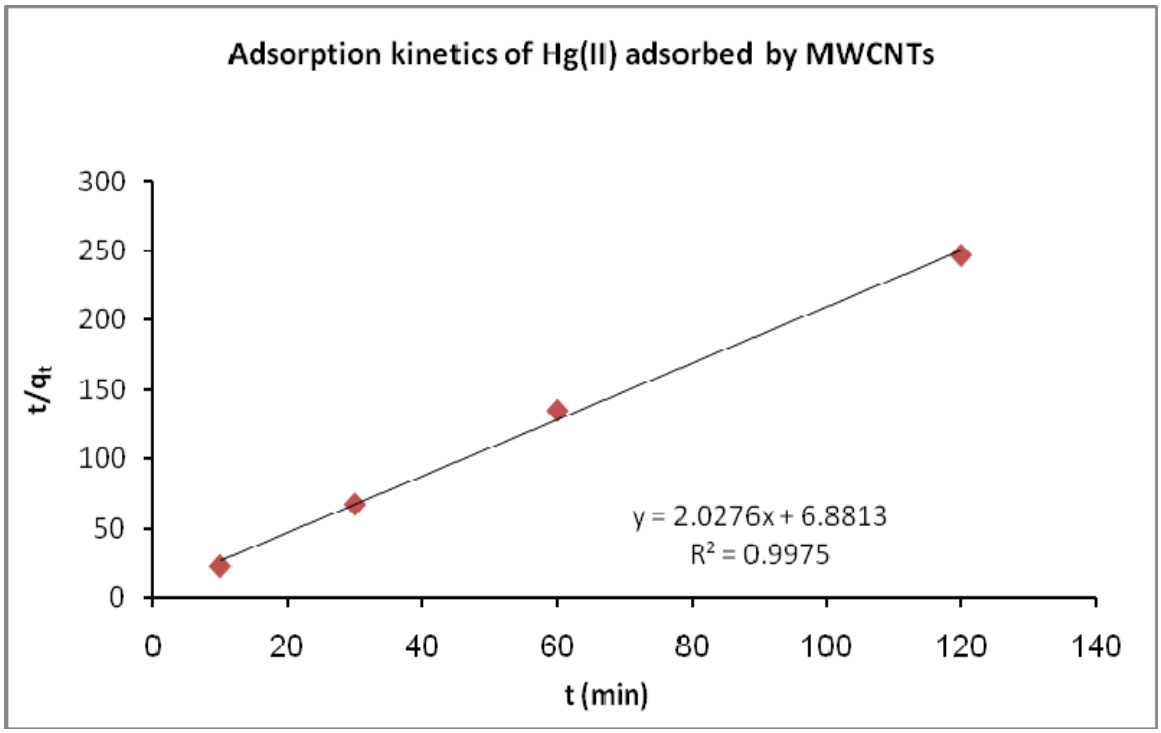

Figure 5.18: Test of pseudo-second-order rate equation for adsorption of various initial Hg (II) concentrations onto MWCNTs. (Ci = 0.1 mg/L; Dose = 10 mg/ 50 ml).

Table 5.3: Kinetic parameters of Hg (II) adsorbed on MWCNTs at initial concentrations of 0.1 mg/L

pH	**Pseudo second-order kinetic**		
	q_e	k	r^2
8	0.493	0.018	0.9975

that the kinetic adsorption can be described by a pseudo- second-order rate equation well.

5.4.2 ADSORPTION KINETICS FOR ARSENIC (III)

The adsorption rate of As (III) onto M-CNTs was evaluated by a pseudo-second-order rate equation to simulate the kinetic of adsorption. From the linear plot of t/q_t versus t (Figure 5.19) the value *of k* was calculated from the slope and intercept and summarized in Table 5.4. The correlation coefficient of the pseudo-second order rate equation for the linear plot is 0.996, which suggests that the kinetic adsorption can be described by a pseudo-second-order rate equation well.

5.5 COMPARATIVE ANALYSIS OF VARIOUS ADSORBENTS FOR MERCURY (II) AND ARSENIC (III) REMOVAL

Contamination of water by mercury is serious environmental and health problem. The great concern about mercury pollution is due to its persistence in the environment and biota as well as bioamplification and bioaccumulation along the food chain. Many researches have been conducted on the adsorption of mercury from water with varying degrees of success and efficiency. Organic, inorganic and biological adsorbents have been used for mercury removal from water. The morphology of the adsorbents e.g. surface area, pore size and functional groups is one of the differentiating factors for mercury adsorption efficiency from water. Furthermore, even within the same material researchers have been trying to optimize that material.

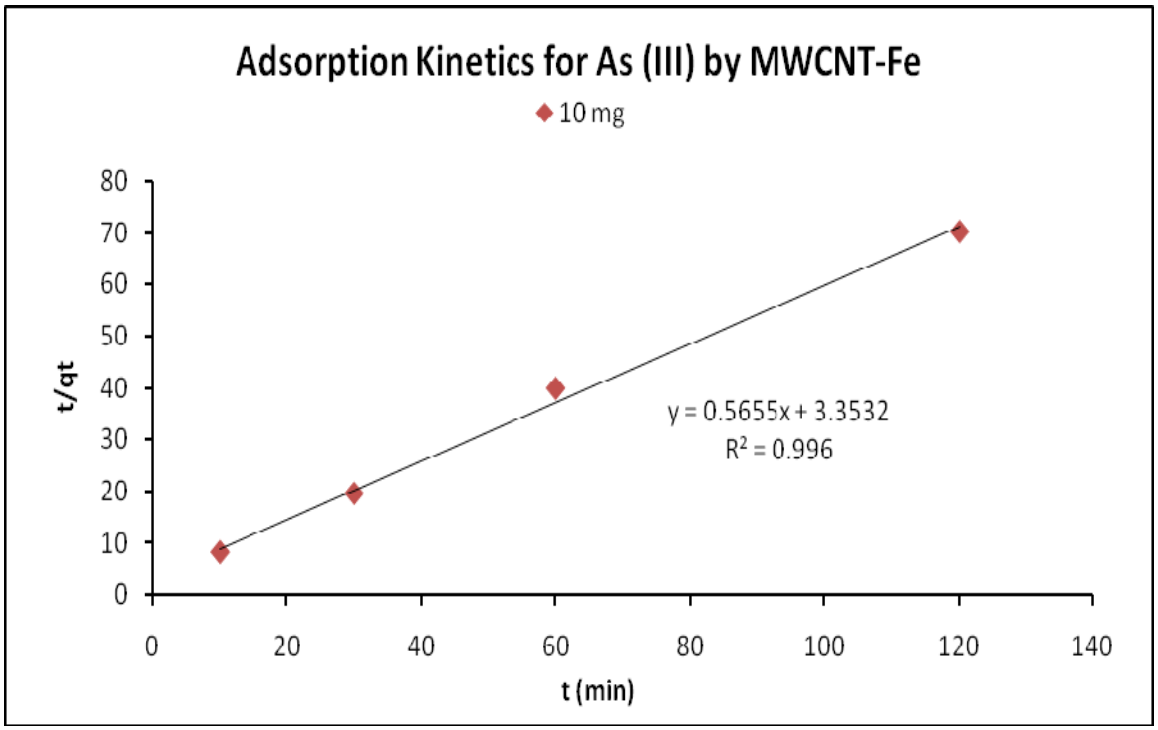

Figure 5.19: Test of pseudo-second-order rate equation for adsorption of various initial As (III) concentrations onto MWCNT-Fe. (Ci = 1 mg/L; Dose = 10 mg/50 ml).

Table 5.4: Kinetic parameters of As (III) adsorbed on M-CNTs at initial concentrations of 1 mg/L

pH	**Pseudo second-order kinetic**		
	q_e	k	r^2
8	1.77	0.466	0.996

For instance Activated Carbon (AC) is used to adsorb mercury from water; different kinds of AC are being manufactured and used e.g. Powdered AC, Granular AC (Abdel-Shafy *et al.*, 1998), AC made from sago waste (Kadirvelu *et al.*, 2004), AC made from organic sewage sludge (Zhang *et al.*, 2005) and among others (Bailey *et al.*, 1998). Additionally various biological species have been used e.g. Bacillus Sp. (Green-Ruiz, 2006) and macroalga *Cystoseira baccata* (Herrero *et al.*, 2005). For comparison purposes, table 5.5 depicts some examples of the adsorbents used for the removal of Hg from water.

Based on table 5.5 and literature, there are many studies on the removal of Hg (II) using various types of adsorbents. However, the removal percentage of each adsorbent differs due to the variation in the operating parameters(pH, agitation speed, dosage, temperature and many more). Thus, this comparative study was conducted to further understand the mechanism of adsorption and compare the types of adsorbents that were previously used to remove Hg (II). There are many studies and reviews that have been conducted to compare the adsorption efficiencies of As (III) by different adsorbents. Table 5.6 is an excerpt that summarizes the outcome of those studies. MWCNT-Fe shows superior adsorption capacity compared to other adsorbents.

Table 5.5: Comparison of various adsorbents and its percentage uptake of Hg (II)

Adsorbent	Condition				% Removal	Reference
	pH	Contact time	Agitation Speed (rpm)	Dosage (g/L)		
PAC	-	150 min	-	7.0	91.4	Abdul-Shafy *et al*., (**1998**)
GAC		18 hrs.				
Quartz	4.3	48 hrs.	-	3.3	58	Sarkar *et al*., (**1999**)
Gippsite	4.8				55	
AC from sago waste	10	120 min	170	2.0-2.4	100	Kadirvelu *et al.*, (**2004**)
Bacillus Sp.	4.5-6	40-60 min	100	2	91.4±4.8 for 0.25 mg/L	Green-Ruiz, (**2006**)
ETS-4	8	24 hrs.	>500	3.45	98±1	Lopes *et al*., (**2009**)
MWCNTs	4-9	120 min	150	0.2	100	This study

Table 5.6: Comparison of various adsorbents and its percentage uptake of As (III)

Adsorbent	Condition				% Removal	Reference
	pH	Contact time	Agitation Speed (rpm)	Dosage (g/L)		
Granular Ferric Hydroxide (GFH)	6-8.5	6 hrs	175	2	97 0.1 mg/L As(III)	Thirunavukkarasu *et al.* (**2003**)
GAC	5-7	12 hrs	-	24	44	Mondal *et al.* (**2007**)
GAC-Fe	9-11	8 hrs		8	92.4	
Iron Oxide Coated Cement	6-8	120 min	180±10	30	89.8 1.35 mg/L As(III)	Kundu and Gupta (**2007**)
MWCNTs	4-9	120 min	150	0.2	0	This study
MWCNT-Fe	7-9	120 min	150	0.4	87.8 10 mg/L As(III)	

CHAPTER 6

CONCLUSION AND RECOMMENDATION

Carbon Nanotubes were found to be efficient for the adsorption of Hg (II) and As (III) in aqueous solutions. The characterization of Hg (II) and As (III) uptake showed that mercury and arsenic adsorption is dependent on pH, agitation speed, dosage of CNTs and contact time. Study of the effects of operational parameters such as pH, CNTs dosage, agitation speed and contact time produced different optimum conditions. Percentage uptake increased with an increase in pH from pH 4 to 8. The optimum pH found in this study is pH 8 in which it gave 100% removal of Hg (II) ions by using MWCNTs and 87.8 % of As (III) ions by using MWCNT-Fe from aqueous solution. The percentage uptake increase gradually with the increase in agitation speed from 50 to 150 rpm, in which 150 rpm gave higher removal for mercury and arsenic. The removal of Hg (II) and As (III) was observed to be optimal for higher dosage of CNTs, in which 10 mg of MWCNTs contribute to 100 % removal of Hg (II) ions and 40 mg of MWCNT-Fe achieved 87.8 % removal of As (III) ions.

The experimental results were analyzed using Langmuir and Freundlich equations. Table 5.1 shows the Langmuir and Freundlich adsorption isotherm constants for the adsorption of mercury (II). The experimental data of this study for both mercury (II) and arsenic (III) are extremely well described by both isotherm

models with correlation coefficients (R^2) close to 1. The values obtained demonstrate that CNTs is a good adsorbent for the removal of mercury and arsenic from wastewaters.

A comparative analysis was conducted at the end of this study to explore the effectiveness of other adsorbents that were used to remove Hg (II) and As (III). Based on this analysis, other adsorbents could be more efficient. However, the potential of CNTs should not be underestimated since the application of CNTs as Carbon Nanofilter provides a competitive advantage in terms of cost-effectiveness and scale of operation. Although the cost of CNTs is expensive, but the benefits outweigh the cost since CNTs have high adsorption capacity and can be used for large scale operation compared to other adsorbents. In addition, this study reported that the treatment process only requires mild agitation speed for the removal of Hg (II) and As (III), thus it will benefit the industry due to its low power consumption. Yet further study is recommended to focus on the cost-effectiveness of CNTs.

In conclusion, from all of these analyses, it is demonstrated that CNTs can be used as adsorbents for the removal of Hg (II) and As (III) ions from water and wastewater. However, further study must be done to further validate the effectiveness of this method in terms of cost and large scale treatment of Hg (II) and As (III) in the industry. Further study and investigations can be done such as:

1. The study of adsorbent dosage should include the particle size characterization and determination of surface area of adsorbent.

2. Study should be conducted using the real wastewater solution from selected industry to verify its effectiveness on the actual application.
3. Production of CNTs should be conducted to obtain the highest purity.
4. The effects of CNTs on human health should be studied thoroughly in order to protect the public from future hazards if any.
5. Descriptive studies should be conducted to elucidate the mechanism of adsorption and recover the metal loaded adsorbent.
6. Validation study should be conducted to verify the optimization equation that was developed from this study.

Last but not least, the objectives of this project which are to remove Hg (II) and As (III) using CNTs and the optimization of process parameters was achieved based on the successful outcome of this study. In addition, the adsorption kinetics of CNTs was developed and the results indicate the strong affinity of Hg (II) and As (III) ions on the surface of CNTs. Hopefully, the outcome of this study will benefit the public and protect environment from future contamination.

REFERENCES

Abdel-Shafy, Hussein I., Abdel-Sabour, Mamdouh F., Aly, Raouf O. (**1998**). "*Adsorption of nickel and mercury from drinking water stimulant by activated carbon*". Environmental Management and Health 9/4:170–175.

Ando, Yoshinori; Zhao, Xinluo; Sugai, Toshiki and Kumar, Mukul; (**2004**); "*Growing Carbon Nanotubes*". Materials Today October 2004, 22-29.

Badruzzaman B. M., Harvey C. F., Swartz C., Keon-Blute A. N., Yu W., Hemond M. A. Ali, J. Jay, R. Beckie, V. Niedan, D. Brabander, P. Oates, K. Ashfaque, S. Islam, H., and Ahmed M. F. (**2004**) *Arsenic Mobility and Groundwater Extraction in Bangladesh***,** *Science* 2002 298: 1602-1606

Bacsa, Wolfgang S. (**2006**). **"**Who Discovered Carbon Nanotubes?". CARBON 44: 1621.

Bailey et al. (**1998**). "*A Review of Potentially Low-Cost Sorbents for Heavy Metals*". PII: S0043-1354(98)00475-8.

Beckvar, Nancy, Jay Field, Sandra Salazar, Rebecca Hoff (**1996**). *Contaminants in Aquatic Habitats at Hazardous Waste Sites: Mercury*; NOAA Technical Memorandum NOS ORCA 100. Seattle: Hazardous Materials Response and Assessment Division, National Oceanic and Atmospheric Administration. 74 pp.

Berber, Savas, Kwon, Young-Kyun and Tománek, David (**2000**). "*Unusually High Thermal Conductivity of Carbon Nanotubes*". Physical Review Letters, Volume 84, Number 20, Pages 4613-4616.

Bethune, D. S.; Klang, C. H.; de Vries, M. S.; Gorman, G.; Savoy, R.; Vazquez, J. and Beyers, R. (**1993**). "*Cobalt-catalyzed growth of carbon nanotubes with single-atomic-layer walls*", Nature **363**, 605 - 607; doi: 10.1038/363605a0

Black, Bryan (**1999**); Arsenic: Answers to Questions Commonly Asked by Drinking Water Professionals, American Water Works Association, ISBN-9781583210581

Bonaventura, Celia and Johnson, Franklin M. (**1997**). "*Healthy Environments for Healthy People: Bioremediation Today and Tomorrow*" *Environmental Health Perspectives Supplements* Volume 105, Number S1, February 1997**.**

Bonzongo, J.J., Heim, K.J., Y. Chen, W.B. Lyons, J.J. Warwick, G.C. Miller and P.J. Lechler. (**1996**). Mercury pathways in the Carson River-Lahontan Reservoir System, Nevada, USA. Environmental Toxicology and Chemistry 15(5):677-683.

Chen, C. L., Li, X. L., Wang, X. K. (**2007**). "*Application of oxidized multi-wall carbon nanotubes for Th(IV) adsorption*". Radiochimica Acta, Volume 95: 261-266.

Cheng *et al.* (**1998**); "*Bulk morphology and diameter distribution of single-walled carbon nanotubes synthesized by catalytic decomposition of hydrocarbons*"; Chemical Physics Letters Volume 289, Issues 5-6, Pages 602-610.

Chin Ching-Ju Monica, Shih, Li-Chieh, Tsai, Hen-Je, Liu, Ta-Kang, (**2007**). "*Adsorption of o-xylene and p-xylene from water by SWCNTs*". Carbon 45:1254–1260.

Collins, P. G. and Avouris, P. (**2000**); "*Nanotubes for Electronics*". Scientific American, 238:62-9

Daenen, M. et al. (**2003**); "*The Wondrous World of Carbon Nanotubes*". Eindhoven University of Technology.

Dai et al. (**1996**); "*Single-wall nanotubes produced by metal-catalyzed disproportionation of carbon monoxide*". Chemical Physics Letters Volume 260, Issues 3-4, Pages 471-475

Di, Ze-Chao, Jun Ding, Xian-Jia Peng, Yan-Hui Li, Zhao-Kun Luan, Ji Liang; (**2006**). "*Chromium adsorption by aligned carbon nanotubes supported ceria nanoparticles*" Chemosphere 62: 861–865.

Dresselhaus, M. S., Dresselhaus, G. and Satio, (**1995**); "*Physics of Carbon Nanotubes*". Carbon, Vol. 33, No. 7, pp. 883-891.

Ebbesen, Thomas W. (**1996**); Carbon nanotubes: preparation and properties. CRC Press; ISBN 9780849396021.

Ebbesen, T. W. and Ajayan P. M. (**1992**); "*Large-scale synthesis of carbon Nanotubes*". Nature **358:** 220 - 222; doi:10.1038/358220a0

Endo, M. *et al.* (**1993**); "*The production and structure of pyrolytic carbon nanotubes (PCNTs)*" Journal of Physics and Chemistry of Solids 54 (12), Pages 1841-1848.

Environmental Health Criteria 18 Arsenic WHO Geneva. (**1981**), Page 42. ISBN 92 4 154078 8.

Falvo, M.R., G.J. Clary, R.M. Taylor II, V. Chi, F.P. Brooks Jr., S. Washburn and R. Superfine, (**1997**). "*Bending and buckling of carbon nanotubes under large strain*". Nature, Vol 389, No 6651, pp. 582-584.

Fendorf, S. E.; Matthew, J. E.; Grossel, P.; Sparks, D. L.; (**1997**). Arsenate and chromate retention mechanism on goethite. 1. Surface structure. *Environmental Science and Technology* **3:**315–320

Ferguson J. F, Gavis J. (**1972**), Review of the arsenic cycle in natural waters. Water Res 6:1259–74.

Fuhrman, Hülya Genç (**2004**); Arsenic removal from water using seawater-neutralized red mud (Bauxsol). *Environmental & Resources DTU*. ISBN 87-89220-75-7

Gill, GA, KW Bruland. (**1990**). Mercury speciation in surface freshwater systems in California and other areas. *Environmental Science and Technology 24*(9):1392-1400.

Goessler, W.; Kuehnelt, D.; (**2002**). Analytical methods for the determination of arsenic and arsenic compounds in the environment. In W. T. Frankenberger, Jr. (Ed.) "Environmental Chemistry of Arsenic". p. 27. Marcel Dekker, Inc., New York. ISBN 0824706765

Green-Ruiz, Carlos (**2006**). "*Mercury (II) removal from aqueous solutions by nonviable Bacillus sp. from a tropical estuary*". Bioresource Technology 97:1907–1911.

Guo, T.; Nikolaev, P.; Thess, A.; Colbert, D.T. and Smalley, R.E. (**1995**); "*Catalytic growth of single-walled nanotubes by laser vaporization*". Chemical Physics Letters Volume 243, Issues 1-2:49-54.

Herrero et al. (**2005**). "*Removal of inorganic mercury from aqueous solutions by biomass of the marine macroalga Cystoseira baccata*". Water Research 39:3199–3210.

Hontelez, John; Lymberidi, Elena (**2005**); *ZERO MERCURY: Key issues and policy recommendations for the EU Strategy on Mercury*. European Environmental Bureau p 143.

Hsieh, Shu-Huei and Horng, Jao-Jia (**2007**). "*Adsorption behavior of heavy metal ions by carbon nanotubes grown on microsized Al_2O_3 particles*". Journal of University of Science and Technology Beging, Volume 14, Number 1, Page 77.

Hülya Genç Fuhrman (**2004**); Arsenic removal from water using seawater-neutralized red mud (Bauxsol). *Environmental & Resources DTU*. ISBN 87-89220-75-7

Iijima S. (**1991**), "*Helical Microtubules of Graphitic Carbon*". Nature, Vol. 354, pp. 56-58

Iijima, Sumio and Ichihashi, Toshinari (**1993**); "*Single-shell carbon nanotubes of 1-nm diameter*", Nature, **363**, 603-605.

Inskeep, W. P., T. R. McDermott, and S.E. Fendorf (**2002**). Arsenic (V/III) cycling in soils and natural waters: Chemical and microbiological processes. In W. T. Frankenberger, Jr. (Ed.) "Environmental Chemistry of Arsenic". p. 183. Marcel Dekker, Inc., New York. ISBN 0824706765

Issi**,** J.P. *et al.* (**1995**); "*Electronic Properties of Carbon Nanotubes: Experimental Results*". Carbon Nanotubes, Pages 121-128.

Jones, Alan B.; Slotton, Darell G. (**1996**); Mercury Effects, Sources and Control Measures. A Special Study for the San Francisco Estuary Institute (SFEI) under the Regional Monitoring Program (RMP) Contribution #20. www.sfei.org/rmp/reports/**mercury**/**mercury**.pdf

José-Yacamán, M., Miki-Yoshida, M., and Rendón, L. (**1993**). "*Catalytic growth of carbon microtubules with fullerene structure"*. Applied Physics Letters. 62: 657.

Jung, S.-H.; Kim, M.-R.; Jeong, S.-H.; Kim, S.-U.; Lee, O.-J.; Lee, K.-H.; Suh, J.-H.; Park, C.-K. (**2003**); "*High-yield synthesis of multi-walled carbon nanotubes by arc discharge in liquid nitrogen*". Applied Physics A Materials Science & Processing, Volume 76, 2:285-286.

Kadirvelu, K., Kavipriya, M., Karthika, C., Vennilamani, N., Pattabhi, S. (**2004**). "*Mercury (II) adsorption by activated carbon made from sago waste*". Carbon 42:745–752.

Kandah, M.I. and Meunier, J.-L.; (**2007**). "*Removal of nickel ions from water by multi-walled carbon nanotubes*". Journal of Hazardous Materials 146:283–288

Krätschmer, W.; Lamb, Lowell D.; Fostiropoulos, K.; and Huffman, Donald R.; (**1990**). "*C_{60}: a new form of carbon*". Nature 347, 354–358. http://www.nature.com/physics/looking-back/kraetschmer/index.html

Krauss, T. D. et al. (**2005**); "*Single Carbon Nanotube Optical Spectroscopy*". ChemPhysChem 6, 1–6 DOI: 10.1002/cphc.200400408.

Kroto, H.W.; Heath, J. R.; O'Brien, S. C.; Curl, R. F. and Smalley, R. E. (**1985**)" *C_{60}: Buckminsterfullerene*". Nature **318,** 162-163. http://www.nature.com/physics/looking-back/kroto/index.html

Kundu, Sanghamitra and Gupta, A.K. (**2007**). "*Adsorption characteristics of As (III) from aqueous solution on iron oxide coated cement (IOCC)*". Journal of Hazardous Materials 142:97–104.

Lambert, J. M.; Ajayan, P. M.; Bernier, P.; Planeix, J. M.; Brotons, V.; Coq, B. and Castaing, J. (**1994**). "*Improving conditions towards isolating single-shell carbon nanotubes*". Chemical Physics Letters Volume 226, Issues 3-4:364-371

Lauwerys, R. R., Buchet, J. P. & Roels, H. (**1979**), "The determination of trace levels of arsenic in human biological materials". *Arch. Toxicol.,* 41: 239-247.

Li, et al. (**2002**), "*Lead adsorption on carbon nanotubes*". Chemical Physics Letters 357:263–266

Li, et al. (**2003**), "*Adsorption of fluoride from water by aligned carbon nanotubes*". Materials Research Bulletin 38:469-476

Li, et al. (**2003**), "*Adsorption of cadmium (II) from aqueous solution by surface oxidized carbon nanotubes*". Carbon 41:1057–1062

Li, et al. (**2003**), "*Competitive adsorption of Pb^{2+}, Cu^{2+} and Cd^{2+} ions from aqueous solutions by MWCNT*". Carbon 41 (2003) 2787–2792

Li, Yan-Hui, Shuguang Wang, Anyuan Cao, Dan Zhao, Xianfeng Zhang, Cailu Xu, Zhaokun Luan, Dianbo Ruan, Ji Liang, Dehai Wu, Bingqing Wei; (**2001**).

Li, Yan-Hui, Yanqiu Zhu, Yimin Zhao, Dehai Wu, Zhaokun Luan (**2006**). "*Different morphologies of carbon nanotubes effect on the lead removal from aqueous solution*". Diamond & Related Materials 15:90 – 94.

"*Adsorption of fluoride from water by amorphous alumina supported on carbon nanotubes*". Chemical Physics Letters 350:412–416.

Liang, Hua-Ding and Han, De-Man (**2006**). "*Multi-Walled Carbon Nanotubes as Sorbent for Flow Injection On-Line Microcolumn Preconcentration Coupled with Flame Atomic Absorption Spectrometry for Determination of Cadmium and Copper*". Analytical Letters, 39: 2285–2295

Long, R.Q. and Yang, R.T. (**2001**). "*Carbon Nanotubes as Superior Sorbent for Dioxin Removal*". J. Am. Chem. Soc., 123: 2058.

Lopes, C. B., Otero, M., Lin, Z., Silva, C. M., Rocha, J., Pereira, E. and Duarte, A.C. (**2009**). "*Removal of Hg^{2+} ions from aqueous solution by ETS-4 microporous titanosilicate—Kinetic and equilibrium studies*". Chemical Engineering Journal 151:247–254.

Lu, C. and Chiu, H.; (**2006**). "*Adsorption of zinc (II) from water with purified carbon nanotubes*". Chemical Engineering Science 61:1138 – 1145

Lu, Chungsying, Chung, Yao-Lei, Chang, Kuan-Foo, (**2005**). "*Adsorption of trihalomethanes from water with carbon nanotubes*". Water Research 39:1183–1189.

Lu, Chungsying, Su, Fengsheng, (**2007**). "*Adsorption of natural organic matter by carbon nanotubes*". Separation and Purification Technology 58:113–121.

Marinković, Slobodan N. (**2008**); " *Review: Carbon Nanotubes*". *J. Serb. Chem. Soc. 73* (8–9) 891–913.

Masciangioli T. and W. Zhang, (**2003**). "*Environmental nanotechnology: Potential and pitfalls*". Environmental Science and Technology 37, 102A–108A.

Massachusetts Department of Environmental Protect (MADEP) (**1996**). Mercury: Forms, Fate & Effects (Chapter 2). http://www.mass.gov/dep/toxics/stypes/hgch2.htm

Meyyappan M. and Srivastava D. (**2000**). "*Carbon Nanotube -A big Revolution in a Technology that Thinks Very, Very, Very Small*". IEEE Potentials, August/September, 16-18.

Mohan, D., Pittman, C.U. Jr. (**2007**); Arsenic removal from water/wastewater using adsorbents - A critical review. Journal of Hazardous Materials 142:1–53

Mondal, P., Balomajumder, C., Mohanty, B.; (**2007**). "*A laboratory study for the treatment of arsenic, iron, and manganese bearing ground water using Fe^{3+} impregnated activated carbon: effects of shaking time, pH and temperature*". Journal of Hazardous Materials, Volume 144, Issues 1-2, Pages 420-426.

Monthioux, Marc and Kuznetsov, Vladimir L. (**2006**). "*Who should be given the credit for the discovery of carbon nanotubes?* *Carbon* 44. [6]

Ng, J. C. (**2005**). "*Environmental contamination of arsenic and its toxicological impact on humans*". *Environ Chem*; 2:146–60.

Norman, Nicholas C., Chemistry of arsenic, antimony, and bismuth, Springer (**1998**) p1. ISBN-9780751403893.

Paradise, M., Goswami, T. (**2007**). "*Carbon nanotubes – Production and industrial applications*". Materials and Design 28:1477–1489

Peng, Xianjia, Luan, Zhaokun, Di, Zechao, Zhang, Zhongguo and Zhu, Chunlei; (**2005**). "*Carbon nanotubes-iron oxides magnetic composites as adsorbent for removal of Pb(II) and Cu(II) from water*". Carbon 43:855–894.

Robertson, D.H., Brenner, D.W., Mintmire J.W.; (**1992**) "*Energetics of nanoscale graphitic tubules*", Phys. Rev. B 45: 12592.

Ruoff, R. S. and Loren, D. C. (**1995**); "*Mechanical and Thermal Properties of Carbon Nanotubes*". Carbon, Volume 33, Issue 7, Pages 925-930.

Sarkar, D., Essington, M. E. and Misra, K. C. (**1999**). "*Adsorption of Mercury(II) by Variable Charge Surfaces of Quartz and Gibbsite*". Soil Sci. Soc. Am. J. 63:1626–1636.

Satio, R.; Fujita, M.; Dresselhaus, G. and Dresselhaus, M. S (**1992**); *Electronic structure of chiral graphene tubules*. Applied Physics Letters (ISSN 0003-6951), vol. 60, 18:2204-2206.

Savage N. and Diallo M., (**2005**). "*Nanomaterials and water purification: opportunities and challenges*". Journal of Nanoparticle Research 7: 331–342.

Senese, Fred (**2000**). "Who discovered carbon?"; Frostburg State University. Retrieved on 05/03/2009

Sharma, V. K. and Sohn, Mary (**2009**); Aquatic arsenic: Toxicity, speciation, transformations, and remediation. Environment International 35:743–759

Smith, AH, Hopenhayn C, Bates MN, Goeden HM, Picciotto IH, Duggan HM, et al. (**1992**). Cancer risks from arsenic in drinking water. *Environ Health Perspective* 97:259–67.

Stafiej, Anna and Pyrzynska, Krystyna; (**2007**). "*Adsorption of heavy metal ions with carbon nanotubes*". Separation and Purification Technology 58:49–52.

Stetter, J. R., Maclay, G.J. (**2004**). "*Carbon Nanotubes and Sensors: a Review*". Advanced Micro and Nanosystems, Vol 1, Pages 357-382.

Subcommittee on Arsenic in Drinking Water, National Research Council (NRC) (**1999**); Arsenic in Drinking Water. *The National Academies Press*: 177-192

Suhr, J., Victor, P., Ci, L., Sreekala, S., Zhang, X., Nalamasu, O. and Ajayan P. M. (**2006**). "Fatigue resistance of aligned carbon nanotube arrays under cyclic compression". *Nature Nanotechnology* 2, 417 – 421.

Tang Z. K. ; Sun H. D. ; Wang J. ; Chen J. ; Li G. (**1998**); "*Mono-Sized Single-Wall Carbon Nanotubes Formed In Channels Of $AlPO_4$-5 Single* Crysta"l. Applied Physics Letters, Vol. 73, 16: 2287-2289.

Tasis, Dimitrios; Tagmatarchis, Nikos; Bianco, Alberto and Maurizio Prato (**2006**). "*Chemistry of Carbon Nanotubes*". Chem. Rev. 106:1105-1136.

Thess, A.; Lee, R.; Nikolaev, P.; Dai, H.; Petit, P.; Robert, J.; Xu, C., Lee, Y.H.; Kim, S.G.; Rinzler, A.G.; Colbert, D.T.; Scuseria, G.E.; Tománek, D. J.; Fischer, E. and Smalley, R.E. (**1996**); "*Crystalline ropes of metallic carbon nanotubes*" Science **273**, 483-487.

Thirunavukkarasu, OS, Viraraghavan, T and Subramanian, KS (**2003**). "*Arsenic removal from drinking water using granular ferric hydroxide*" Water SA Vol. 29 No. 2:161-170.

Thostenson *et al.* (**2001**); "*Advances in the science and technology of carbon nanotubes and their composites: a review*". Composites Science and Technology 61:1899–1912.

Treacy, M. M. J., Ebbesen, T. W. and Gibson, J. M. (**1996**). "*Exceptionally high Young's modulus observed for individual carbon nanotubes*". Nature **381**, 678 - 680; doi:10.1038/381678a0 .

U.S. EPA (**1997**); Office of Research and Development. Capsule Report, Aqueous Mercury Treatment. EPA-625-R-97-004. http://www.epa.gov/ORD/NRMRL/pubs/625r97004/625r97004.pdf

U. S. ENVIRONMENTAL PROTECTION AGENCY. Accessed April 2009. http://www.epa.gov/safewater/arsenic/index.html

U. S. ENVIRONMENTAL PROTECTION AGENCY, (**1998**). "*Water Recycling and Reuse: The Environmental Benefits*". Accessed December 2007. http://www.epa.gov/region09/water/recycling/index.html

U.S. EPA-OSW Human Health Risk Assessment Protocol (HHRAP) (**1998**). http://www.weblakes.com/Mercury/mercury_methylation.html

Villaescusa, Isabel, Bollinger, Jean-Claude (**2008**), Arsenic in drinking water: sources, occurrence and health effects (a review), Rev Environ Sci Biotechnol 7:307–323

Virender K. Sharma, Mary Sohn (**2009**); Aquatic arsenic: Toxicity, speciation, transformations, and remediation. *Environment International* 35 743–759

Walters, D. A., Ericson, L. M., Casavant, M. J., Liu, J., Colbert, D. T., Smith, K. A. and R. E. Smalley (**1999**). "*Elastic strain of freely suspended single-wall carbon nanotube ropes*". Applied Physics Letters, Volume 74, Number 25, Pages 3803-3805.

Wang, H.J., Zhou, A.L., Peng, F., Yu, H., Chen, L.F. (**2007**). "*Adsorption characteristic of acidified carbon nanotubes for heavy metal Pb(II) in aqueous solution*". Materials Science and Engineering A 466:201–206.

West General Inc. 2005. Mercury solubility – mercury hydroxide curve. January. http://www.westgeneral.com/outofthebox/compounds/hgsol.html

World Health Organization (**2006**); Guidelines for drinking-water quality, 3rd edition, incorporating first addendum. ISBN 92 4 154696 4, http://www.who.int/water_sanitation_health/dwq/gdwq3rev/en/index.html

Xianjia Peng, Yanhui Li, Zhaokun Luan, Zechao Di, Hongyu Wang, Binghui Tian, Zhiping Jia, (**2003**). "*Adsorption of 1,2-dichlorobenzene from water to carbon nanotubes*". Chemical Physics Letters 376:154–158.

Ye, Chao, Gong, Qianming, Lu, Fangping, Liang, Ji; (**2007**). "*Adsorption of Middle Molecular Weight Toxins on Carbon Nanotubes*". Acta Phys.-Chim. Sin., 23(9): 1321-1324

Yu, Min-Feng, Files, Bradley S., Arepalli, Sivaram and Ruoff, Rodney S. (**2000**). "*Tensile Loading of Ropes of SingleWall Carbon Nanotubes and their Mechanical Properties*". Physical Review Letters, Volume 84, Number 24, Pages 5552-5555.

Zhang, Fu-Shen, Nriagua, Jerome O., Itohb, Hideaki (**2005**). "*Mercury removal from water using activated carbons derived from organic sewage sludge*" Water Research 39:389–395.

Zheng, L. X et al. (**2004**); "*Ultralong single-wall carbon nanotubes*". Nature Materials, Volume 3, Issue 10: 673-676.

APPENDIX A

EXPERIMENTAL DATA

APPENDIX (A)

EXPERIMENTAL DATA

1. THE EXPERIMENTAL DATA OF THE ADSORPTION OF MERCURY (II) BY MWCNTS:

Sample No.	pH	CNTs Dose (mg)	rpm	Time (min)	C_i (mg/L)	C_f (mg/L)	% removed	Adsorption Capacity qt (mg/g)
1	4	5	50	10	0.066	0.041	37.73	0.249
2	4	10	50	10	0.066	0.032	51.06	0.169
3	5	5	50	10	0.093	0.032	65.38	0.608
4	5	10	50	10	0.093	0.045	51.83	0.241
5	7	5	50	10	0.100	0.052	48.10	0.481
6	7	10	50	10	0.100	0.050	50.40	0.252
7	8	5	50	10	0.099	0.049	50.40	0.499
8	8	10	50	10	0.099	0.042	57.88	0.287
9	9	5	50	10	0.104	0.063	39.13	0.407
10	9	10	50	10	0.104	0.059	43.46	0.226
11	4	5	50	30	0.066	0.023	64.89	0.430
12	4	10	50	30	0.066	0.018	72.06	0.239
13	5	5	50	30	0.093	0.048	48.11	0.450
14	5	10	50	30	0.093	0.036	61.08	0.285
15	7	5	50	30	0.100	0.046	54.20	0.542
16	7	10	50	30	0.100	0.060	40.30	0.202
17	8	5	50	30	0.099	0.044	55.66	0.551
18	8	10	50	30	0.099	0.043	56.97	0.282
19	9	5	50	30	0.104	0.054	48.27	0.502
20	9	10	50	30	0.104	0.038	63.85	0.332
21	4	5	50	60	0.066	0.040	39.69	0.265
22	4	10	50	60	0.066	0.050	23.51	0.080
23	5	5	50	60	0.093	0.049	47.57	0.445
24	5	10	50	60	0.093	0.025	72.54	0.338
25	7	5	50	60	0.100	0.035	65.40	0.654
26	7	10	50	60	0.100	0.028	72.30	0.362

Sample No.	pH	CNTs Dose (mg)	rpm	Time (min)	C_i (mg/L)	C_f (mg/L)	% removed	Adsorption Capacity qt (mg/g)
27	8	5	50	60	0.099	0.027	72.93	0.722
28	8	10	50	60	0.099	0.021	78.38	0.388
29	9	5	50	60	0.104	0.039	62.98	0.655
30	9	10	50	60	0.104	0.031	69.90	0.364
31	4	5	50	120	0.066	0.025	62.29	0.413
32	4	10	50	120	0.066	0.019	71.60	0.237
33	5	5	50	120	0.093	0.022	75.89	0.707
34	5	10	50	120	0.093	0.024	74.59	0.348
35	7	5	50	120	0.100	0.040	60.40	0.604
36	7	10	50	120	0.100	0.027	72.80	0.364
37	8	5	50	120	0.099	0.046	53.94	0.534
38	8	10	50	120	0.099	0.016	83.74	0.415
39	9	5	50	120	0.104	0.027	74.52	0.775
40	9	10	50	120	0.104	0.026	75.10	0.391
41	4	5	100	10	0.066	0.035	46.87	0.312
42	4	10	100	10	0.066	0.027	58.17	0.193
43	5	5	100	10	0.093	0.036	61.30	0.572
44	5	10	100	10	0.093	0.026	72.00	0.336
45	7	5	100	10	0.100	0.038	62.00	0.620
46	7	10	100	10	0.100	0.042	57.60	0.288
47	8	5	100	10	0.099	0.036	64.14	0.635
48	8	10	100	10	0.099	0.037	62.73	0.311
49	9	5	100	10	0.104	0.042	59.42	0.618
50	9	10	100	10	0.104	0.044	57.60	0.300
51	4	5	100	30	0.066	0.025	62.44	0.414
52	4	10	100	30	0.066	0.025	62.44	0.207
53	5	5	100	30	0.093	0.024	74.38	0.693
54	5	10	100	30	0.093	0.027	70.38	0.328
55	7	5	100	30	0.100	0.035	65.40	0.654
56	7	10	100	30	0.100	0.032	68.20	0.341
57	8	5	100	30	0.099	0.035	65.05	0.644
58	8	10	100	30	0.099	0.037	63.03	0.312
59	9	5	100	30	0.104	0.028	73.37	0.763
60	9	10	100	30	0.104	0.028	73.46	0.382
61	4	5	100	60	0.066	0.045	31.91	0.214
62	4	10	100	60	0.066	0.023	65.19	0.216
63	5	5	100	60	0.093	0.021	77.51	0.722

Sample No.	pH	CNTs Dose (mg)	rpm	Time (min)	C_i (mg/L)	C_f (mg/L)	% removed	Adsorption Capacity qt (mg/g)
64	5	10	100	60	0.093	0.014	84.76	0.395
65	7	5	100	60	0.100	0.023	76.80	0.768
66	7	10	100	60	0.100	0.022	77.60	0.388
67	8	5	100	60	0.099	0.037	63.03	0.624
68	8	10	100	60	0.099	0.022	77.98	0.386
69	9	5	100	60	0.104	0.030	71.25	0.741
70	9	10	100	60	0.104	0.024	76.63	0.399
71	4	5	100	120	0.066	0.021	68.55	0.454
72	4	10	100	120	0.066	0.012	81.37	0.269
73	5	5	100	120	0.093	0.015	84.00	0.782
74	5	10	100	120	0.093	0.009	89.95	0.419
75	7	5	100	120	0.100	0.032	67.80	0.678
76	7	10	100	120	0.100	0.015	84.80	0.424
77	8	5	100	120	0.099	0.032	67.88	0.672
78	8	10	100	120	0.099	0.020	79.49	0.394
79	9	5	100	120	0.104	0.031	70.67	0.735
80	9	10	100	120	0.104	0.022	79.04	0.411
81	4	5	150	10	0.089	0.018	79.64	0.709
82	4	10	150	10	0.089	0.007	92.35	0.411
83	5	5	150	10	0.093	0.016	82.17	0.765
84	5	10	150	10	0.093	0.015	83.88	0.390
85	7	5	150	10	0.100	0.028	72.36	0.724
86	7	10	150	10	0.100	0.017	83.19	0.416
87	8	5	150	10	0.099	0.028	71.59	0.709
88	8	10	150	10	0.099	0.013	86.42	0.428
89	9	5	150	10	0.104	0.034	66.90	0.696
90	9	10	150	10	0.104	0.014	86.89	0.452
91	4	5	150	30	0.089	0.012	86.96	0.774
92	4	10	150	30	0.089	0.009	90.14	0.401
93	5	5	150	30	0.093	0.014	85.34	0.794
94	5	10	150	30	0.093	0.010	88.73	0.413
95	7	5	150	30	0.100	0.030	69.72	0.697
96	7	10	150	30	0.100	0.024	75.77	0.379
97	8	5	150	30	0.099	0.019	80.51	0.797
98	8	10	150	30	0.099	0.011	89.39	0.442
99	9	5	150	30	0.104	0.031	70.33	0.731
100	9	10	150	30	0.104	0.020	80.51	0.419

Sample No.	pH	CNTs Dose (mg)	rpm	Time (min)	C_i (mg/L)	C_f (mg/L)	% removed	Adsorption Capacity qt (mg/g)
101	4	5	150	60	0.089	0.062	30.09	0.269
102	4	10	150	60	0.089	0.014	84.26	0.375
103	5	5	150	60	0.093	0.012	87.04	0.810
104	5	10	150	60	0.093	0.008	91.56	0.426
105	7	5	150	60	0.100	0.012	88.23	0.882
106	7	10	150	60	0.100	0.003	96.77	0.484
107	8	5	150	60	0.099	0.016	84.34	0.835
108	8	10	150	60	0.099	0.010	89.57	0.443
109	9	5	150	60	0.104	0.026	75.10	0.781
110	9	10	150	60	0.104	0.014	86.85	0.452
111	4	5	150	120	0.089	0.021	75.80	0.675
112	4	10	150	120	0.089	0.000	100.00	0.445
113	5	5	150	120	0.093	0.007	92.94	0.865
114	5	10	150	120	0.093	0.000	100.00	0.465
115	7	5	150	120	0.100	0.007	93.14	0.931
116	7	10	150	120	0.100	0.002	98.10	0.491
117	8	5	150	120	0.099	0.005	95.17	0.942
118	8	10	150	120	0.099	0.002	98.11	0.486
119	9	5	150	120	0.104	0.020	80.85	0.841
120	9	10	150	120	0.104	0.000	99.68	0.518

2. THE EXPERIMENTAL DATA OF THE ADSORPTION ISOTHERMS OF MERCURY (II) ADSORPTION BY MWCNTS:

pH	CNTs Dose (mg)	rpm	Time (min)	C_i (mg/L)	C_e (mg/L)	% removed	Adsorption Capacity q_e (mg/g)
8	10	150	120	0.099	0.002	98.18	0.49
8	10	150	120	0.964	0.742	23.03	1.11
8	10	150	120	5.161	4.300	16.68	4.31
8	10	150	120	9.8	8.563	12.62	6.19
8	20	150	120	0.964	0.488	49.38	1.19
8	20	150	120	5.161	4.500	12.81	1.65
8	20	150	120	9.8	8.936	8.82	2.16
8	40	150	120	0.964	0.479	50.31	0.61
8	40	150	120	5.161	2.854	44.70	2.88
8	40	150	120	9.8	5.800	40.82	5.00

3. THE EXPERIMENTAL DATA OF THE ADSORPTION OF ARSENIC (III) BY MWCNTS:

Sample No.	pH	Wt (mg)	rpm	Time (min)	C_i (mg/L)	C_f (mg/L)	% removed	Adsorption Capacity qt (mg/g)
101	4	5	50	10	1.25	1.25	0.00	0
108	4	10	50	10	1.25	1.25	0.00	0
96	4	5	50	30	1.25	1.25	0.00	0
111	4	10	50	30	1.25	1.25	0.00	0
87	4	5	50	60	1.25	1.25	0.00	0
97	4	10	50	60	1.25	1.25	0.00	0
64	4	5	50	120	1.25	1.25	0.00	0
81	4	10	50	120	1.25	1.25	0.00	0
90	4	5	100	10	1.25	1.25	0.00	0
69	4	10	100	10	1.25	1.25	0.00	0
80	4	5	100	30	1.25	1.25	0.00	0
51	4	10	100	30	1.25	1.25	0.00	0
52	4	5	100	60	1.25	1.25	0.00	0
29	4	10	100	60	1.25	1.25	0.00	0
56	4	5	100	120	1.25	1.25	0.00	0
88	4	10	100	120	1.25	1.25	0.00	0
85	4	5	150	10	1.25	1.25	0.00	0
89	4	10	150	10	1.25	1.25	0.00	0
8	4	5	150	30	1.25	1.25	0.00	0
15	4	10	150	30	1.25	1.25	0.00	0
9	4	5	150	60	1.25	1.25	0.00	0
7	4	10	150	60	1.25	1.25	0.00	0
36	4	5	150	120	1.25	1.25	0.00	0
33	4	10	150	120	1.25	1.25	0.00	0
119	5	5	50	10	1.25	1.25	0.00	0
113	5	10	50	10	1.25	1.25	0.00	0
98	5	5	50	30	1.25	1.25	0.00	0
107	5	10	50	30	1.25	1.25	0.00	0
106	5	5	50	60	1.25	1.25	0.00	0
73	5	10	50	60	1.25	1.25	0.00	0
83	5	5	50	120	1.25	1.25	0.00	0
43	5	10	50	120	1.25	1.25	0.00	0
86	5	5	100	10	1.25	1.25	0.00	0
68	5	10	100	10	1.25	1.25	0.00	0
65	5	5	100	30	1.25	1.25	0.00	0
71	5	10	100	30	1.25	1.25	0.00	0
92	5	5	100	60	1.25	1.25	0.00	0
48	5	10	100	60	1.25	1.25	0.00	0

Sample No.	pH	Wt (mg)	rpm	Time (min)	C_i (mg/L)	C_f (mg/L)	% removed	Adsorption Capacity qt (mg/g)
28	5	5	100	120	1.25	1.25	0.00	0
17	5	10	100	120	1.25	1.25	0.00	0
41	5	5	150	10	1.25	1.25	0.00	0
30	5	10	150	10	1.25	1.25	0.00	0
5	5	5	150	30	1.25	1.25	0.00	0
13	5	10	150	30	1.25	1.25	0.00	0
2	5	5	150	60	1.25	1.25	0.00	0
3	5	10	150	60	1.25	1.25	0.00	0
38	5	5	150	120	1.25	1.25	0.00	0
34	5	10	150	120	1.25	1.25	0.00	0
46	7	5	50	10	1.25	1.25	0.00	0
112	7	10	50	10	1.25	1.25	0.00	0
116	7	5	50	30	1.25	1.25	0.00	0
110	7	10	50	30	1.25	1.25	0.00	0
103	7	5	50	60	1.25	1.25	0.00	0
100	7	10	50	60	1.25	1.25	0.00	0
79	7	5	50	120	1.25	1.25	0.00	0
67	7	10	50	120	1.25	1.25	0.00	0
72	7	5	100	10	1.25	1.25	0.00	0
91	7	10	100	10	1.25	1.25	0.00	0
50	7	5	100	30	1.25	1.25	0.00	0
45	7	10	100	30	1.25	1.25	0.00	0
47	7	5	100	60	1.25	1.25	0.00	0
6	7	10	100	60	1.25	1.25	0.00	0
18	7	5	100	120	1.25	1.25	0.00	0
57	7	10	100	120	1.25	1.25	0.00	0
31	7	5	150	10	1.25	1.25	0.00	0
70	7	10	150	10	1.25	1.25	0.00	0
61	7	5	150	30	1.25	1.25	0.00	0
16	7	10	150	30	1.25	1.25	0.00	0
23	7	5	150	60	1.25	1.25	0.00	0
11	7	10	150	60	1.25	1.25	0.00	0
35	7	5	150	120	1.25	1.25	0.00	0
37	7	10	150	120	1.25	1.25	0.00	0
105	8	5	50	10	1.25	1.25	0.00	0
104	8	10	50	10	1.25	1.25	0.00	0
94	8	5	50	30	1.25	1.25	0.00	0
118	8	10	50	30	1.25	1.25	0.00	0
84	8	5	50	60	1.25	1.25	0.00	0
95	8	10	50	60	1.25	1.25	0.00	0
82	8	5	50	120	1.25	1.25	0.00	0
114	8	10	50	120	1.25	1.25	0.00	0

Sample No.	pH	Wt (mg)	rpm	Time (min)	C_i (mg/L)	C_f (mg/L)	% removed	Adsorption Capacity qt (mg/g)
49	8	5	100	10	1.25	1.25	0.00	0
99	8	10	100	10	1.25	1.25	0.00	0
75	8	5	100	30	1.25	1.25	0.00	0
40	8	10	100	30	1.25	1.25	0.00	0
54	8	5	100	60	1.25	1.25	0.00	0
63	8	10	100	60	1.25	1.25	0.00	0
74	8	5	100	120	1.25	1.25	0.00	0
42	8	10	100	120	1.25	1.25	0.00	0
44	8	5	150	10	1.25	1.25	0.00	0
32	8	10	150	10	1.25	1.25	0.00	0
20	8	5	150	30	1.25	1.25	0.00	0
25	8	10	150	30	1.25	1.25	0.00	0
4	8	5	150	60	1.25	1.25	0.00	0
1	8	10	150	60	1.25	1.25	0.00	0
21	8	5	150	120	1.25	1.25	0.00	0
10	8	10	150	120	1.25	1.25	0.00	0
109	9	5	50	10	1.25	1.25	0.00	0
115	9	10	50	10	1.25	1.25	0.00	0
120	9	5	50	30	1.25	1.25	0.00	0
117	9	10	50	30	1.25	1.25	0.00	0
60	9	5	50	60	1.25	1.25	0.00	0
55	9	10	50	60	1.25	1.25	0.00	0
78	9	5	50	120	1.25	1.25	0.00	0
62	9	10	50	120	1.25	1.25	0.00	0
77	9	5	100	10	1.25	1.25	0.00	0
102	9	10	100	10	1.25	1.25	0.00	0
39	9	5	100	30	1.25	1.25	0.00	0
53	9	10	100	30	1.25	1.25	0.00	0
58	9	5	100	60	1.25	1.25	0.00	0
76	9	10	100	60	1.25	1.25	0.00	0
27	9	5	100	120	1.25	1.25	0.00	0
59	9	10	100	120	1.25	1.25	0.00	0
66	9	5	150	10	1.25	1.25	0.00	0
93	9	10	150	10	1.25	1.25	0.00	0
14	9	5	150	30	1.25	1.25	0.00	0
19	9	10	150	30	1.25	1.25	0.00	0
26	9	5	150	60	1.25	1.25	0.00	0
22	9	10	150	60	1.25	1.25	0.00	0
12	9	5	150	120	1.25	1.25	0.00	0
24	9	10	150	120	1.25	1.25	0.00	0

4. THE EXPERIMENTAL DATA OF THE ADSORPTION OF ARSENIC (III) BY MWCNT-FE:

Sample No.	pH	Wt (mg)	rpm	Time (min)	C_i mg/L	C_e (mg/L)	% removed	Adsorption Capacity q_e (mg/g)
1	8	5	50	10	0.962	0.805	16.32	1.57
2	8	10	50	10	0.962	0.719	25.26	1.22
3	8	5	50	30	0.962	0.723	24.84	2.39
4	8	10	50	30	0.962	0.655	31.91	1.54
5	8	5	50	60	0.962	0.752	21.83	2.1
6	8	10	50	60	0.962	0.661	31.29	1.51
7	8	5	50	120	0.962	0.718	25.36	2.44
8	8	10	50	120	0.962	0.62	35.55	1.71
9	8	5	100	10	0.962	0.741	22.97	2.21
10	8	10	100	10	0.962	0.642	33.26	1.60
11	8	5	100	30	0.962	0.716	25.57	2.46
12	8	10	100	30	0.962	0.625	35.03	1.69
13	8	5	100	60	0.962	0.688	28.48	2.74
14	8	10	100	60	0.962	0.617	35.86	1.73
15	8	5	100	120	0.962	0.659	31.50	3.03
16	8	10	100	120	0.962	0.516	46.36	2.23
17	8	10	150	120	1.15	0.260	77.45	4.47
18	8	10	150	120	5.05	4.332	14.23	3.60
19	8	10	150	120	10.39	9.061	12.81	6.66
20	8	20	150	120	0.96	0.347	63.91	3.07
21	8	20	150	120	5.05	3.794	24.89	6.29
22	8	20	150	120	10.39	8.894	14.41	7.49
23	8	40	150	120	0.96	0.117	87.84	4.23
24	8	40	150	120	5.05	2.602	48.49	12.25
25	8	40	150	120	10.39	7.473	28.09	14.60

VISTAE

Name:	Salman Faleh Al-Khaldi
Mail Address:	P. O. Box 458, Abqaiq 31311, Kingdom Of Saudi Arabia
Contacts:	Work Phone: 03/572-4399
	+966507669933
	Email: salman.khaldi.2@aramco.com

Education/Training:

Education:	BS in Chemistry from MTSU, USA (May-1996)
	MS in Environmental Science

Career History:

12/2004-Present Team Leader, Environmental Lab Section, Southern Area Lab Division, Southern Area Engineering Department, Saudi Aramco

Head of a group responsible for the analysis of environmental water analyses (Geochemical, trace metals, nutrients and bacteriological analyses). The section is responsible for conducting all responsibilities of producing high quality water analyses of samples received from Environmental Protection Department i.e. Groundwater, Sewage treatment plants, and community water samples. The responsibilities include and not limited to manpower management, work optimization, data verifications and reporting, quality control, method development, and instrumentation troubleshooting.

Jul/2007-Dec/2008 Environmental Scientist, Environmental Protection Department, Environmental Engineering Division, Saudi Aramco

I worked in the Land and Groundwater Protection Unit. The major activities of this unit include but not limited to:

- Consults on waste and waste management issues.
- Advises on the handling, treatment, and disposal of solid, liquid, hazardous and toxic wastes.
- Evaluates and pre-qualifies waste management contractors, and monitors both Saudi Aramco and contract waste management facilities.
- Performs waste minimization assessments.
- Monitors groundwater wells and deep well disposal of industrial wastewater, and reports on the results of specific groundwater investigations.
- Reviews engineering design packages including Land Use Permits and hydrotest water disposal plans.

06/2006-09/2006 Supervisor for Qurayyah Sea water Lab Unit Southern Area Lab
04/2003-08/2003 Division, Southern Area Engineering Department, Saudi Aramco

The major objective of the Qurayyah Laboratory is to provide analytical support to operations in maximizing the production of seawater while ensuring that the system is protected against chemical and bacterial corrosion. The unit comprises of laboratories at Qurayyah (which operates a 24 hour shift operation) and UWSS. The unit's operational area encompasses the Seawater Treatment Plant, Shipping Lines, UWSS Pumping Facility and the Surge Tanks. The monitoring program includes a wide range of physical, chemical and microbiological parameters essential for operations and engineering personnel to meet production quality standards. The unit further provides technical support in chemical treatment processes, chemical usage and system data evaluation.

12/2002-11/2004 Lab Scientist, Qurayyah Sea water Lab Unit, Southern Area Lab Division, Southern Area Engineering Department, Saudi Aramco

Responsible for the monitoring program of Qurayyah Sea water Lab unit which includes a wide range of physical, chemical and microbiological parameters essential for operations and engineering personnel to meet production quality standards. The unit further provides technical support in chemical treatment processes, chemical usage and system data evaluation.

06/2000-11/2002 Field Coordinator, Technical Support Lab Unit, Southern Area Lab Division, Southern Area Engineering Department, Saudi Aramco

Responsible for the scheduling and coordination of field sampling and testing of oilfield plant and community facilities in Abqaiq, Shedgum and Aindar areas; also companywide Public Health monitoring for bacterial contamination. Treatment chemicals evaluation and monitoring of boilers during chemical cleaning are other examples of services provided.

06/99-05/2000 Lab Scientist, Technical Support Lab Unit, Southern Area Lab Division, Southern Area Engineering Department, Saudi Aramco

I was responsible for the evaluation, compatibility and performance of oilfield chemicals corrosion, scale, demulsifies and biocides used in the oilfield facilities in Abqaiq, Shedgum and AinDar areas.

09/1998-05/1999 Lab Scientist, Analytical Support Lab Unit, Southern Area Lab Division, Southern Area Engineering Department, Saudi Aramco

I worked for the analytical unit where both routine and non-routine analyses are conducted in support to a wide range of Saudi Aramco operations. Automated systems are used, wherever possible, to provide a cost effective and fast response to proponent requests. Major services carried out by the Unit include: Geochemical analysis of produced, utilities, and potable waters; Trace metal analysis for corrosion monitoring and scaling tendency evaluations; Scale/solids analysis.

11/1997-08/1998 Production Engineer, Abqaiq Production Engineering Div., Southern Area Engineering Department, Saudi Aramco

I worked as a production engineer responsible for Ain Dar GOSP-3. My duties included monitoring production oil wells and maintaining the production rate of oil well also gathering well information for reservoir management.

04/1997-10/1997 Corrosion Engineer, Abqaiq Operation Engineering Div., Southern Area Engineering Department, Saudi Aramco

I worked as a corrosion engineer responsible for Abqaiq, Shedgum and Ain Dar areas' facilities. My duties included monitoring oilfield chemicals residuals and corrosion/scaling potentials.

11/1996-03/1997 Lab Scientist, Technical Support Lab Unit, Southern Area Lab Division, Southern Area Engineering Department, Saudi Aramco

After graduation from Middle Tennessee State University in the USA, I was assigned to work as a Lab Scientist in the Technical Support Lab Unit. Part of this unit's responsibilities was to collect Oil, water and Gas samples and perform on-site testing.